ABSTRACT

A study is presented of two aspects of plant adaptation to soil waterlogging. The first part of this study is an investigation into the relation between the uptake of oxygen by plant root tips and the external concentration of oxygen. A range of plant species was collected and grown in the glasshouse in both flooded and unflooded sand cultures. Experiments were carried out on these plants after at least one month's growth in the glasshouse, and also on plants collected from the wild without any pre-treatment in the glasshouse. Oxygen uptake measurements were carried out using excised root apices in a Rank Memebrane Oxygen Electrode assembly. It was found in nearly all experiments that the rate of oxygen uptake was highly dependent on the external oxygen concentration in both flood-tolerant and flood-sensitive species. Samples which had been grown in a flooded sand culture, however, were less dependent on the supply of external oxygen than those which had been grown in an unflooded sand culture.

These results were interpreted with the aid of a simple mathematical model of oxygen uptake in a plant root apex. The model was designed to predict the relation between oxygen uptake rate and the external concentration of oxygen for roots with different porosities, different rates of uptake and possessing respiratory systems with different affinities for oxygen. Using this model, it was found that a normal plant root apex, in which the respiratory systems have a high affinity for oxygen and in which the presence of intercellular air spaces allows a rapid radial movement of oxygen, should exhibit a rate of oxygen uptake which is largely independent of the external concentration of oxygen. From this prediction and from theoretical calculations on the movement of oxygen within individual root cells, it was concluded that the high dependence of oxygen uptake on external oxygen concentration which was found in the experiments was largely an artefact resulting

from flooding of the intercellular air spaces under the *in vitro* conditions of the experiments. Affinity for oxygen and the ability to maintain high rates of oxygen uptake under conditions of low oxygen availability are not therefore considered to be criteria by which flood-tolerant and flood-intolerant species can be distinguished.

The second part of this study was an investigation into the energy relations of excised plant root systems, by the measurement of ATP/ADP ratios under anoxia. Root systems were harvested from plants which had previously been grown under a flooded or an unflooded sand culture regime in the glasshouse, and were incubated under nitrogen gas in deoxygenated phosphate buffer for up to 4 hours. Control samples were incubated in air-saturated buffer under an atmosphere of air. It was found that ATP/ADP ratios were lower when the excised root systems were incubated under nitrogen than when they were incubated in an aerobic environment. However, the values obtained suggest a higher energy charge in the root tissues under anoxia than has generally been reported by other workers. No difference was found between flood-tolerant and flood-sensitive species, but it is pointed out that since the experiments did not measure the total size of the adenylate pool, such differences may have been overlooked. It is suggested that energy charge measurements may be more useful as a general indication of the metabolic activity within the root tissue rather than as a criterion for distinguishing flood tolerant and flood intolerant plant species.

DECLARATION

I hereby declare that this thesis has been composed by myself, and that it is a record of work which has been done by myself. This has not been accepted in any previous application for a degree. Any other sources of information have been specifically acknowledged.

Signed

The Oxygen Uptake and Energy Charge under Hypoxia and Anoxia of Excised Plant Roots from Flood-tolerant and Flood-sensitive Species.

A thesis presented for the degree of MSc at the University of St. Andrews 1980

by

Andrew J. McCreath, BSc

ACKNOWLEDGEMENTS

I would like to thank Professor R.M.M. Crawford for his valuable assistance and encouragement during the course of my research at St. Andrews University. Thanks are also due to the technical staff of the Department of Botany for their assistance, to Mr. N. Smirnoff for the provision of much of the plant material used in my experiments and to Dr. A. Barclay for some stimulating discussions.

CERTIFICATE

I hereby certify that Andrew J. McCreath has been engaged upon research from October 1978 onwards under my supervision to prepare the accompanying thesis for the degree of Master of Science.

Signed

Prof. R.M.M. Crawford

St. Andrews

October 1980

STATEMENT

I, Andrew J. McCreath, was born on February 15th, 1956, and was educated at George Watson's College, Edinburgh, and subsequently at the University of Aberdeen from which I graduated in June, 1978, with the degree of Bachelor of Science. I was admitted as a research student of the University of St. Andrews in October 1978 in accordance with Ordinance General No. 12. The thesis was completed in October 1980.

SUMMARY

A study is presented of two aspects of plant adaptation to soil waterlogging. The first part of this study is an investigation into the relation between the uptake of oxygen by excised plant root tips and the concentration of oxygen in the external solution. It was found in experiments on several species that the rate of oxygen uptake was highly dependent on the external oxygen concentration, and that this dependence was lower in samples which had previously been grown in a flooded sand culture. These results have been interpreted with the aid of a mathematical model designed to predict the rate of oxygen uptake given certain properties of the root tissue. From the predictions made by this model, and from the results of other workers, it is concluded that the high dependence of oxygen uptake on external oxygen concentration is largely an artefact resulting from the flooding of the intercellular air spaces of the root tissue under the *in vitro* conditions of the experiments. Affinity for oxygen and the ability to maintain high rates of oxygen uptake under conditions of low oxygen availability are not therefore considered to be criteria by which flood-tolerant and flood-intolerant species can be distinguished.

The second part of this study is an investigation into the energy relations of excised plant root systems, by the measurement of ATP/ADP ratios under anoxia. It was found that ATP/ADP ratios were lower when the excised root systems were incubated under nitrogen than when they were incubated in an aerobic environment. However, the values obtained suggest a higher energy charge in the root tissues under anoxia than has generally been reported by other workers. No difference was found between flood-tolerant and flood-intolerant species, but it is pointed out that since the experiments did not measure the total size of the adenylate pool, such differences may have been overlooked. It is suggested that energy charge measurements may be more useful as a general indication of the metabolic activity within the root tissue rather than as a criterion for distinguishing flood tolerant and flood intolerant plant species.

CONTENTS

GENERAL INTRODUCTION

The primary effect of soil waterlogging is a drastic reduction in the availability of oxygen, the diffusion of oxygen through water being approximately four orders of magnitude slower than diffusion through air. Flooding a previously aerobic soil leads to an immediate drop in the oxygen supply, which may be totally depleted within several hours to a few days, depending on the oxygen demand by chemical and biological processes (EVANS and SCOTT, 1955; TURNER and PATRICK, 1968). Despite the total lack of oxygen characteristic of flooded soils, many plant species are able to survive under such conditions. Such species may be classified as 'flood-tolerant' and can be broadly divided into two groups according to their ability to withstand prolonged flooding. On the one hand, there are those species which require adequate soil aeration for active growth but which are nevertheless capable of surviving long periods of soil waterlogging in a dormant state. On the other hand, however, there are many species which are able to maintain active growth during periods of soil flooding. In contrast to these flood-tolerant species are those which show signs of physiological damage upon the onset of flooding. Such 'flood-sensitive' species are either unable to endure even temporary conditions of soil waterlogging, or their growth is retarded to such an extent that they are unable to compete with better-adapted flood-tolerant species. Clearly, an understanding of flooding-tolerance can only be achieved by comparative studies of these two types of plant species in order to elucidate the survival mechanisms which enable wetland plants to endure the adverse conditions of waterlogged soils.

The reduction in soil aeration which follows flooding leads to the development of strong reducing conditions in the soil, and the production of toxic substances in high quantities. Manganic and Ferric compounds, for example, become reduced to the more soluble Manganous and Ferrous forms and produce symptoms of poisoning in plant species

poorly adapted to such conditions (DIONNE and PESANT, 1976; BENAC, 1976; ROBSON and LONERAGAN, 1970; BARTLETT, 1961). Survival in anaerobic soils, therefore, necessitates the evolution of detoxification mechanisms. However, the main pre-requisite for the survival of any plant species in a waterlogged soil must be the ability to endure the lack of molecular oxygen available in the soil environment.

In most flood-tolerant species, the onset of flooding induces extensive development of the intercellular gas space system in the root tissues, along with a reduction in the rate of aerobic respiration (ARMSTRONG, 1978). A similar response is also found in many flood-sensitive species (YU et al, 1969) but the extent of the response does not approach that characteristic of wetland species. Such morphological changes will lead to an increase in root porosity and an enhancement of the gaseous diffusion of oxygen from the aerial portions of the plant to the root system. This observation has led a number of authors to propose that survival in waterlogged soils is achieved through increased internal ventilation, so that unimpeded aerobic respiration is able to continue throughout the root system. Innumerable studies have indeed shown that there is a downward movement of gaseous oxygen through the root systems of flood-tolerant species (ARMSTRONG,1964, 1967; LAMBERS, 1976; PHILIPSON and COUTTS, 1977c; VARTAPETIAN, 1978) and also some flood-sensitive species (GREENWOOD, 1967a, b; LUXMOORE and STOLZY, 1972).

The assertion that such internal oxygen diffusion is sufficient to maintain uninhibited aerobic respiration within the root system depends on an accurate knowledge of the relationship between oxygen concentration and aerobic respiration. Investigations into this relationship have aroused a certain degree of controversy in recent years. A number of studies using excised root portions in in vitro experiments have shown a high dependence of aerobic respiration on the external concentration of oxygen (BERRY and NORRIS, 1949a;

LUXMOORE et al, 1970). Such studies show that oxygen uptake is independent of oxygen concentration until a certain point, termed the critical oxygen pressure (COP) is reached, below which oxygen uptake shows a hyperbolic relationship to the external oxygen concentration. COPs measured in such experiments are usually relatively high, the values reported rarely being lower than 0.1 atm (ARMSTRONG and GAYNARD, 1976). This would indicate that for unrestricted aerobic respiration, a wetland plant would have to possess a ventilating mechanism capable of maintaining an internal oxygen concentration of greater than 0.1 atm throughout the root system. However, ARMSTRONG and GAYNARD (1976) have pointed out that in vitro experiments may lead to flooding of the cortical air spaces. As this will increase the diffusional impedance to oxygen movement, they conclude that COPs obtained in such experiments overestimate the true COP characteristic of the intact plant. In experiments on intact plants, they estimated the COP for root respiration to be 0.025atm and 0.020atm for Rice and Eriophorum angustifolium respectively. Evidence of internal oxygen concentrations larger than these values (VALLANCE and COULT, 1951; ARMSTRONG, 1967) would therefore support the hypothesis that internal oxygen diffusion is adequate to maintain full aerobic respiration in many wetland species.

A number of studies, however, have shown that the root tissues of many flood-tolerant species are characterised by metabolic adaptations to ameliorate the normally harmful effects of anaerobiosis. Removal of the oxygen supply to plant tissues commonly results in an acceleration of glycolysis, with the consequent rapid evolution of carbon dioxide and the production of ethanol as the end-product of anaerobic respiration. This accumulation of ethanol, a plant toxin, is undoubtedly a major cause of flooding damage in flood-

sensitive species. It has been shown that in flood-sensitive species, the onset of flooding leads not only to an increase in glycolysis but also to a large increase in alcohol dehydrogenase (ADH) activity. By contrast, flood-tolerant species show a considerably less marked increase in glycolysis and ADH activity upon flooding (CRAWFORD, 1966, 1967; CRAWFORD and McMANMON, 1968). Some evidence has been presented which suggests that in some flood-tolerant species, the end-product of glycolysis is malate rather than ethanol, so that toxic quantities of ethanol are not produced under anaerobic conditions (CRAWFORD and TYLER, 1969). LINHART and BAKER (1973) showed that flood-tolerant races of Veronica peregrina accumulated malate under experimental flooding, whereas non flood-tolerant races did not.

Evidence of metabolic adaptations for the survival of low oxygen conditions must be taken to suggest that in many flood-tolerant species, the supply of oxygen from internal aeration is not sufficient to meet the full requirements of aerobic respiration throughout the root tissue. Furthermore, although flood-tolerant species are able to regulate their glycolytic rate under anaerobic conditions, the onset of flooding often still leads to an increased production of ethanol, indicating the existence of anaerobic centres within the root (CRAWFORD, 1967; CRAWFORD and BAINES, 1979).

Recently, the measurement of energy charge (a measure of the relative amounts of ATP and ADP in the adenylate pool) has been used as an extremely sensitive parameter to investigate the effects of anoxia on plant tissues. RAYMOND et al (1978) found that when root systems of intact maize and rice plants were flushed with nitrogen there was a drop in energy charge within the first half hour. PRADET (1978) found a similar response when rice embryos and coleoptiles were subjected to anaerobic treatment.

The relative contribution of metabolic adaptations versus internal aeration in flood-tolerant plant species is still not clear.

While some species with extensive gas space development and shallow rooting systems may be able to avoid oxygen shortages within the root tissues, it seems likely that species such as Filipendula ulmaria, which contains only 2% root air space (CRAWFORD and SMIRNOFF, unpublished data), must rely on metabolic adaptation. Furthermore, it is not certain which regions of the root system are responsible for the production of ethanol upon flooding. It has been shown that even in an atmosphere of air, ethanol can be detected in root tips (BETZ, 1957; RUHLAND and RAMSHORN, 1938), suggesting that even in the presence of an efficient ventilating mechanism some increase in glycolysis is inevitable in the meristematic regions under flooded conditions.

It is quite plausible to suggest that while internal oxygen diffusion may be adequate to meet the respiratory requirements of the sub-apical regions of the root system, under anaerobic soil conditions, the meristematic regions will be subjected to an oxygen stress. This arises from the high respiratory activity of the root tip zone, coupled with a low diffusion coefficient of oxygen because of the much lower development of the air space system (LUXMOORE and STOLZY, 1972b). Such a suggestion is supported by the discovery (see above) that ethanol is found in root tips growing in an atmosphere of air. LUXMOORE and STOLZY (1972b) have suggested that, in general, the root tip zone may be more dependent on soil aeration rather than internal aeration for its oxygen supply. They estimate that the ratio between the area available for internal aeration to soil aeration through liquid is approximately 12.5% in maize.

It is reasonable to expect, therefore, that root tip zones from species with differing sensitivities to flooding may respond

differently to conditions of low soil oxygen. The root tip of a flood-tolerant species, for example, may be metabolically adapted to rely on anaerobic respiration to meet its energy requirements, or it may be capable of maintaining a high rate of aerobic respiration even at very low concentrations of soil oxygen.

Little information is available in the literature regarding the effects of low oxygen tension on aerobic respiration in the root tip zone in particular. Those studies which have been carried out have generally been confined to only a few species, notably those of agricultural significance. In order to obtain a more complete picture, with particular reference to flooding tolerance, the major part of this project was an investigation into the effects of hypoxia on aerobic respiration in the root tip. A wide range of species was used, including flood-tolerant and flood-sensitive examples, so that the results obtained could be considered within a general ecological framework. To complement this study, a short investigation was also carried out into the effects of anoxia on energy relations within plant root systems from a few selected species. It was hoped that the results of these two investigations would shed more light on the relative contributions of metabolic adaptations and internal oxygen diffusion to flooding tolerance.

SECTION 1

The Effect of External Oxygen Concentration on Aerobic Respiration in the Root Tip.

1.1 INTRODUCTION

It has already been outlined in the General Introduction that the behaviour of the root tip zone in particular, under conditions of low oxygen tension, is likely to be of crucial importance in determining the ability of a plant species to survive on an anaerobic soil. ARMSTRONG (1964, 1971) has shown that the permeability of the root wall in certain wetland species declines rapidly in the subapical regions of the root. Towards the root tip zone, however, the wall is highly permeable to oxygen (ARMSTRONG, 1967), so that any leakage of oxygen into the surrounding medium as a result of oxygen diffusion will tend to be greater near the apical region of the root. This effect was also observed by PHILIPSON and COUTTS (1980) in Pinus contorta. Thus, in many flood-tolerant species growing in waterlogged soils, the root tip may be surrounded by a small region of aerobic soil maintained by oxygen leakage from those regions of the root immediately behind the apex. Even if it is accepted that the direct supply of oxygen to the root tip from internal aeration is relatively small (LUXMOORE and STOLZY, 1972b), the indirect supply as a result of oxygen leakage into the soil may be much higher. Whether or not such a supply is adequate to maintain unrestricted aerobic respiration, however, will depend on the ability of the root tip to utilise oxygen available in the external medium.

Three main factors will affect the uptake of oxygen by the root tip zone. These are: a) the permeability of the root wall to oxygen; b) the diffusional impedance to oxygen movement within the root tissue; and c) the affinity of the respiring tissue for oxygen.

Experiments by ARMSTRONG (1967), GREENWOOD (1967) and LUXMOORE et al (1970) indicate the permeability of the apical root wall to be relatively high. GREENWOOD (1967), for example, found the wall resistance in mustard seedlings equivalent to a liquid diffusion

pathway of 12μm. ARMSTRONG and WRIGHT (1975) suggest that the high permeabilities obtained may be due to cytoplasmic streaming in the epidermal layers. The indications are, therefore, that there is a very low resistance to oxygen movement across the apical root epidermis.

Reports from in vitro experiments indicate there to be a high diffusional resistance to oxygen movement in the root tip. BERRY and NORRIS (1949) calculated the diffusion coefficient for oxygen to be approximately 7×10^{-6} cm^2 sec^{-1} in the apical 5mm of excised onion root tips at 15°C. They point out, however, that such calculated diffusion coefficients must be thought of as an average of a number of separate coefficients within the root tissue. Nevertheless, after consideration of the possible sources of error, they consider the calculated coefficient to be an accurate estimate of the true rate of penetration of oxygen into the tissue. Such estimates would suggest that diffusion is a strongly limiting factor in the aerobic respiratory rate in root tissue. It has been pointed out in the General Introduction, however, that there has been recent criticism of such in vitro estimates on the grounds that flooding of the intercellular air spaces may lead to a higher diffusional impedance than actually exists in the intact root.

The cytochrome enzymes are known to have an extremely high affinity for oxygen, their activity remaining undiminished even at very low oxygen concentrations (WINZLER, 1941; YOCUM and HACKETT, 1957). There has been a certain amount of interest recently, however, in the existence of cyanide-resistant respiratory pathways, a subject reviewed by SOLOMOS (1977). Such 'alternate' oxidative pathways appear to be widespread in higher plants and microorganisms (HENRY and NYNS, 1975), though their significance is not yet clear. Although the nature of the alternate oxidase is not yet known, its affinity for oxygen is known to be lower than that of cytochrome oxidase,

perhaps by as much as ten times (SOLOMOS, 1977). Clearly, therefore, a root tissue in which a high proportion of respiratory activity was due to the alternate pathway would show a higher dependence on the external oxygen concentration than one in which the cytochrome pathway was predominant. It appears unlikely, however, that the alternate pathway is coupled with oxidative phosphorylation (SOLOMOS,1977), so that a reduction in the activity of this pathway due to low oxygen concentration might not affect the energy-producing reactions within the cell. Moreover, LAMBERS and SMAKMAN (1978) reported that there was no correlation between possession of the alternate pathway and flooding tolerance in plants of the Senecio genus. LAMBERS and STEINGROVER (1978), however, showed that the activity of the alternate oxidative pathway was considerably reduced when plants of Senecio aquaticus were grown in culture solutions of low oxygen tension.

It is clear from the foregoing discussion that the factors which will be of the greatest importance in determining the respiratory activity of the root tip zone under a low oxygen tension are the permeability of the tissue to oxygen and the nature of the respiratory pathways present. In the following investigation, oxygen uptake rates have been measured over a range of oxygen concentrations in excised root tips from a wide variety of plant species. The results are interpreted in relation to the known ability of the species used to withstand waterlogging and also to the conditions under which the samples were grown. A mathematical model has also been developed in order to predict the respiratory behaviour of a hypothetical root tip whose respiratory and physical properties are clearly defined. Predictions from this model are compared with the experimental results in an attempt to determine the changes which occur in the root tip zone to facilitate survival in waterlogged soils. A short investigation was also carried out into cyanide-resistant respiration in the Senecio genus to assist in estimating the relative contribution of the alternate

pathway to the overall behaviour of the root tip.

1.2 MATERIALS AND METHODS

a) Plant Material

Initially, samples were obtained by carefully digging up plants from various locations and storing them in plastic bags before excising the root apices. In such cases, oxygen uptake measurements were always made within 24 hours of the plant being dug up.

Subsequently, a selection of species were collected from the wild and grown in the glasshouse for several weeks before being harvested. Each sample was grown either under a 'flooded' or an 'unflooded' regime. In the 'unflooded' regime, the plants were grown in a freely drained sand culture under mercury lamps (light intensity 8 - 10,000 lux) and watered once weekly with one-fifth strength modified Hoagland's solution adjusted to a pH of 6.0 (see Appendix I). In the flooded regime, the plants were first grown under the same conditions as the unflooded plants for two weeks. After this initial period, the sand culture was kept fully waterlogged with the same Hoagland's solution, which was changed once a month. Transpiration losses were made up twice a week with distilled water.

Table 1 summarises the growth conditions and the species used in each of the oxygen uptake experiments.

Measurements of cyanide-resistant respiration were carried out on 6-month-old seedlings of *Senecio jacobaea* and *S. aquaticus*. These were grown in the glasshouse in an unflooded sand culture exactly as described above.

b) Measurement of Oxygen Uptake

All oxygen uptake measurements were carried out *in vitro* using

SPECIES	GROWTH CONDITIONS	FIGURE
Ammophila arenaria	Glasshouse, unflooded	19
	Glasshouse, flooded	31
	Glasshouse, unflooded	30
	Glasshouse, flooded	38
	Glasshouse, unflooded	39
Brachypodium sylvaticum	Glasshouse, unflooded	24
Caltha palustris	Glasshouse, unflooded	11
Chamaenerion angustifolium	Wasteground, unflooded	12
	Wasteground, unflooded	13
Deschampsia caespitosa	Glasshouse, unflooded	23
	Glasshouse, unflooded	37
	Glasshouse, flooded	36
Digitalis purpurea	Roadside ditch, waterlogged	17
Glyceria fluitans	Glasshouse, unflooded	20
	Glasshouse, unflooded	27
	Glasshouse, flooded	26
Juncus effusus	Waterlogged field	15
Oryza sativa	Glasshouse, unflooded	18
Phalaris arundinacea	Glasshouse, unflooded	22
	Glasshouse, flooded	32/34
	Glasshouse, unflooded	33/35
Plantago lanceolata	Glasshouse, unflooded	25
Ranunculus repens	Roadside, unflooded	14
Senecio jacobaea	Forest track, unflooded	16
	Glasshouse, unflooded	21
	Glasshouse, unflooded	29
	Glasshouse, flooded	28

Table 1.1 - Growth Conditions and Species used in Oxygen Uptake Measurements.

This table shows the species used in each oxygen uptake experiment, and the conditions under which they were grown or collected. Samples bracketed together were grown together and harvested on the same date. The right-hand column lists the corresponding graphs of oxygen uptake *versus* oxygen concentration.

excised roots in a Rank membrane-electrode assembly (Fig 1.1). The oxygen electrode was set up according to the maker's instructions as follows: The platinum electrode, bathed in a solution of saturated KCl, is separated from the sample chamber by a thin, oxygen permeable membrane made from dialysis tubing. The electrode was polarised with a voltage of 0.6V using the control box supplied with the electrode, and the current through the electrode was monitored by means of a chart recorder. At the polarising voltage used, the current which flows through the electrode is directly proportional to the concentration of oxygen in the sample chamber solution, and this was checked by filling the sample chamber with solutions of known oxygen concentration.

The temperature in the sample chamber was kept constant by circulating water from a water bath through the water-jacket built into the electrode assembly. In all experiments, the temperature was kept at 20°C ± 0.5°C.

In the sample chamber, a small glass-coated magnetic stirrer rotating at approximately 500 r.p.m. kept the medium stirred and ensured that diffusion of oxygen across the membrane was not limiting the readings obtained. The stopper for the sample chamber has a small capillary tube drilled up the centre, designed for the addition of small liquid samples without disturbing the experiment. The stopper was inserted slowly and pushed down until the meniscus of the buffer in the sample chamber lay about halfway up this capillary tube, taking care that no air bubbles were trapped beneath the stopper. Because of the small diameter of the capillary, any exchange of oxygen between the buffer and the atmosphere was negligible.

The buffer used in the sample chamber was initially 0.1M Sodium Phosphate buffer, pH 6.0 , containing 2% sucrose. On all experiments conducted after 28/2/79, however, 0.1M Potassium Phosphate buffer of the same pH and also containing 2% sucrose was used.

At the start of each experiment, the plant sample was removed from its pot and the root system gently washed in a basin of water to

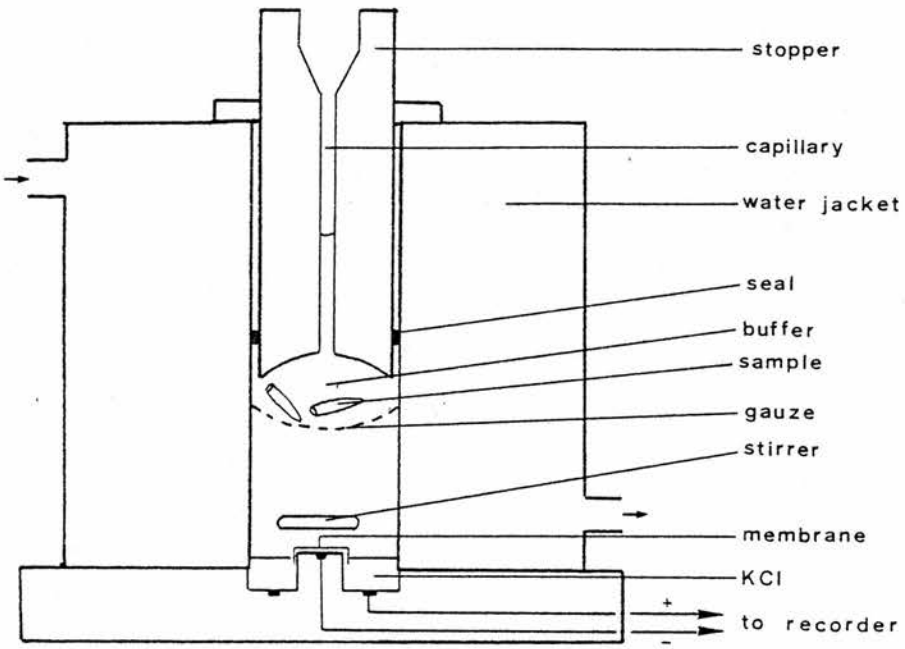

Fig 1.1 - Diagram of oxygen electrode assembly used to measure rates of oxygen uptake in excised root tips.

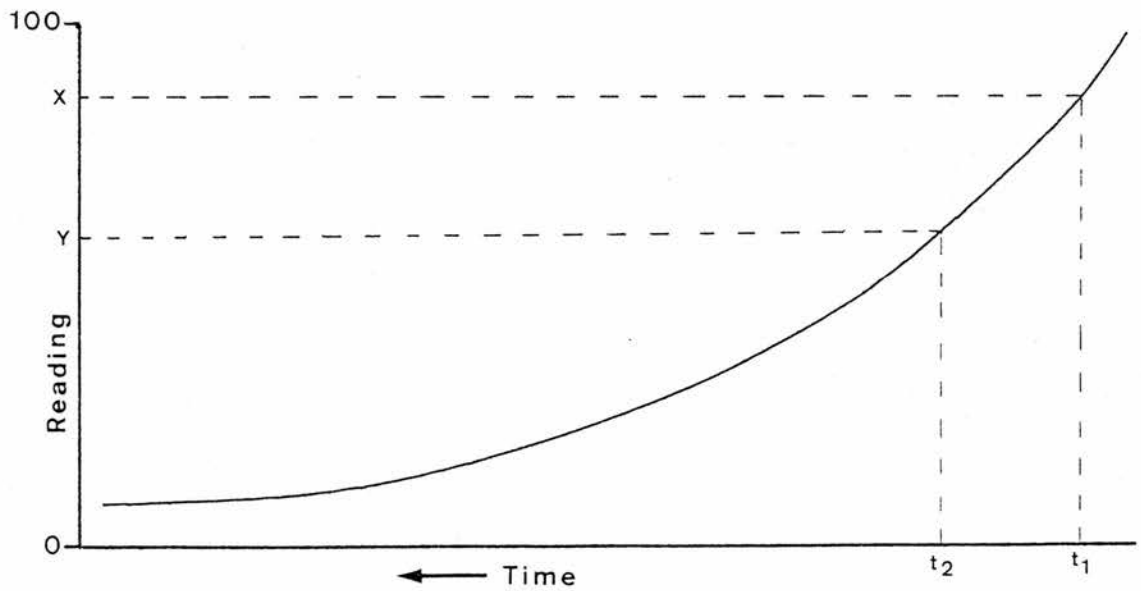

Fig 1.2 - Typical response curve obtained on the chart recorder during the course of oxygen uptake measurements.

remove sufficient soil to expose the required amount of root. The apical 1 cm from between six and ten main roots (depending on the size of the roots) was carefully removed, washed in distilled water and then placed in a 0.02% solution of Mercuric Chloride for several minutes for surface sterilization.

While the roots were in the Mercuric Chloride, the sample chamber of the oxygen electrode was filled with 3ml buffer and the stirrer activated, while the lid was off. This had the effect of saturating the buffer with air, and when a steady reading was obtained from the electrode, the recorder was set at its maximum reading of 100. Thus, a reading on the recorder of 100 was taken as the reading for air-saturated buffer, containing oxygen at a partial pressure of 0.21 atm (9ppm).

With the buffer air-saturated, the root tips were removed from the mercuric chloride solution, washed in distilled water, and then placed in the sample chamber, supported on a piece of fine-mesh aluminium gauze to prevent them from fouling the stirrer. The stopper was then placed over the buffer as already described.

By means of the chart recorder, the change in oxygen concentration with time as a result of root respiration could then be followed until a point was reached where oxygen uptake by the roots ceased. A typical response curve is shown in figure 1.2. When respiration had ceased (i.e. there was no further change in oxygen concentration with time), the root tips were removed and a few crystals of sodium dithionite were added to the buffer in the sample chamber. This reduced all the remaining oxygen and the resulting reading on the chart recorder was taken as the reading for completely deoxygenated buffer. Ideally it should be zero, but there is always a slight leakage of current across the electrode. Finally, the root tips were placed in an oven at 95°C overnight to obtain their dry weight.

From a curve such as that shown in figure 1.2, the rate of oxygen uptake by the root tips can be calculated at all oxygen concentrations

between that of air-saturated buffer and deoxygenated buffer. For example (fig 1.2), if X is the reading obtained on the chart recorder at time t1 minutes, and Y is the reading obtained at time t2 minutes, then the rate of oxygen uptake between points X and Y is given by the formula:

$$Q = \frac{(X-Y) \times A \times B \times 60}{(100-Z) \times 32 \times (t2-t1) \times D} \quad \text{umoles } O_2/\text{g dry weight/hour}$$

where:

A = volume (ml) of buffer in the sample chamber (= 3ml)
B = solubility of O_2 in water at 20 C (= 9μg/ml)
Z = recorder reading corresponding to deoxygenated buffer
D = dry weight (g) of the root tips

The oxygen concentration in the buffer corresponding to this rate of uptake would be taken as the average concentration between readings X and Y, given by:

$$(O_2) = \frac{((X + Y) - 2Z) \times B}{(200 - 2Z) \times 32} \quad \text{mM}$$

Strictly speaking, these formulae are only accurate for situations in which the change in oxygen concentration with time shows a linear response. However, by making (t2-t1) small, the errors involved in applying these formulae to a non-linear response are minimized.

In some later experiments, this standard method was slightly modified in order to speed up the experiment. The electrode was prepared and calibrated as already described, and the roots placed in the sample chamber. The initial rate of uptake was determined, and then the oxygen concentration in the sample chamber was lowered rapidly, by about 10%, by introducing a small bubble of nitrogen into the sample chamber. Once the desired drop in oxygen concentration was obtained, the bubble was expelled and the rate of oxygen uptake at the new oxygen concentration determined. A typical response from the recorder chart is shown in figure 1.3. From points A to B, the initial rate of oxygen uptake was determined using the previous formula.

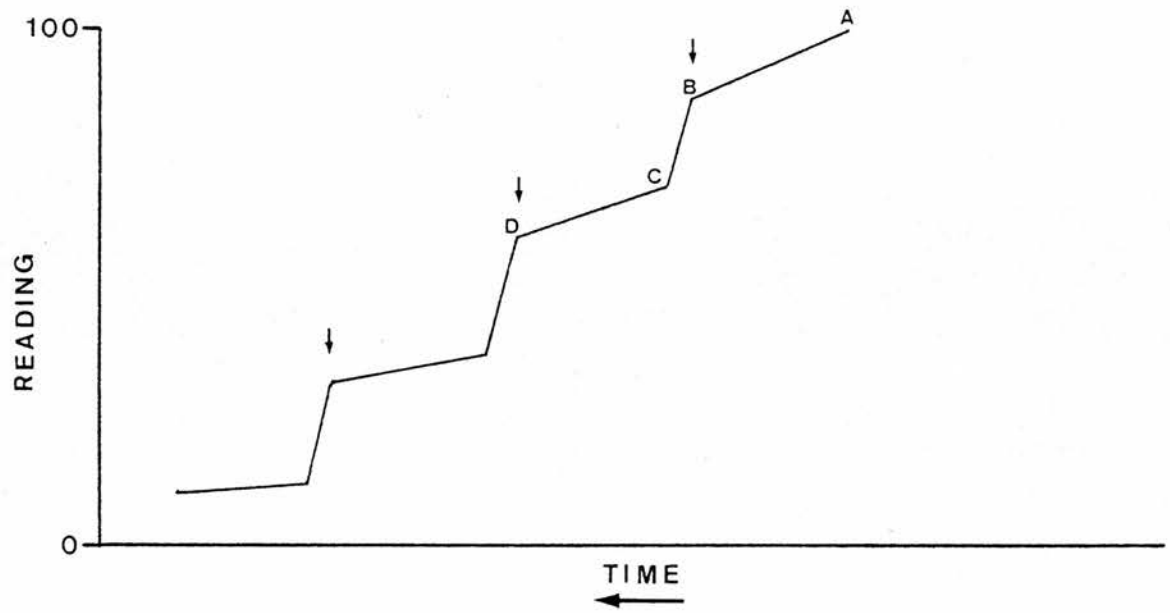

Fig 1.3 - Response curve obtained on the chart recorder with nitrogen bubbles introduced into the sample chamber at intervals (arrows) (see text).

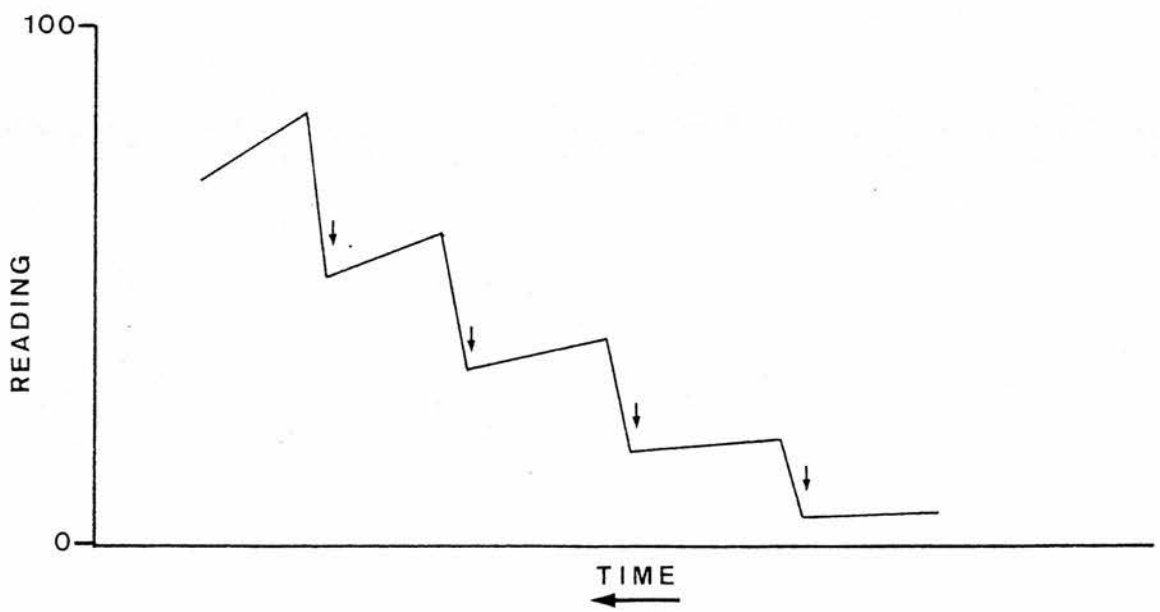

Fig 1.4 - Response curve obtained on the chart recorder with air bubbles introduced into the sample chamber at intervals (arrows) (see text).

Between points B and C, the oxygen concentration was lowered by introducing the nitrogen bubble. The bubble was then expelled, and the rate of oxygen uptake at the new oxygen concentration determined between points C and D. This process was repeated until an oxygen concentration was reached at which respiration fell to zero.

Another variation, which was only employed in a few experiments, was to start the experiment with deoxygenated buffer, and gradually increase the oxygen concentration by introducing small air bubbles between determinations in a manner similar to that described above. A typical response from the recorder chart is shown in figure 1.4. Wherever this method was used, an appropriate indication is given along with the graph of oxygen uptake versus oxygen concentration.

The typical response of oxygen uptake to declining oxygen concentration is shown in figure 1.5. The hyperbolic shape of the graph, which will be discussed later, is quite characteristic, and analagous to the type of curve which is usually obtained when the rate of reaction for an enzyme is plotted against the substrate concentration. By analogy with enzyme kinetics, therefore, it is possible to calculate a value for the Michaelis Constant (Km) and for the maximum rate of oxygen uptake (Vmax). It must be emphasized, however, that the meaning of these values must be interpreted with care. Nevertheless, it was hoped that they would provide a convenient means of comparing the results from different species.

The usual method for calculating these values is to fit a regression line through a plot of 1/v against 1/s, where v = rate of reaction and s = substrate concentration. There are a number of objections to this method, however, not least being the fact that the most unreliable observations (those obtained at low substrate concentration) often have the greatest influence on the slope of the line (MARKUS et al, 1976). A more accurate method was therefore sought and the final choice was the direct linear plot procedure (EISENTHAL and CORNISH-BOWDEN, 1974).

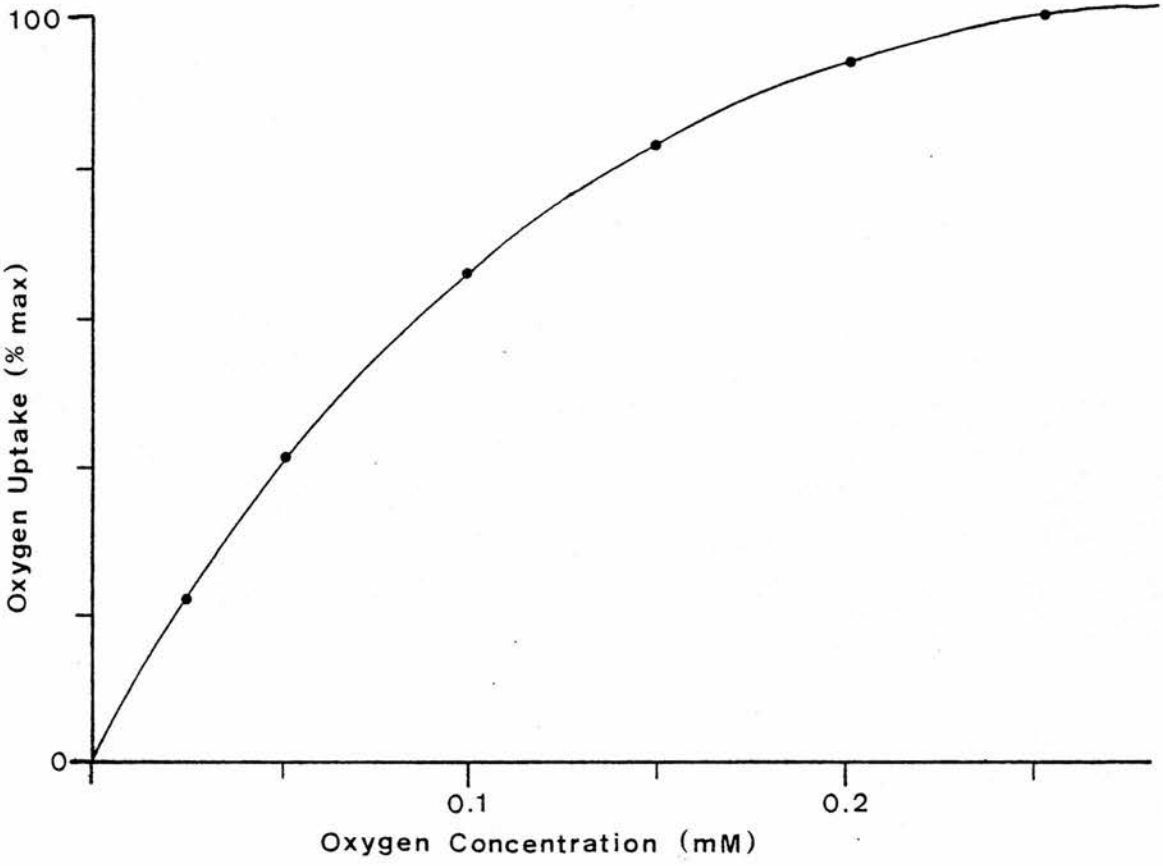

Fig 1.5 - Typical response of root oxygen uptake to declining oxygen concentration in the bathing medium.

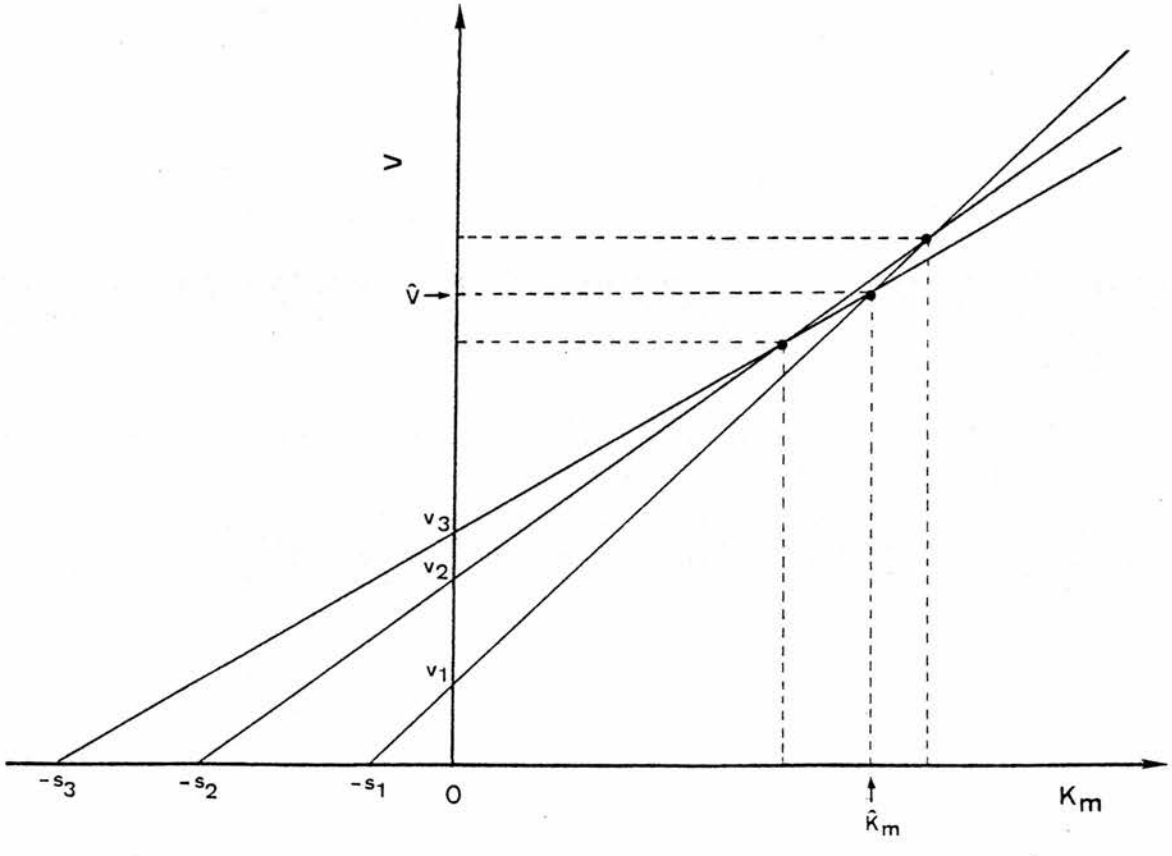

Fig 1.6 - Direct linear plot used to estimate Km and Vmax (see text).

This method was chosen because of its simplicity and reliability. For each observation (see fig 1.6), -s is marked off on the Km axis, v is marked off on the Vmax axis, and a line drawn through the two points. For n such observations, there will be $\frac{1}{2}n(n-1)$ intersections, and each intersection provides an estimate of Vmax and Km. The best estimate of Vmax or Km is provided by the median value of each series. For an even number of values, the mean of the middle two estimates is taken.

From each graph of oxygen uptake versus oxygen concentration, 9 points were selected at evenly spaced oxygen concentrations, and these 9 points were used to calculate Km and Vmax values. To save time, all calculations were carried out using a program for the Texas Instruments TI-59 Programmable Calculator and Printer (see Appendix II). In many cases, respiration fell to zero before the oxygen concentration fell to zero, and the procedure for calculating Km values was modified slightly. If Z is the oxygen concentration at which respiration (oxygen uptake) ceased, then each observation (Q = oxygen uptake, O = oxygen concentration) was entered as (Q, (O - Z)) for the purpose of calculation. The true Km was then given as: Km = Km (calculated) + Z.

c) Air Space Measurement

An exploratory experiment was carried out to determine to what extent the in vitro conditions used to measure oxygen uptake may lead to flooding of the intercellular air spaces. In this experiment, 1 cm lengths of root were cut from a rice plant which had previously been grown in unflooded sand culture, and divided into two samples. One sample was incubated in the oxygen electrode under identical conditions to those used in oxygen uptake measurements, for two hours, after which the root air space content was determined. The second sample, however, was not incubated in the oxygen electrode, and the air space content was measured immediately.

Determination of air space was carried out by weighing intact and homogenized roots in pycnometer bottles. The following formula is used to calculate percentage air space on a volume/volume basis:

$$\% \text{ air space} = \frac{c - b}{d - b + a} \times 100$$

where:
a = root fresh weight
b = weight of bottle + intact roots + water
c = weight of bottle + homogenized roots + water
d = weight of bottle + water
(the density of water is taken as $1 g/cm^3$)

d) Measurement of Cyanide-Resistant Respiration

It is well known that cytochrome oxidase is extremely sensitive to inhibition by cyanide. Recently, it has also been shown that the alternate oxidase can be inhibited by hydroxamic acids (SCHONBAUM et al, 1971). The appropriate use of both these inhibitors, therefore, provides a means of determining the relative contributions of the cytochrome and alternate oxidative pathways in plant tissues. The rate of oxygen uptake is measured before and after the addition of inhibitor, the difference between the two rates providing a measure of the degree of inhibition of respiration by the inhibitor.

Oxygen uptake measurements were carried out using a Rank Membrane Oxygen Electrode assembly, as described previously. The only difference in the use of the electrode was that the potassium phosphate buffer was adjusted to an alkaline pH (7.3) to avoid the liberation of poisonous HCN gas.

Root tips were harvested, sterilised and placed in the electrode in air-saturated buffer. During the course of each experiment, while inhibitors were being added, the buffer was periodically re-saturated with air to ensure that respiration was not being limited by lack of oxygen. The initial rate of oxygen uptake was measured, and then quantities of inhibitor were added and the effect on uptake was

noted. Since only the degree of inhibition was being investigated, the slope of the line on the recorder chart was taken as a direct measure of the rate of oxygen uptake, without calculating rates per dry weight of tissue. Figure 1.7 shows a typical response of a sample to the addition of inhibitor. The degree of inhibition caused by the addition of inhibitor is calculated from the following formula:

$$\% \text{ Inhibition} = \frac{(\frac{V1}{V2})\ S1 \quad - \quad S2}{(\frac{V1}{V2})\ S1} \quad x \quad 100$$

where:
V1 = original volume of buffer
V2 = volume of original buffer + inhibitor solution
S1 = slope of trace before addition of inhibitor
S2 = slope of trace after addition of inhibitor

Two inhibitors were used - namely potassium cyanide and salicyl hydroxamic acid (SHAM). A stock solution of KCN was prepared with a strength of 0.62M, dissolved in distilled water. Preparation of the SHAM solution was more difficult, as it is not readily soluble in aqueous solution. Initially, attempts were made to use SHAM dissolved in ethanol. This quickly proved unsatisfactory, however, since ethanol itself is toxic to plant root tissues and also appeared to have a direct physical effect on the electrode reading. A more satisfactory method was to add the SHAM to some of the buffer used in the electrode, and dissolve it by heating over a small bunsen flame. The SHAM remained dissolved in this solution for some hours after cooling, allowing adequate time to conduct the experiment. The final strength of stock solution prepared by this method was 0.1M.

The inhibitors were added to each sample, either together or singly, through the small capillary tube in the lid of the electrode in quantities of 0.1ml at a time. By measuring the degree of inhibition after each aliquot of inhibitor was added, it was possible to plot the percentage inhinition against concentration of inhibitor.

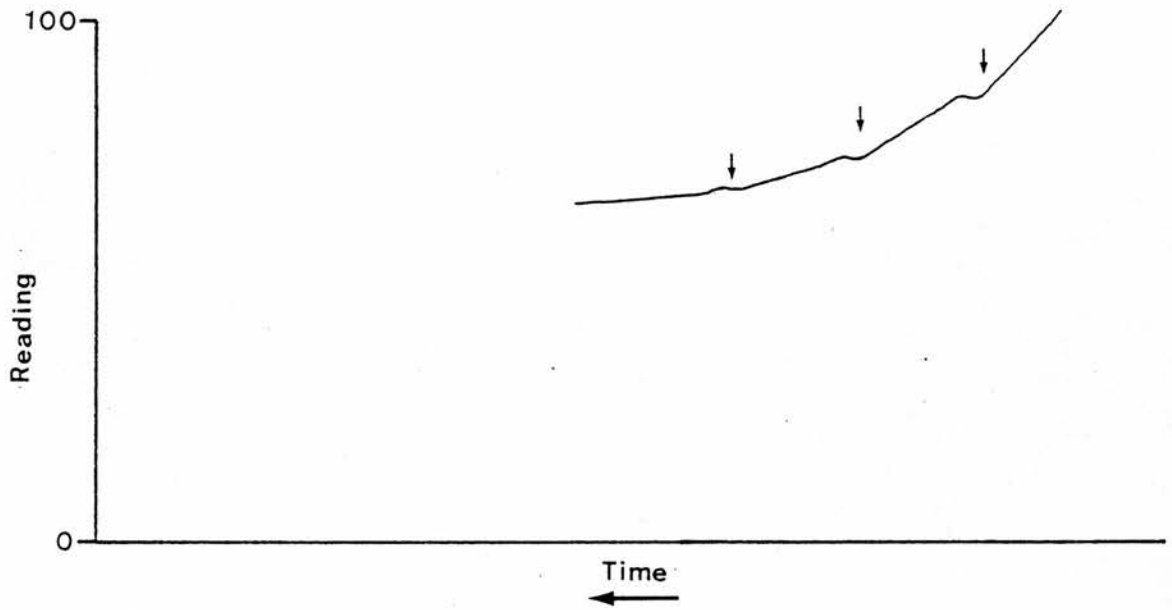

Fig 1.7 - Typical response curve obtained on the chart recorder with the addition of metabolic inhibitor at intervals (arrows).

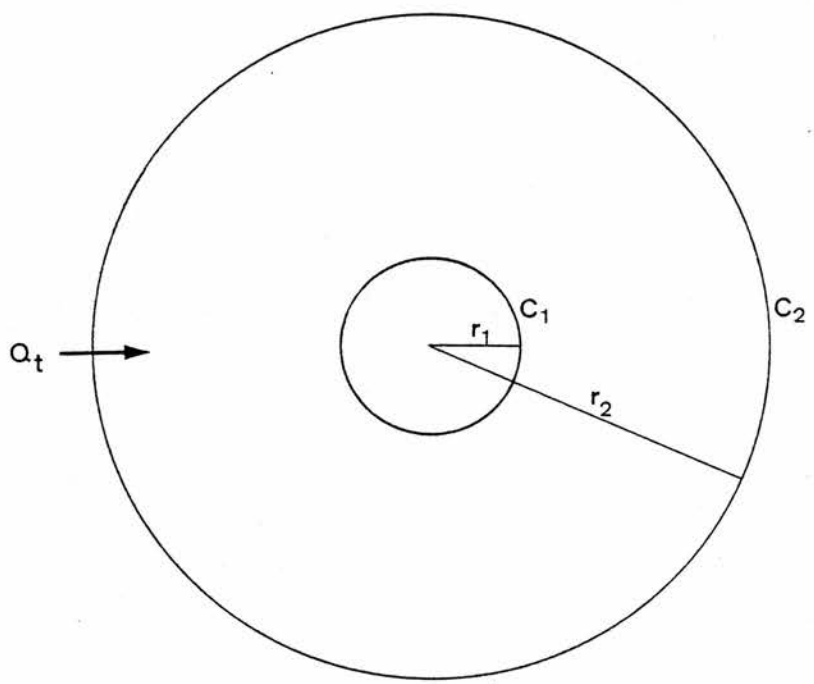

Fig 1.8 - Cross-section of a hollow cylinder with inner and outer radii r1 and r2 respectively (see text).

e) Root Tip Oxygen Uptake Model

A number of factors could be responsible, either singly or together, for the type of response shown in figure 1.5. For example, the decline in oxygen uptake with decreasing oxygen concentration might be due to a low affinity of root respiration for oxygen, or the movement of oxygen across the root might be limited by diffusion, or there may be more than one respiratory system present in the root. To assist in understanding the processes involved, therefore, it was decided to construct a simple model, using the Texas Instruments TI-59 Programmable Calculator and Printer. The program was designed to predict what the response of root oxygen uptake to hypoxia would be, given certain properties of the root and the respiratory systems.

The main assumptions made for this simple model are:

1) that the diffusional impedance to oxygen movement is uniform throughout the root;
2) that the potential maximum rate of oxygen uptake is also uniform throughout the root;
3) that the rate of oxygen uptake at any point within the root is dependent on the oxygen concentration according to the Michaelis-Menton relationship;
4) that there are no special boundary conditions at the root surface.

The model was intended to predict the behaviour of an excised root tip respiring in the experimental conditions of the oxygen electrode, described previously. Consequently, the more complex effects of rhizosphere respiration and oxygen diffusion through the soil are not considered. For simplicity, only the radial movement of oxygen across the root is considered, any movement of oxygen through the ends being disregarded.

Despite these limitations and assumptions, model predictions were in good agreement with the experimental results, indicating

that the model is a fairly accurate representation of the root tip.

Consider a hollow cylinder of inner and outer radii r1 and r2 respectively (fig 1.8). If the concentration of diffusing substance at surface r1 is C1, and that at surface r2 is C2, then at equilibrium the rate (Q) at which diffusing substance moves radially through unit length of cylinder is given by:

$$Q = \frac{2\pi D\ (C2-C1)}{Ln(r2/r1)} \qquad \text{(CRANK, 1956)} \qquad (1.1)$$

If C1 and Qt are known, then rearranging equation 1.1 gives:

$$C2 = \frac{Qt\ Ln(r2/r1)}{2\pi D} + C1 \qquad (1.2)$$

where D, the diffusion coefficient, is uniform throughout the cylinder.

If the cylinder in figure 1.8 is considered to be a section of root with a single respiring surface at r1, and an oxygen uptake of Q , then if the oxygen concentration at surface r1 is C1, the external oxygen concentration,C2, isgiven by equation 1.2, with due regard for units. Equation 1.2 forms the basis of the model. It should be noted that the hollow centre is merely a peculiarity resulting from the way in which the model is constructed. In the final model, this hollow centre is made very small so that the model closely approximates the structure of the living, solid root tip.

Figure 1.9 shows a hypothetical hollow root, this time divided into 3 concentric cylinders. The radius of the hollow centre is r1, and the three concentric cylinders have outer radii r2, r3 and r4. In this model root there are three respiring surfaces lying at radii r1, r2 and r3, with corresponding rates of oxygen uptake of Q1, Q2 and Q3 and oxygen concentrations of C1, C2 and C3. The oxygen concentration at the outer surface is C4. From equation 1.2 it follows that:

$$C2 = \frac{Q1\ Ln(r2/r1)}{2\pi D} + C1 \qquad (1.3)$$

$$C3 = \frac{(Q1+Q2)\ \mathrm{Ln}(r3/r2)}{2\pi D} + C2 \qquad (1.4)$$

$$C4 = \frac{(Q1+Q2+Q3)\ \mathrm{Ln}(r4/r3)}{2\pi D} + C3 \qquad (1.5)$$

If Q1 - Q3 are known, the external concentration of oxygen at equilibrium can be calculated for different values of C1. The total rate of oxygen uptake, per unit length, is given by:

$$QT = Q1 + Q2 + Q3 \qquad (1.6)$$

Obviously, no living root is divided into concentric cylinders as shown in figure 1.9. As a first approximation, however, it is possible to consider a root as being divided into a number of imaginary concentric 'cylinders'. If oxygen uptake is distributed uniformly throughout the root, then the oxygen uptake in any 'cylinder' can be considered to be proportional to the area of that cylinder. Thus, in the example above, if QT is the oxygen uptake, per unit length, of the whole root, then the oxygen uptake of the first cylinder, Q1, will be:

$$Q1 = \frac{(r2^2 - r1^2)}{(r4^2 - r1^2)}\ QT \qquad (1.7)$$

The rate of oxygen uptake is, however, concentration dependent. Assuming that this dependence follows the usual Michaelis-Menton relationship, with QT as the maximum rate of oxygen uptake per unit length of root and Km as the oxygen concentration at which uptake is $\frac{1}{2}$QT, then, if C1 is the oxygen concentration at r1, the equation becomes:

$$Q1 = \frac{\dfrac{(r2^2 - r1^2)}{(r4^2 - r1^2)}\ QT}{1 + \dfrac{Km}{C1}} \qquad (1.8)$$

Equation 1.8 can be used to calculate Q2 and Q3 in a similar fashion and these values can be substituted into equations 1.3 to 1.5 to give a more accurate model. The accuracy of the model is

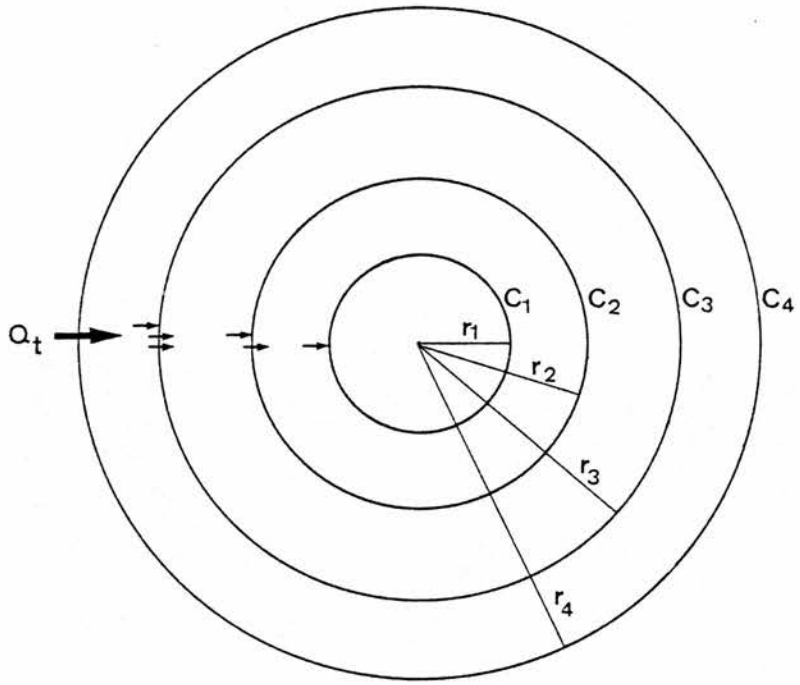

Fig 1.9 - Diagram of a hypothetical hollow root divided into three concentric cylinders (see text).

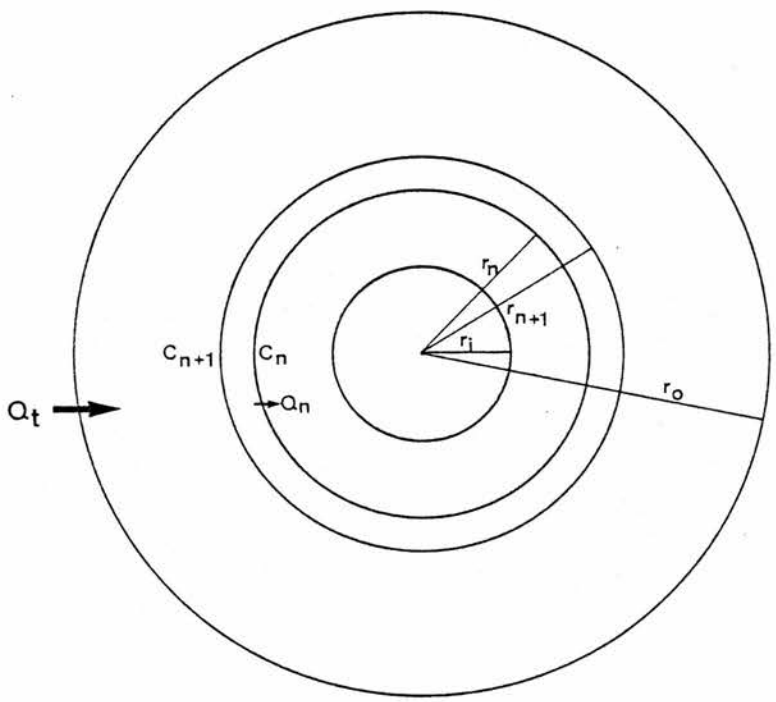

Fig 1.10 - Diagram of a hypothetical hollow root with inner and outer radii ri and ro respectively (see text).

increased still further by dividing the root into a larger number of concentric cylinders, and by making the radius of the hollow centre very small.

Figure 1.10 shows a hollow root with inner radius Ri and outer radius Ro. If Cn is the oxygen concentration at radius Rn, then C(n+1) is given by:

$$C(n+1) = \frac{(Qi + Q(i+1) \ldots + Qn)\ Ln(R(n+1)/Rn)}{2\pi D} + Cn \qquad (1.9)$$

where Qi - Qn are calculated according to equation 1.8

For any given Ci (the oxygen concentration at the centre of the root), the external oxygen concentration, Co, can be calculated by applying equation 1.9 to each succesive 'cylinder' within the root. The total rate of oxygen uptake at that external oxygen concentration is then given as:

$$QT = Qi + Q(i+1) \ldots\ldots + Q(o-1) \qquad (1.10)$$

By choosing a range of values for Ci, the rate of oxygen uptake at a range of external concentrations can be calculated, and hence the behaviour of the root tip can be predicted. The model can be made as accurate as desired (subject to rounding errors) by making the number of concentric cylinders progressively larger, and the radius of the hollow centre progressively smaller. In practice, it was found that dividing the root into 10 cylinders and making the inner radius 1/100th of the outer radius gave results which could be improved only marginally.

Full details of the program used on the calculator are given in Appendix III. Two further refinements were included in this program. Firstly, it was designed so that a critical oxygen concentration could be defined, below which oxygen uptake ceased completely and above which oxygen uptake followed the relationship with oxygen concentration already described. Secondly, provision was made for allowing two

respiratory systems, each with its own value for QT, Km and critical oxygen concentration.

All entries for the program were given in the following units:

Oxygen uptake:	µmoles/cm root/hour
Oxygen concentration:	mM
Diffusion coefficient:	cm^2/sec
Root Radius:	cm

1.3 RESULTS AND DISCUSSION

1) Summary of Results

The results of the experiments in which the rate of oxygen uptake was measured under conditions of hypoxia are shown graphically in figures 1.11 to 1.39 as rate of oxygen uptake (% maximum rate) against oxygen concentration (mM). Table 1.3 summarises the calculated Qmax and Km values for all species and treatments in this series of experiments.

Although not every experiment produced results which could be neatly categorised into a particular type of response, it is nonetheless possible to distinguish three major types of response.

The most common response, typified by Juncus effusus (fig 1.15) and Ranunculus repens (fig 1.14), was a hyperbolic curve, with the rate of oxygen uptake declining with decreasing oxygen concentration. In a few cases, however, a different response was obtained in which the rate of oxygen uptake remained constant until a very low oxygen concentration was reached, at which point the rate of uptake dropped sharply towards zero. A typical example of this type of response was obtained with Caltha palustris (fig 1.11). Finally, a few experiments revealed a peculiar response in which the rate of oxygen uptake declined initially but then remained constant over a short 'middle range' of oxygen concentration, before declining again as the oxygen concentration fell still further. This type of response could be seen with Senecio jacobaea (fig 1.28).

In addition to the shape of the response curve, the graphs also show quite clearly the oxygen concentrations at which oxygen uptake fell to zero. In most cases, this was at zero oxygen concentration, but in a number of examples, oxygen uptake fell to zero before the oxygen concentration within the electrode became zero.

When the results are taken as a whole, no clear correlation

SPECIES	TREATMENT	Km	Qmax	FIGURE
Ammophila arenaria	U	52.8	61.0	19
	F	35.8	258.7	31
	U	179.6	262.0	30
	F*	8.0	101.0	38
	U*	72.9	212.7	39
Brachypodium sylvaticum	U	54.6	549.1	24
Caltha palustris	U	2.5	165.4	11
Chamaenerion angustifolium	U	8.1	264.2	12
	U	14.0	85.7	13
Deschampsia caespitosa	U	4.2	58.4	23
	U*	73.0	460.0	37
	F*	18.6	148.0	36
Digitalis purpurea	F	48.3	288.9	17
Glyceria fluitans	U	41.7	144.6	20
	U	263.3	732.9	27
	F	94.6	309.3	26
Juncus effusus	F	34.9	215.1	15
Oryza sativa	U	24.1	232.4	18
Phalaris arundinacea	U	43.8	129.6	22
	F*	16.6	152.4	32/34
	U*	106.0	432.3	33/35
Plantago lanceolata	U	27.6	264.2	25
Ranunculus repens	U	34.6	342.0	14
Senecio jacobaea	U	89.6	311.2	16
	U	148.5	468.6	21
	U	62.7	432.9	29
	F	22.1	273.8	28

Table 1.3 - Qmax and Km values Calculated from Oxygen Uptake Measurements.

This table shows Km and Qmax values calculated by the Direct Linear Plot method (see text) from the oxygen uptake measurement experiments. Km values are given as % air saturation (100% = 0.268mM) and Qmax values as umoles O_2 /g dry weight /hour. The treatment in each case was either flooded (F) or unflooded (U) (see Table 1.1). An asterisk indicates that the calculated values are the mean of two replicates on the same plant.

KCN CONCENTRATION (mM)	% INHIBITION	% AIR SATURATION RANGE
a) Senecio aquaticus		
1.0	17	70-81
2.0	21	63-71
3.9	24	56-63
5.6	26	79-88
7.3	34	71-79
8.8	31	64-72
10.3	37	56-64
10.3	29	73-82
11.7	33	64-73
13.1	38	56-64
13.1	37	75-84
14.3	42	67-75
15.5	41	61-68
17.7	48	58-64
22.4	45	57-63
b) Senecio jacobaea		
2.0	9	74-80
3.9	6	69-75
5.6	8	65-70
7.3	15	61-67
8.9	14	58-62
10.3	17	56-60
11.7	17	52-57
13.1	25	49-52
13.1	24	73-90
14.3	31	67-73
15.5	38	64-68
16.6	38	61-67
17.7	36	58-62
18.7	38	54-60
19.7	52	52-56
20.7	50	46-53
20.7	46	87-92

Table 1.4 - Effect of Potassium Cyanide on oxygen uptake in two Senecio species.

This table shows the effect on oxygen uptake of the addition of KCN inhibitor. In the right-hand column is given the oxygen content of the solution at the time the inhibitor was added (100 % air saturation = 0.268mM).

SHAM CONCENTRATION (mM)	% INHIBITION	% AIR SATURATION RANGE
a) *Senecio aquaticus*		
3.2	8	69-83
6.3	20	59-69
9.1	28	50-59
11.7	35	42-50
11.7	35	81-90
14.3	40	74-81
16.7	53	70-74
21.1	50	65-70
25	55	60-65
28.6	62	56-60
b) *Senecio jacobaea*		
2.0	29	89-98
3.9	57	64-79
3.9	50	78-85
5.6	53	69-78
7.3	71	61-69

Table 1.5 - Effect of S.H.A.M. on Oxygen Uptake in two Senecio species.

This table shows the effect on oxygen uptake of the addition of SHAM inhibitor. In the right-hand column is given the oxygen content of the solution at the time the inhibitor was added (100% air saturation = 0.268mM).

emerges which can distinguish flooded plants from unflooded ones or flood-tolerant species from flood-sensitive species. However, very striking differences do emerge from those particular experiments in which each species was grown, in the glasshouse, under both flooded and unflooded conditions at the same time and under the same conditions (figs 1.26 - 1.39). In these 'paired' experiments, the unflooded plants showed a rapid decline in oxygen uptake with declining oxygen concentrations. In the flooded plants, however, the rate of oxygen uptake declined much more slowly initially, before dropping more sharply at low oxygen concentrations. This can be seen particularly well in the response of Ammophila arenaria (fig 1.38) in which the rate of oxygen uptake remained virtually constant until an oxygen concentration of about 0.14mM was reached. In complete contrast to this is the response of Phalaris arundinacea (fig 1.35) grown in an unflooded sand culture. These differences are also apparent from the calculated values of Qmax and Km (see Table 1.3). In all cases, Qmax and Km values were much higher in plants which had been grown unflooded.

The clear cut results from these experiments serve to illustrate the importance of good experimental technique, growing plants in controlled conditions in the glasshouse. Experiments on plants which had been collected from the wild were much more inconclusive. Indeed, the same species often produced markedly different results in each experiment (compare, for example, the responses of Chamaenerion angustifolium on two separate occasions, figures 1.12 and 1.13).

The results of the experiments in which the effects of two metabolic inhibitors were investigated are shown graphically in figures 1.41 and 1.42, and also in Tables 1.4 and 1.5. These experiments were of an exploratory nature and were not intended to furnish a large set of data for analysis. They reaffirm the results of LAMBERS and SMAKMAN (1978) in that in the two Senecio species studied there is a sizeable contribution of an alternate, cyanide-insensitive, respiratory chain in the root apex. The apparent discrepancy in the degree of

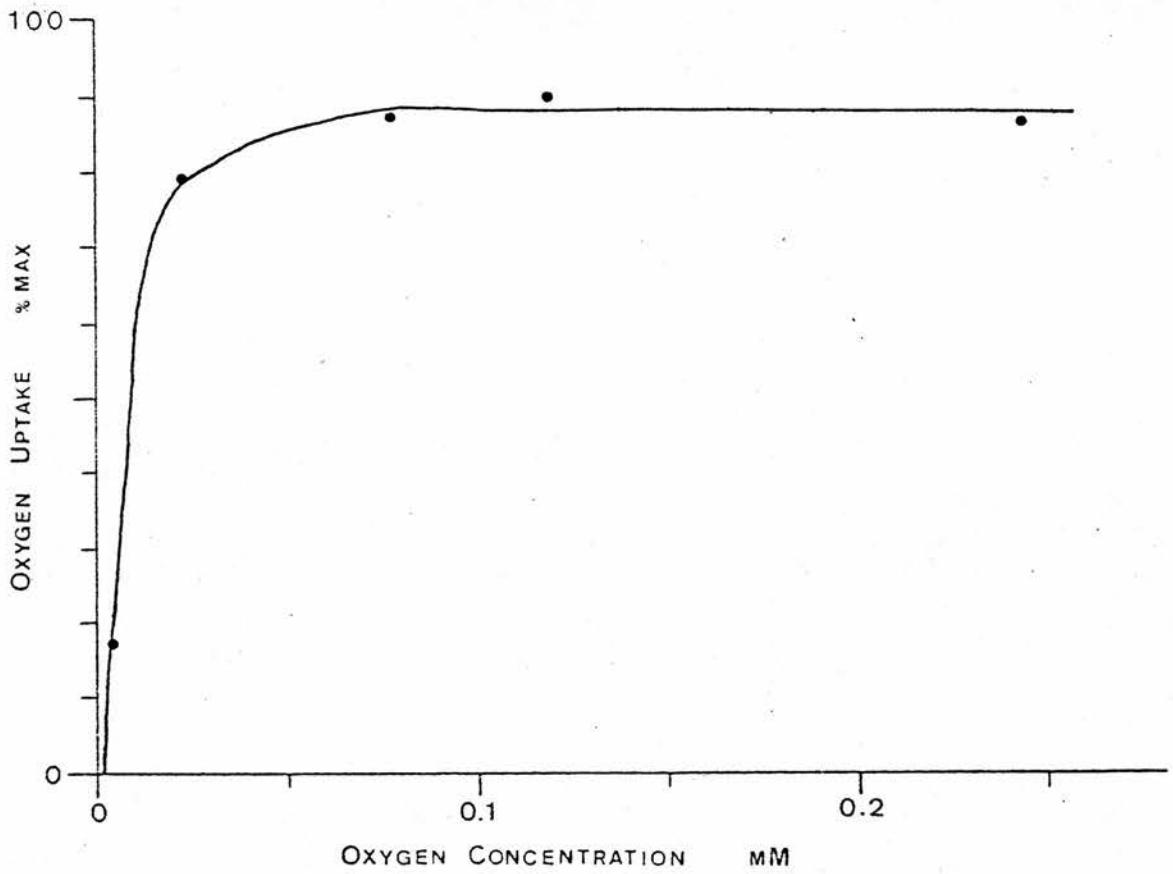

Fig 1.11 - Oxygen uptake vs oxygen concentration in Caltha palustris grown in unflooded sand culture.

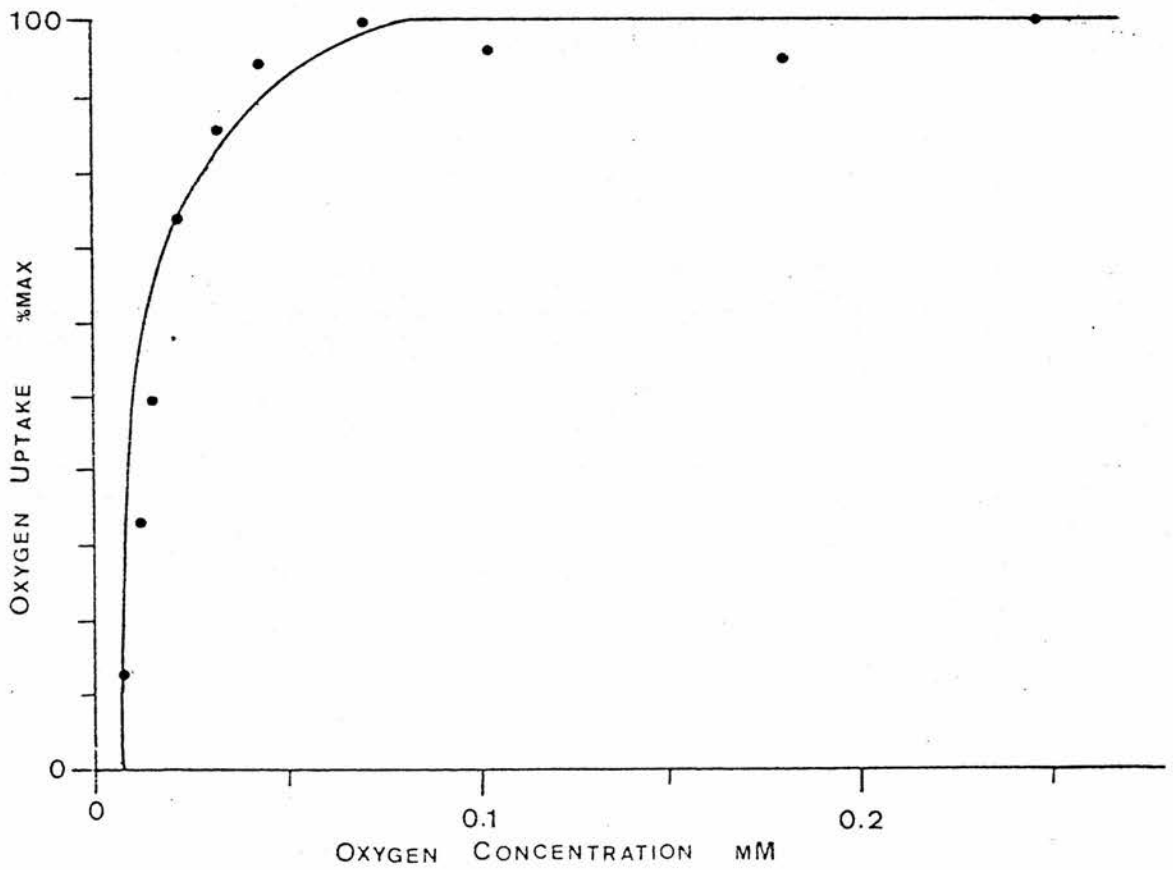

Fig 1.12 - Oxygen uptake vs oxygen concentration in Chamaenerion angustifolium collected from an unflooded site.

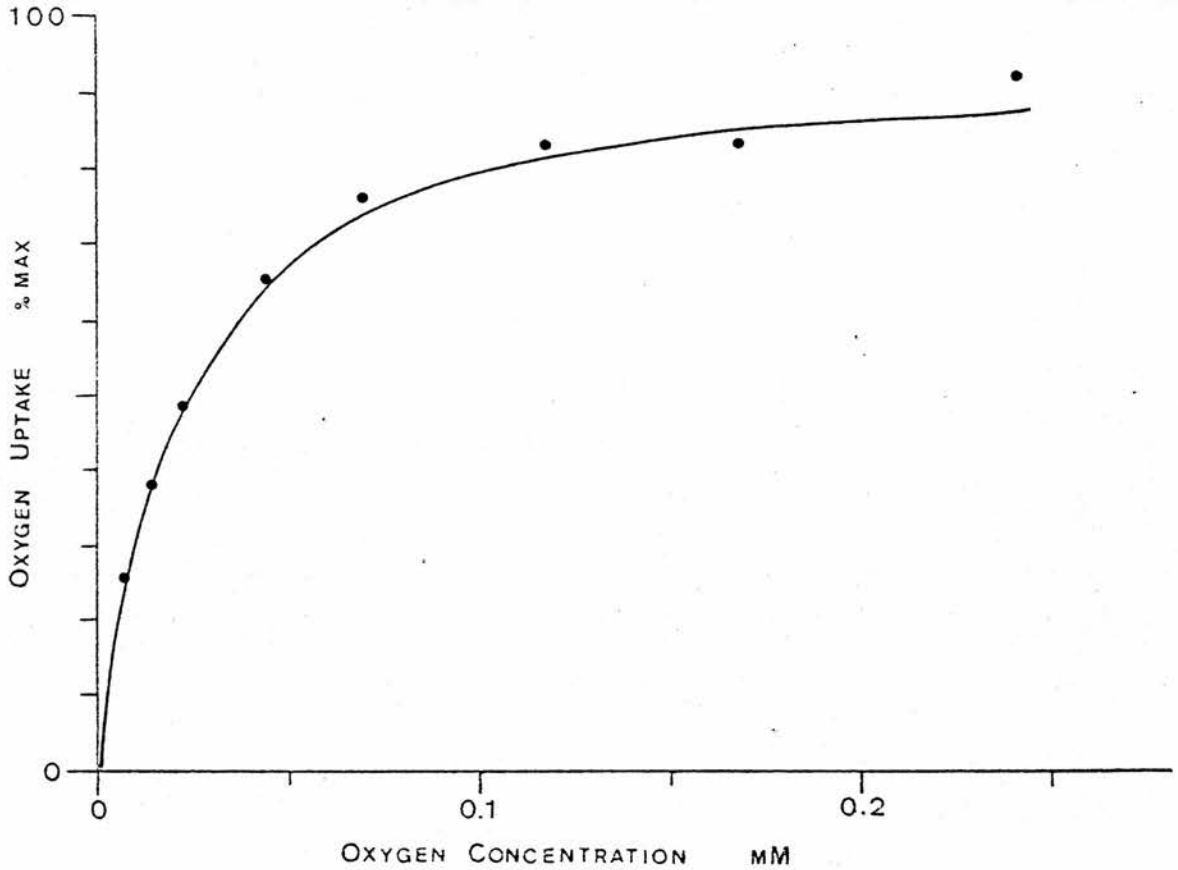

Fig 1.13 - Oxygen uptake vs oxygen concentration in Chamaenerion angustifolium collected from an unflooded site.

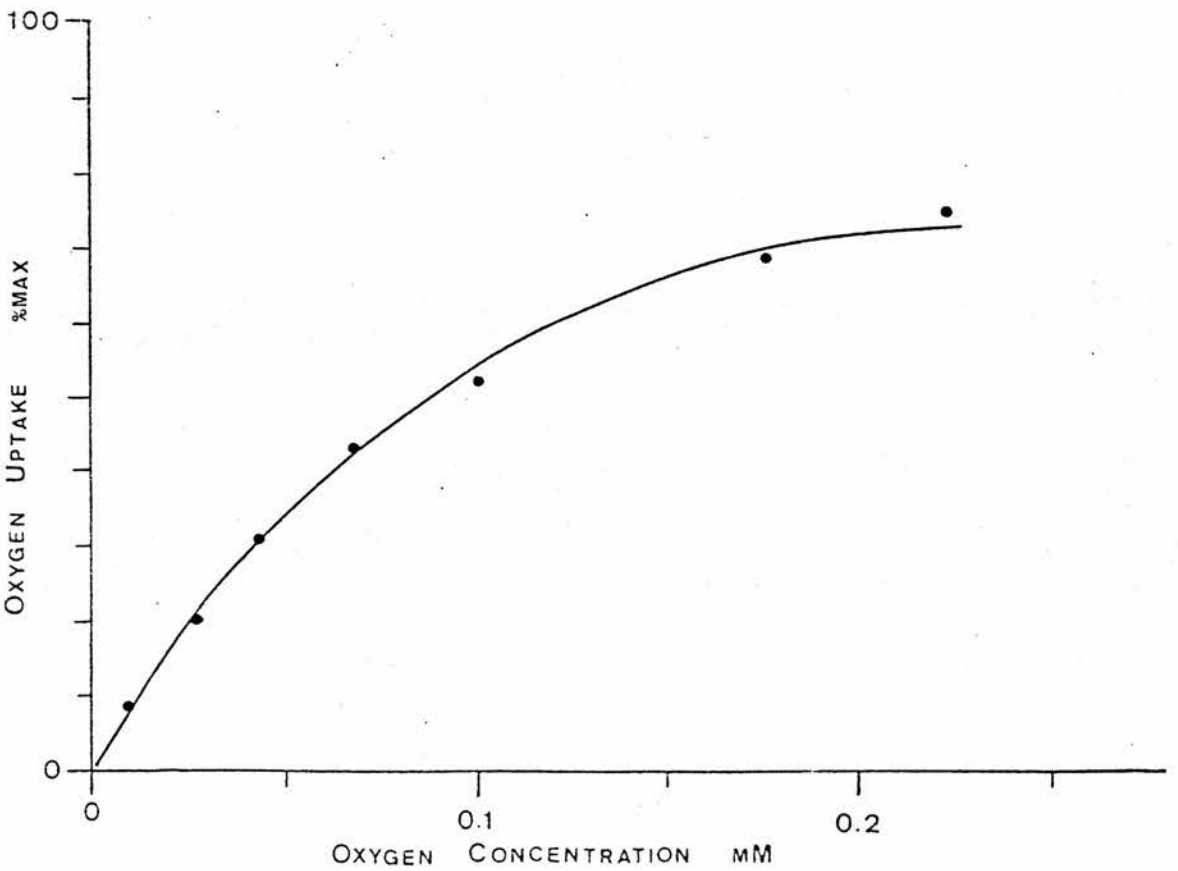

Fig 1.14 - Oxygen uptake vs oxygen concentration in Ranunculus repens collected from an unflooded site.

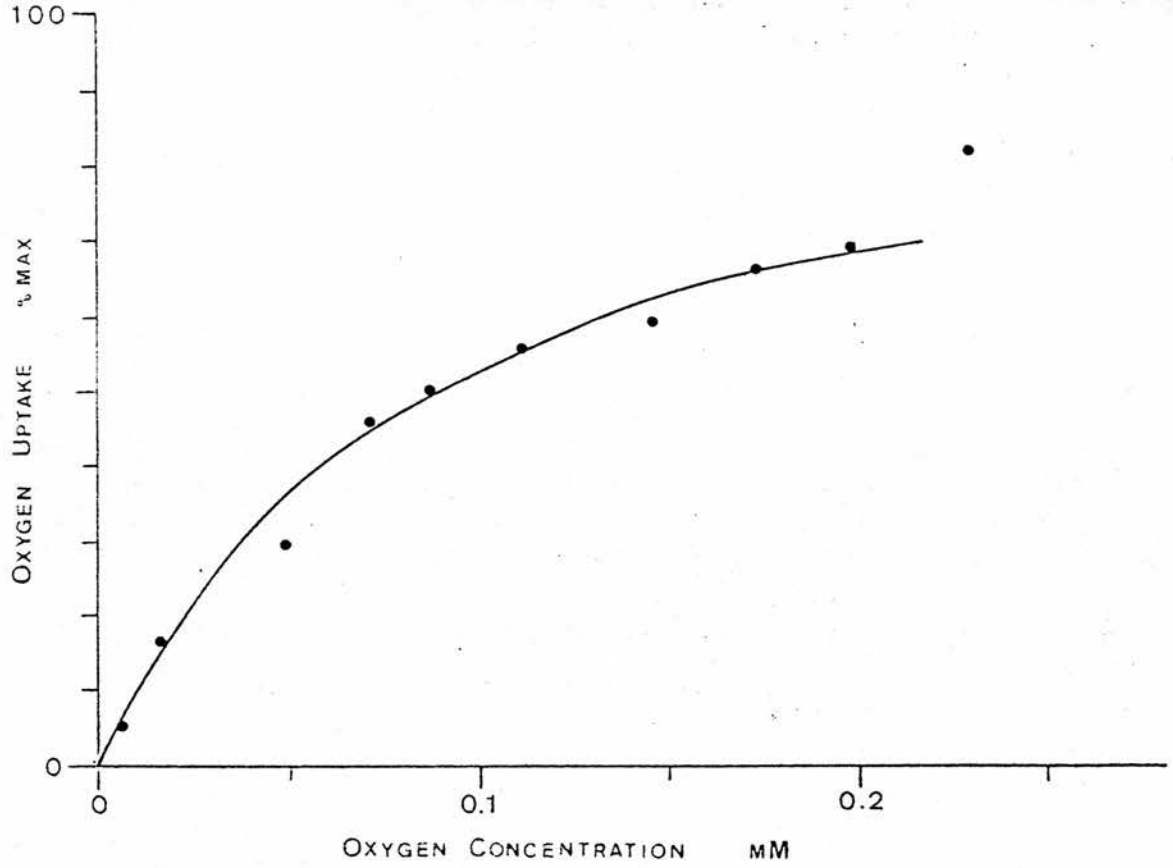

Fig 1.15 - Oxygen uptake vs oxygen concentration in Juncus effusus collected from a flooded site.

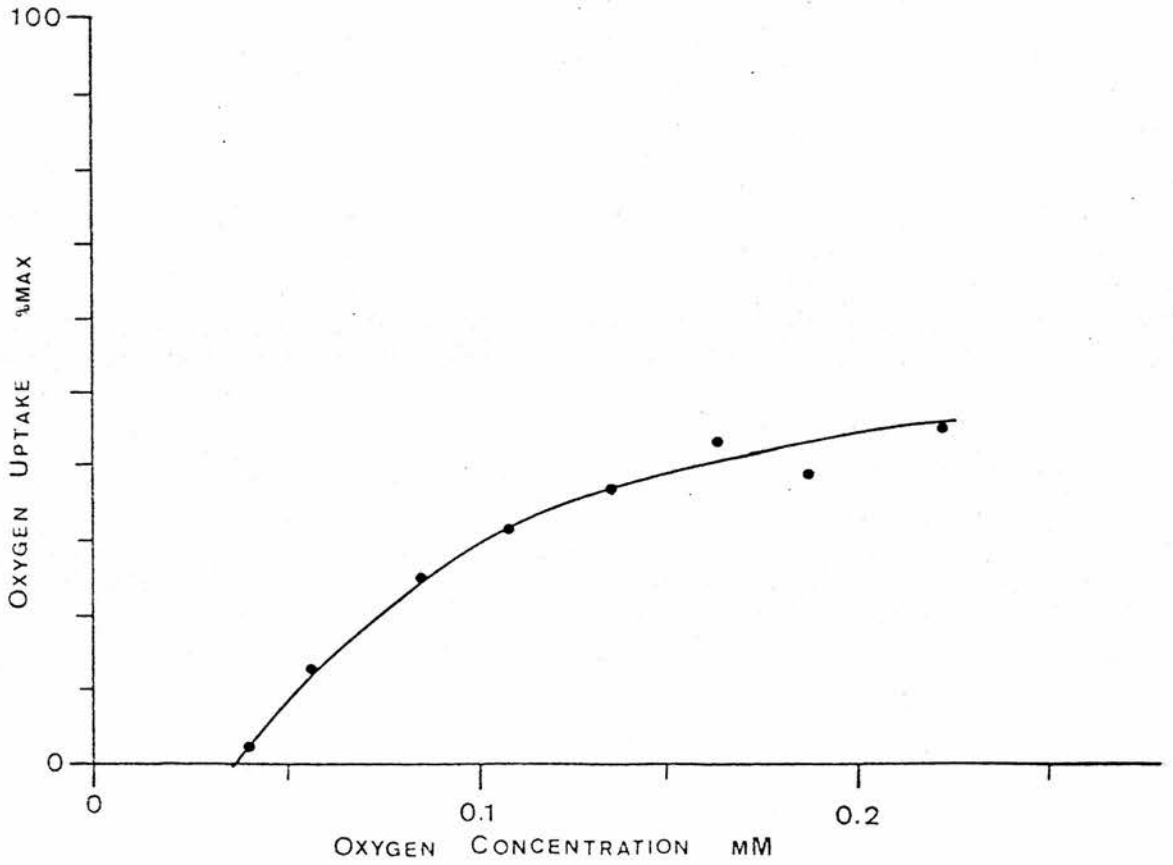

Fig 1.16 - Oxygen uptake vs oxygen concentration in Senecio jacobaea collected from an unflooded site.

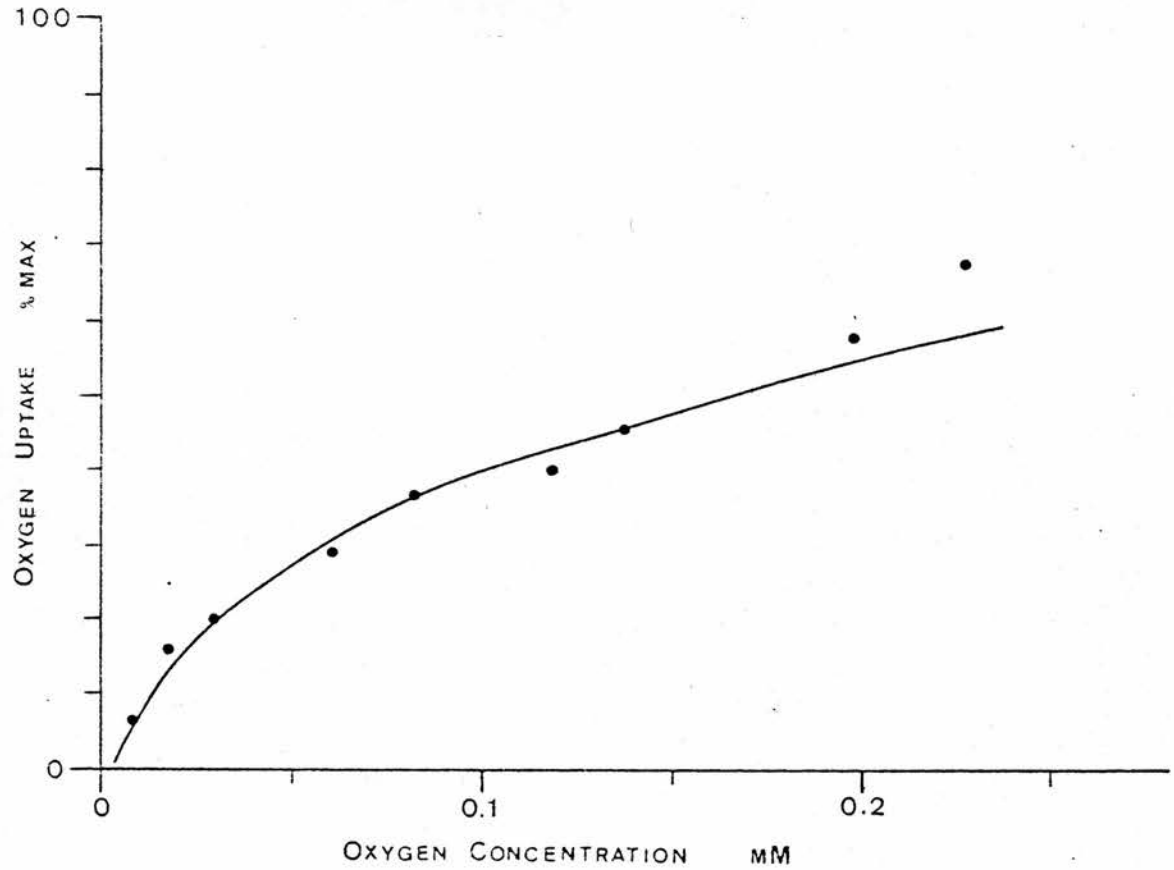

Fig 1.17 - Oxygen uptake vs oxygen concentration in Digitalis purpurea collected from a flooded site.

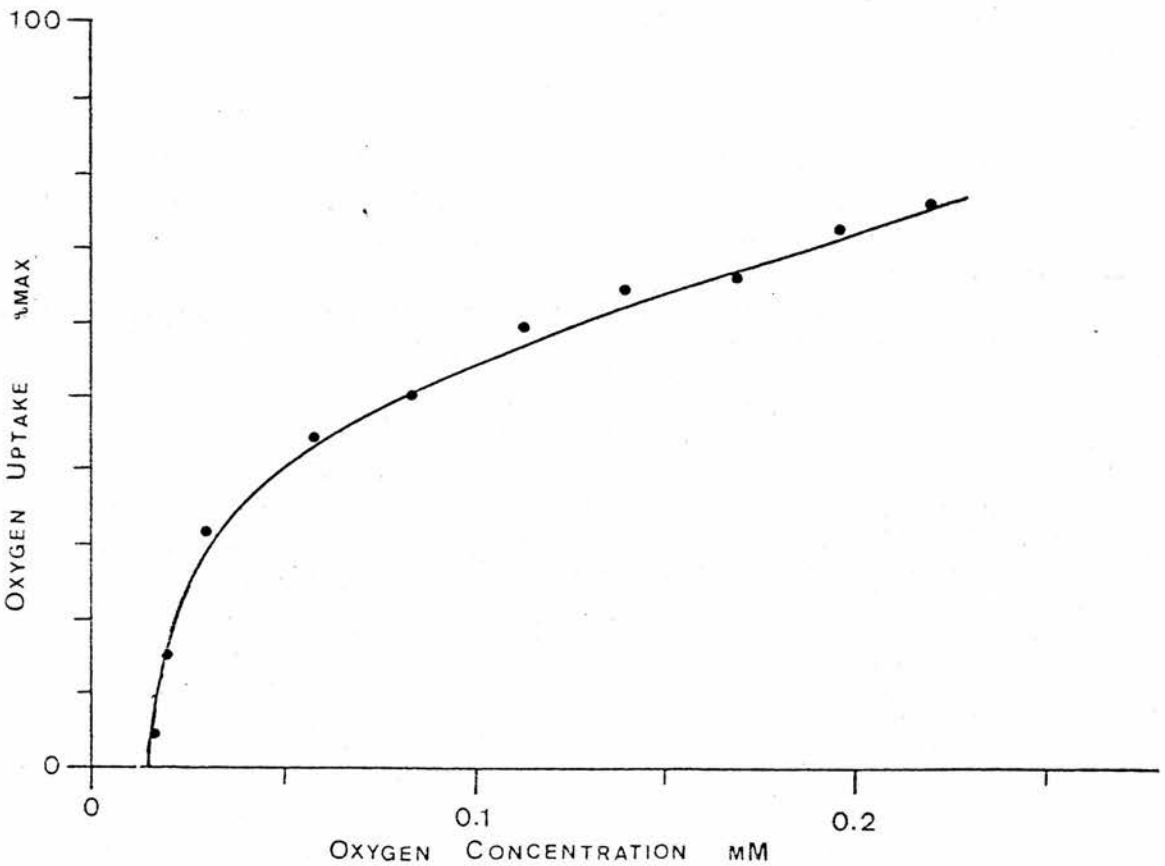

Fig 1.18 - Oxygen uptake vs oxygen concentration in Oryza sativa grown in unflooded sand culture.

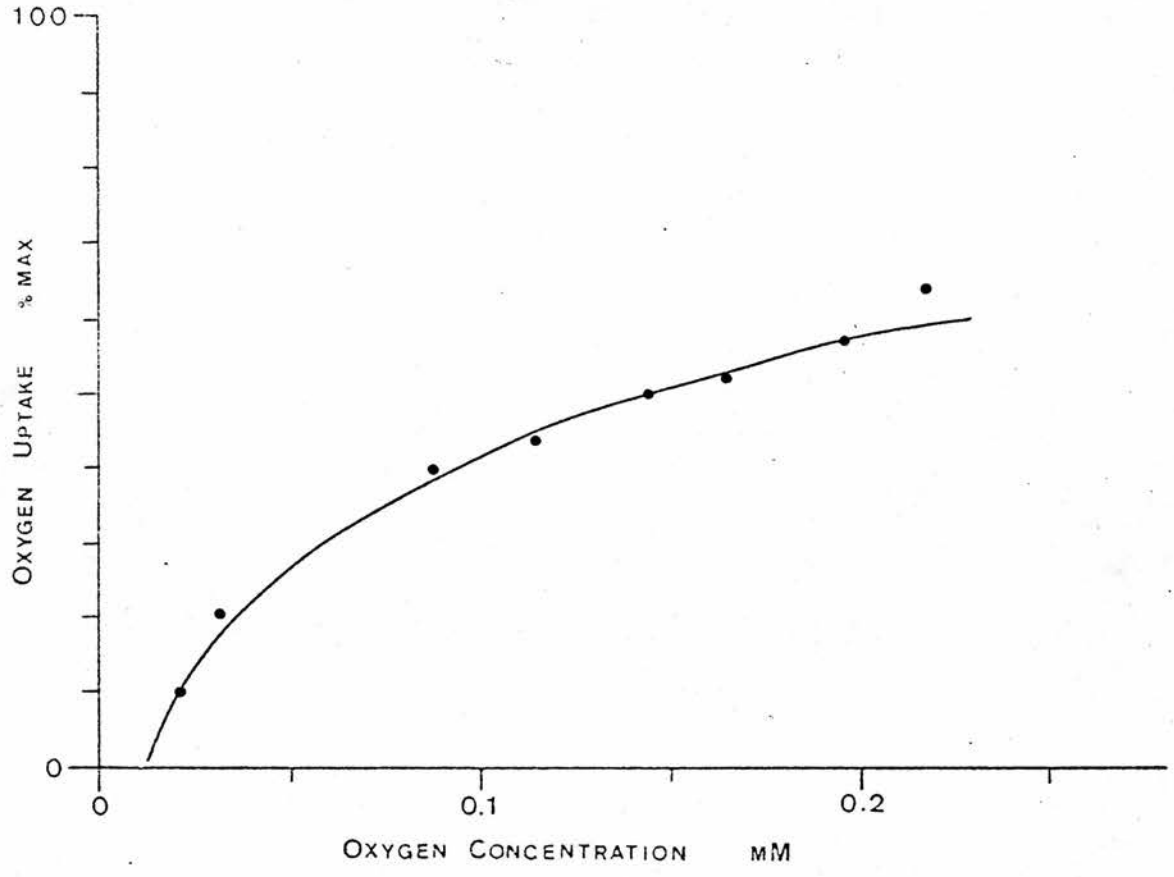

Fig 1.19 - Oxygen uptake vs oxygen concentration in Ammophila arenaria grown in unflooded sand culture.

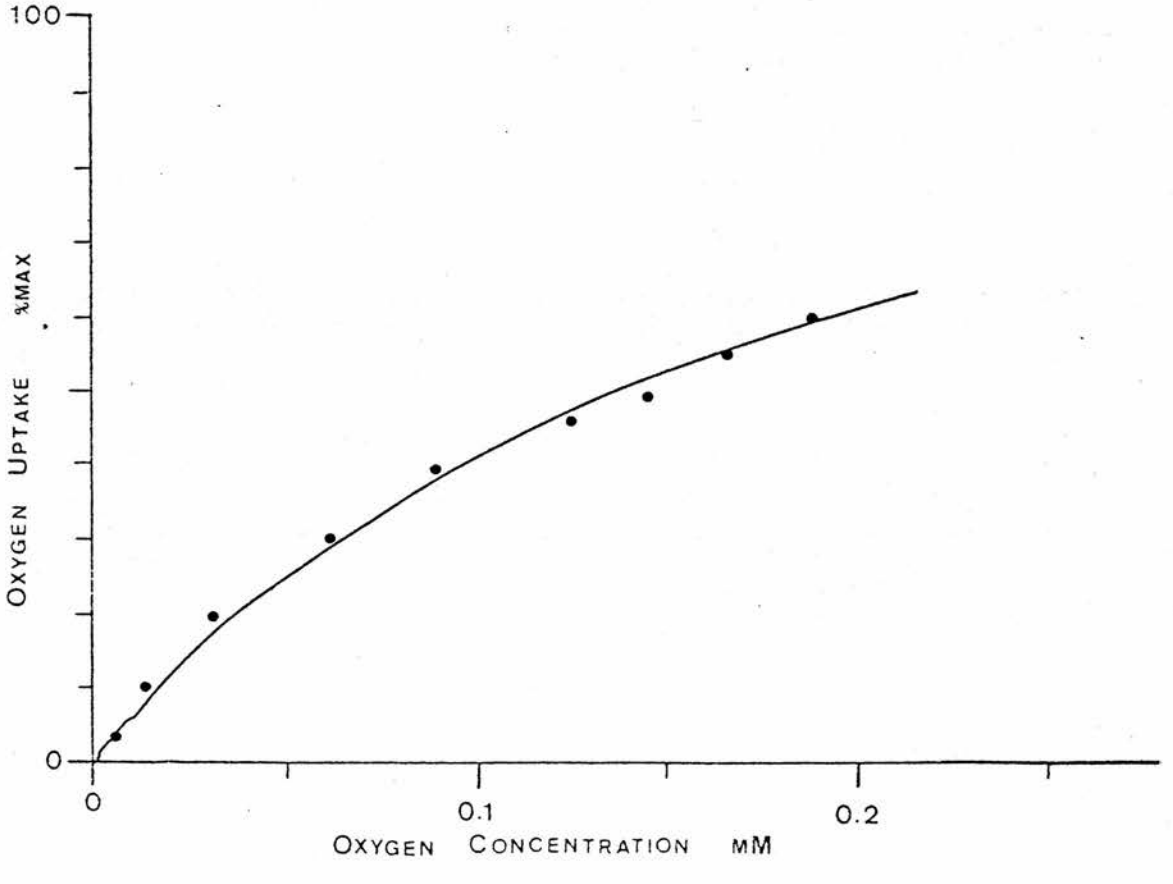

Fig 1.20 - Oxygen uptake vs oxygen concentration in Glyceria fluitans grown in unflooded sand culture.

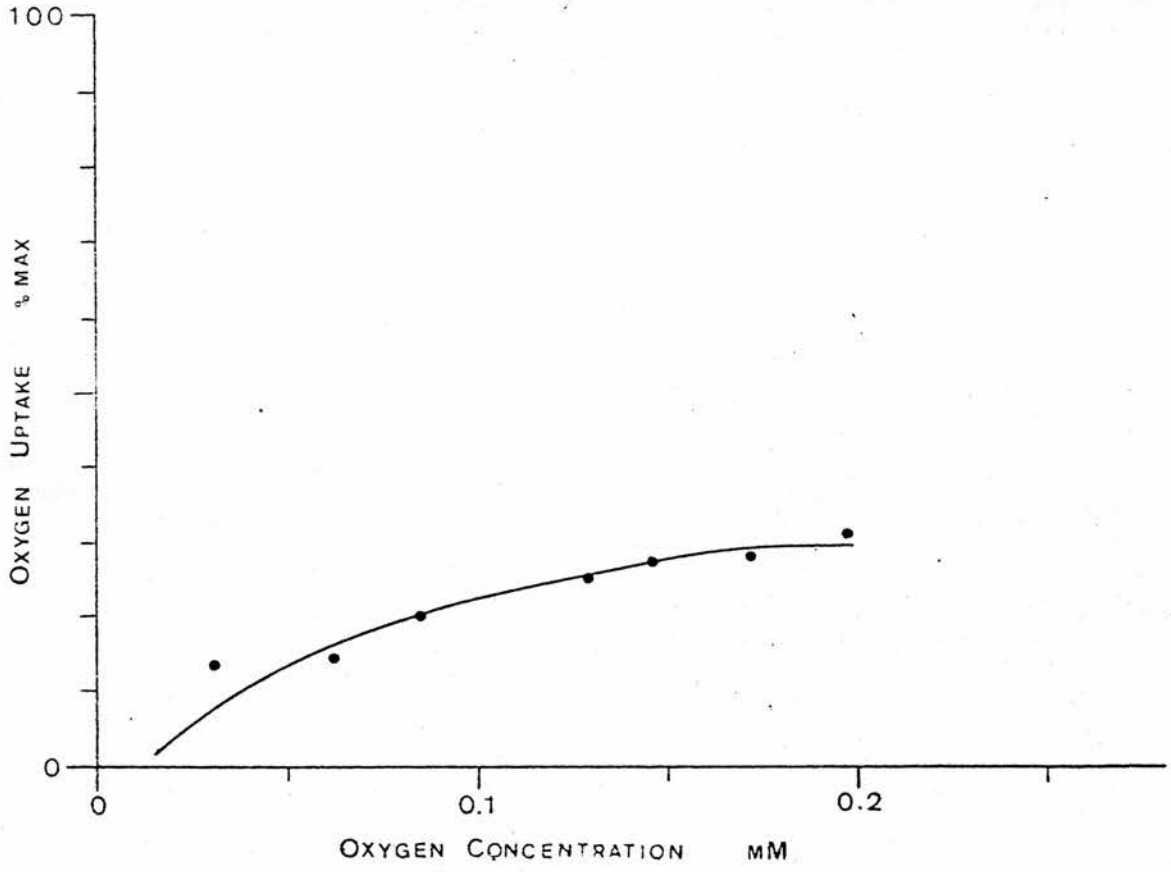

Fig 1.21 - Oxygen uptake vs oxygen concentration in Senecio jacobaea grown in unflooded sand culture.

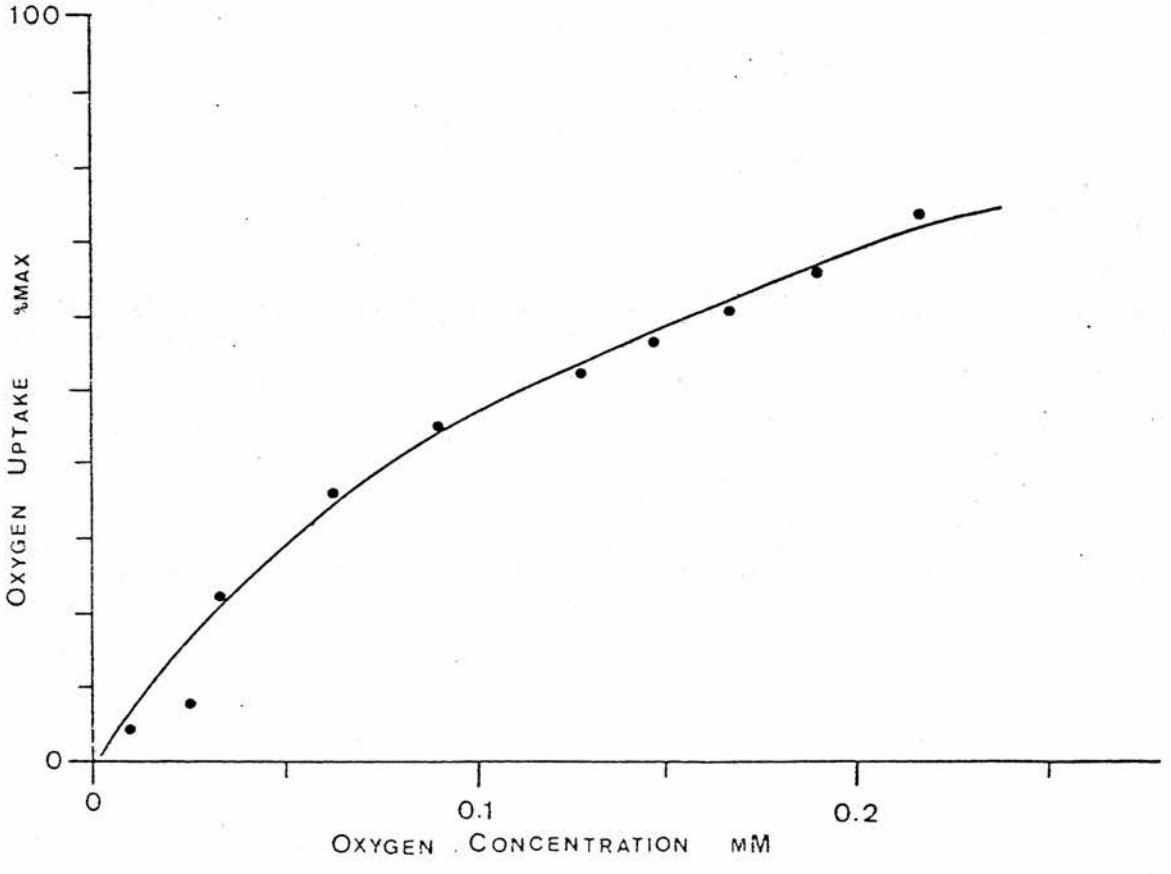

Fig 1.22 - Oxygen uptake vs oxygen concentration in Phalaris arundinacea grown in unflooded sand culture.

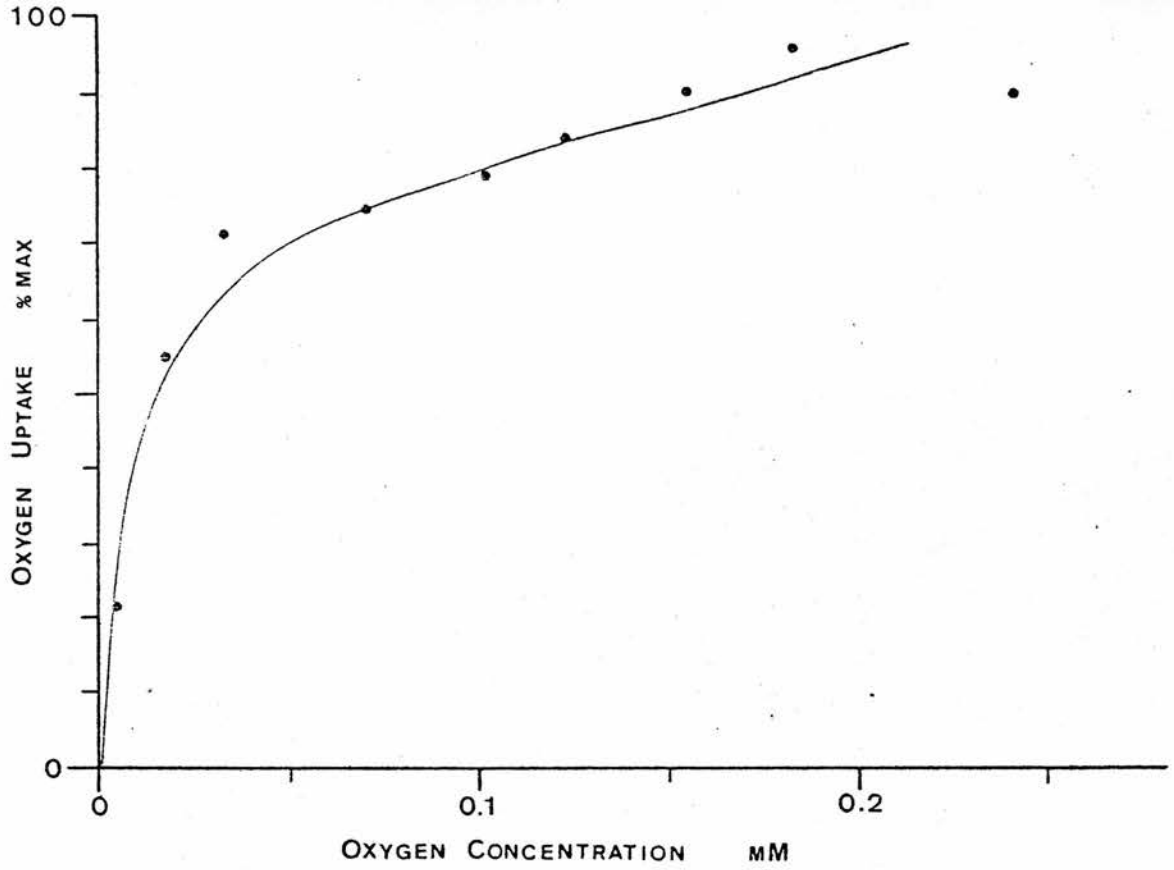

Fig 1.23 - Oxygen uptake vs oxygen concentration in Deschampsia caespitosa grown in unflooded sand culture.

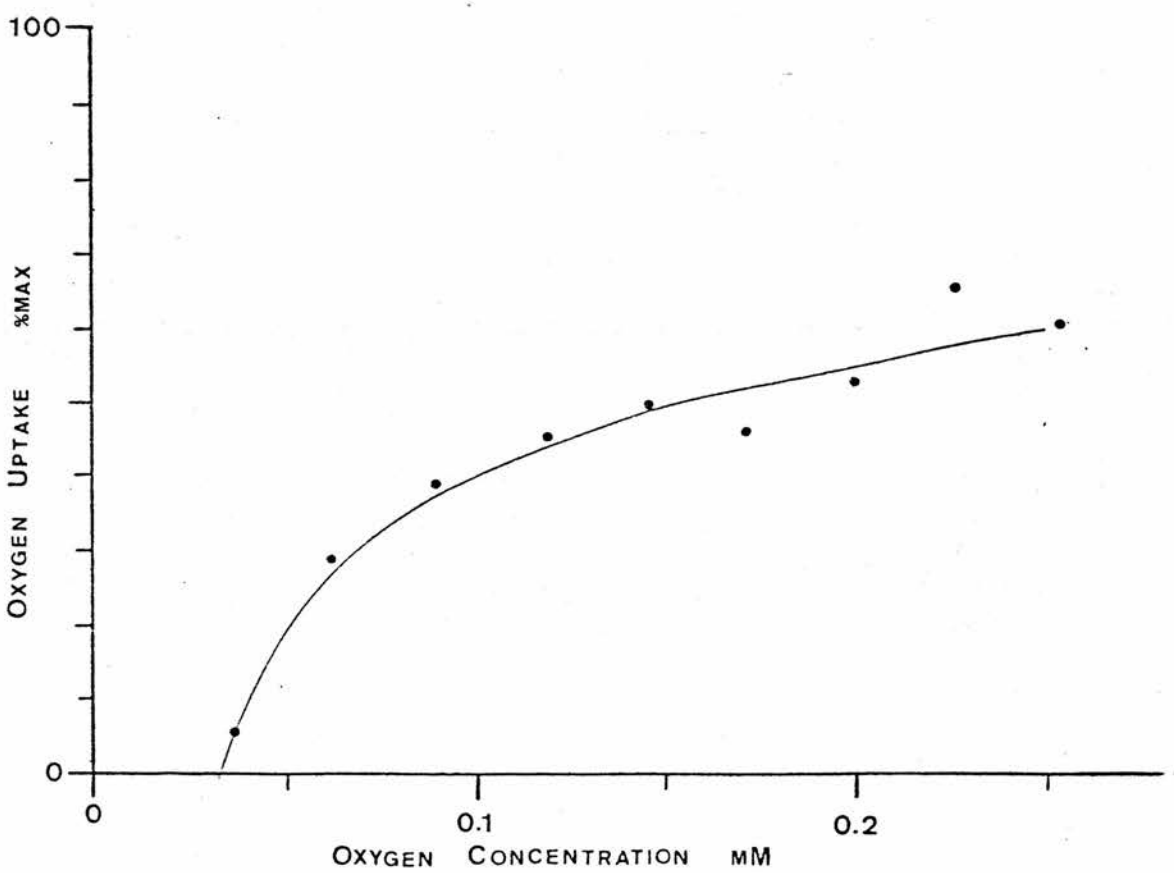

Fig 1.24 - Oxygen uptake vs oxygen concentration in Brachypodium sylvaticum grown in unflooded sand culture.

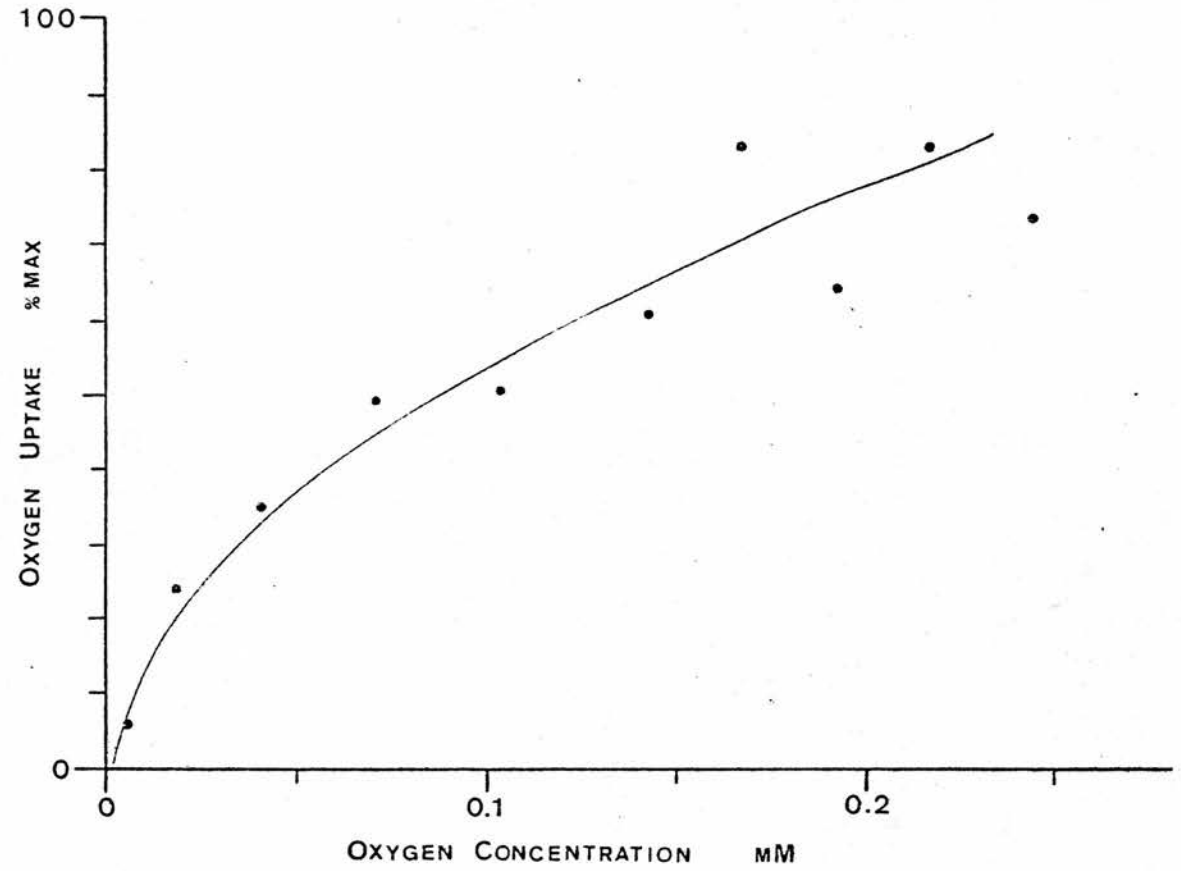

Fig 1.25 - Oxygen uptake vs oxygen concentration in Plantago lanceolata grown in unflooded sand culture.

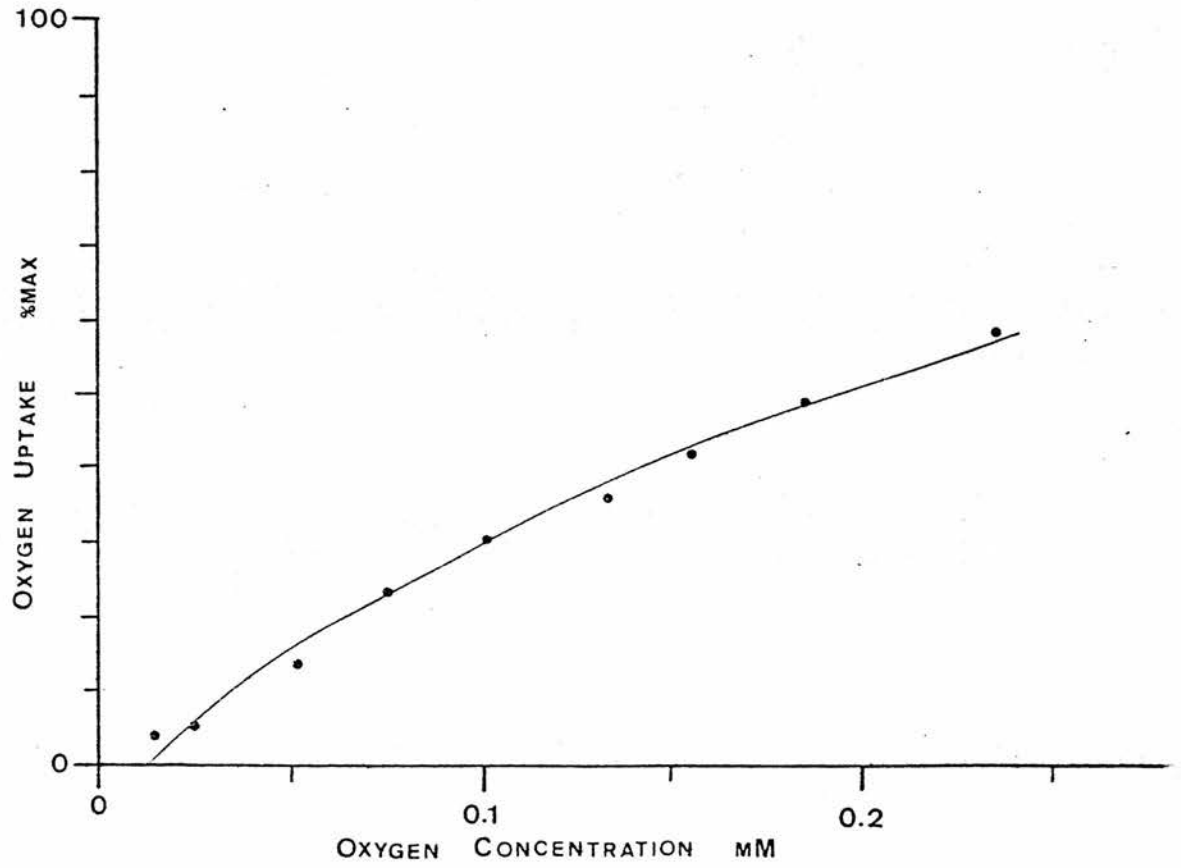

Fig 1.26 - Oxygen uptake vs oxygen concentration in Glyceria fluitans grown in flooded sand culture. Max uptake rate taken as that for Fig 1.27.

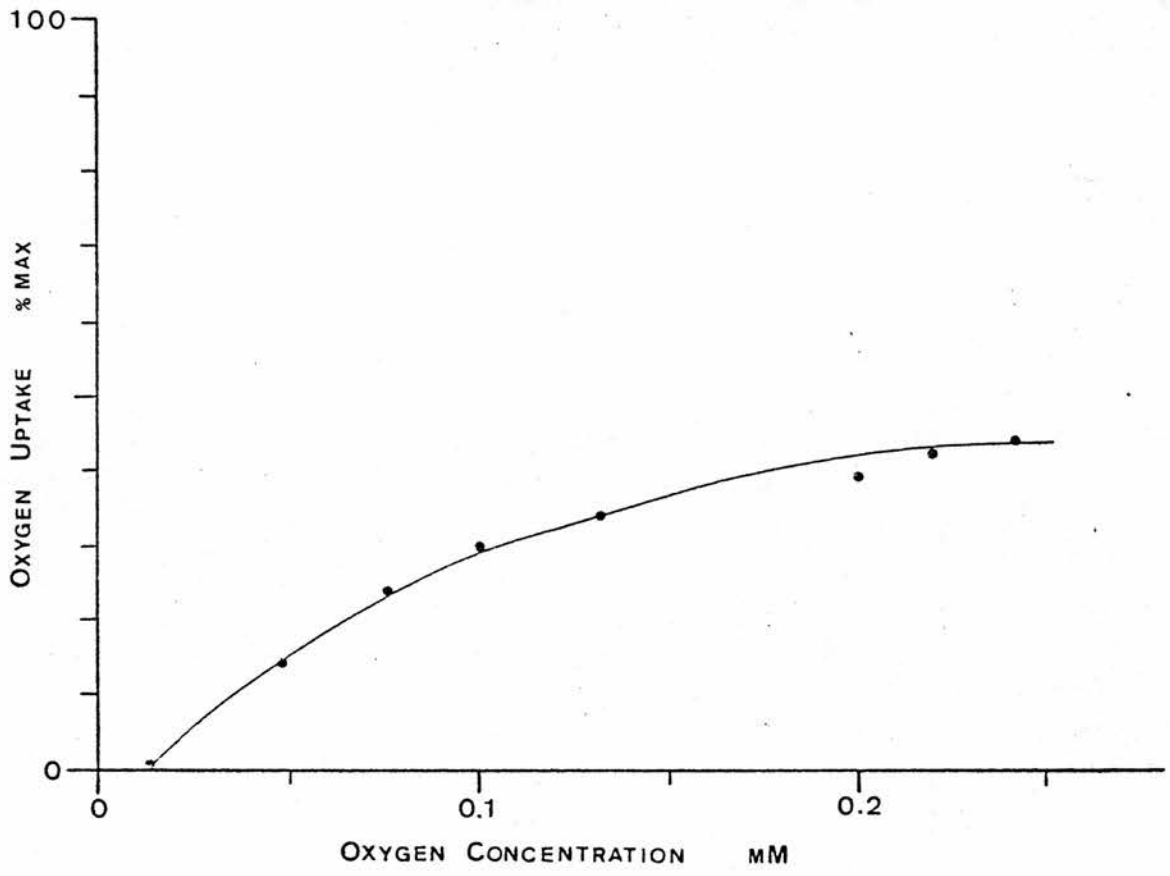

Fig 1.27 - Oxygen uptake vs oxygen concentration in Glyceria fluitans grown in unflooded sand culture.

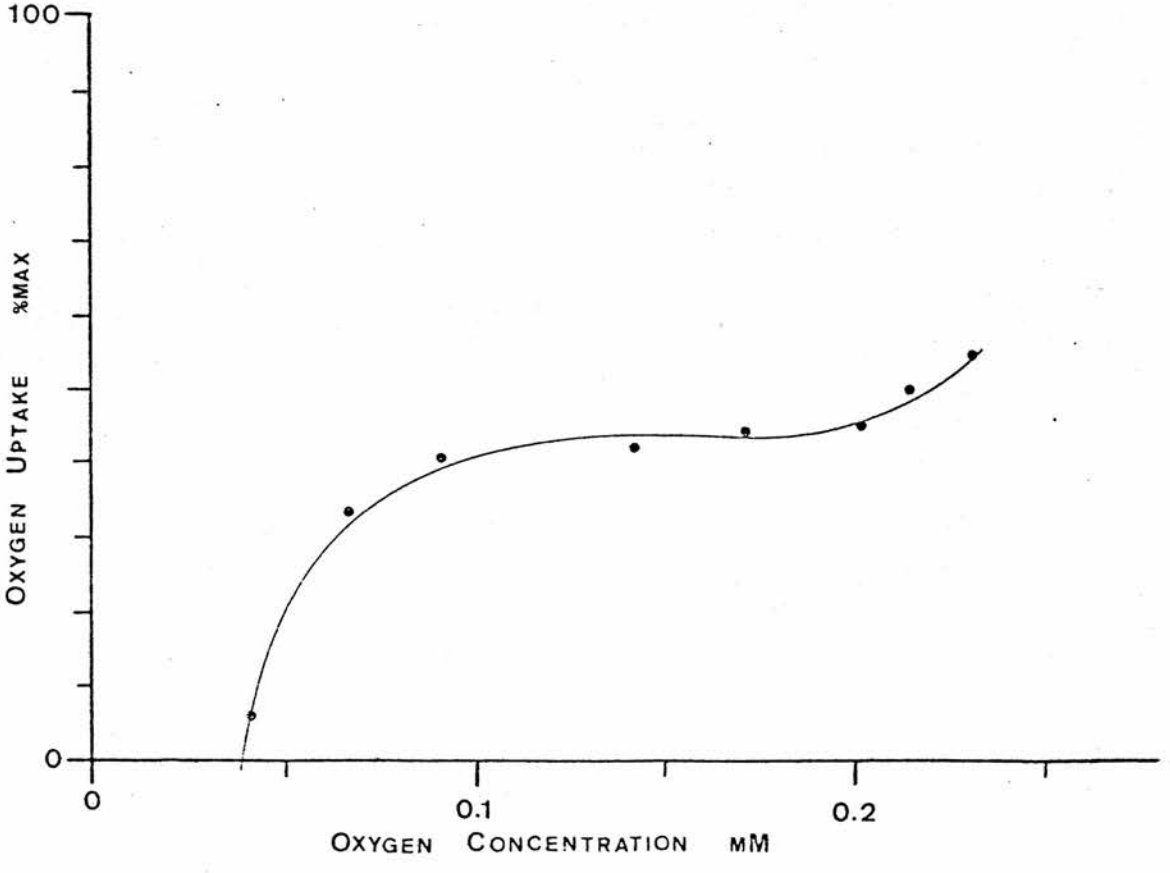

Fig 1.28 - Oxygen uptake vs oxygen concentration in Senecio jacobaea grown in flooded sand culture. Max uptake rate taken as that for Fig 1.29.

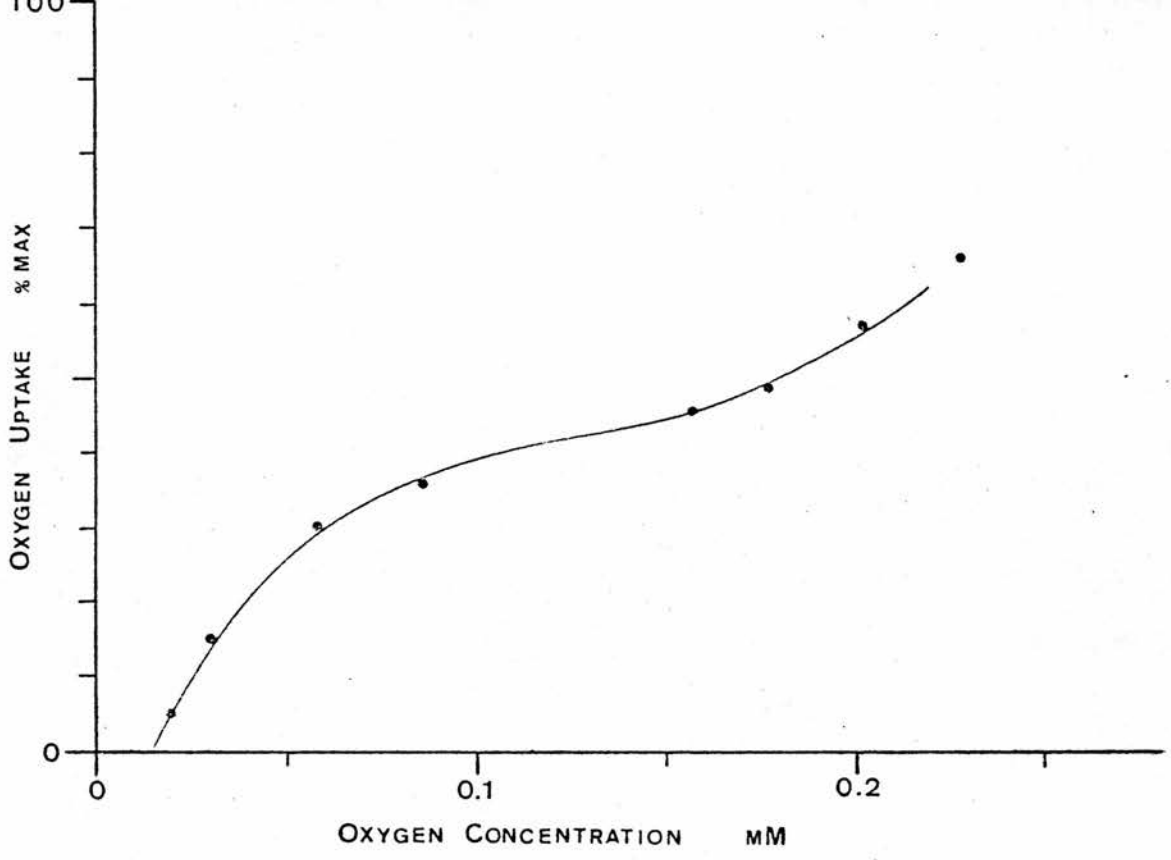

Fig 1.29 - Oxygen uptake vs oxygen concentration in Senecio jacobaea grown in unflooded sand culture.

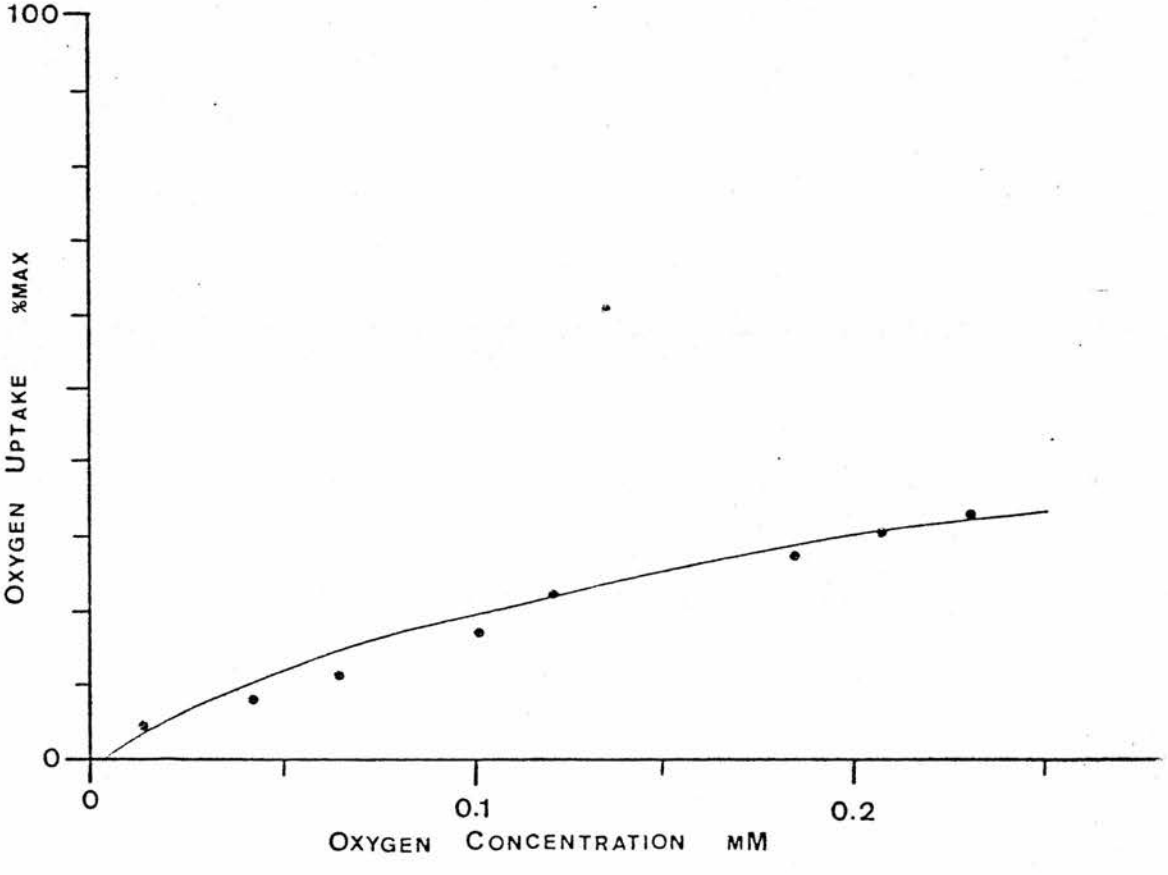

Fig 1.30 - Oxygen uptake vs oxygen concentration in Ammophila arenaria grown in unflooded sand culture.

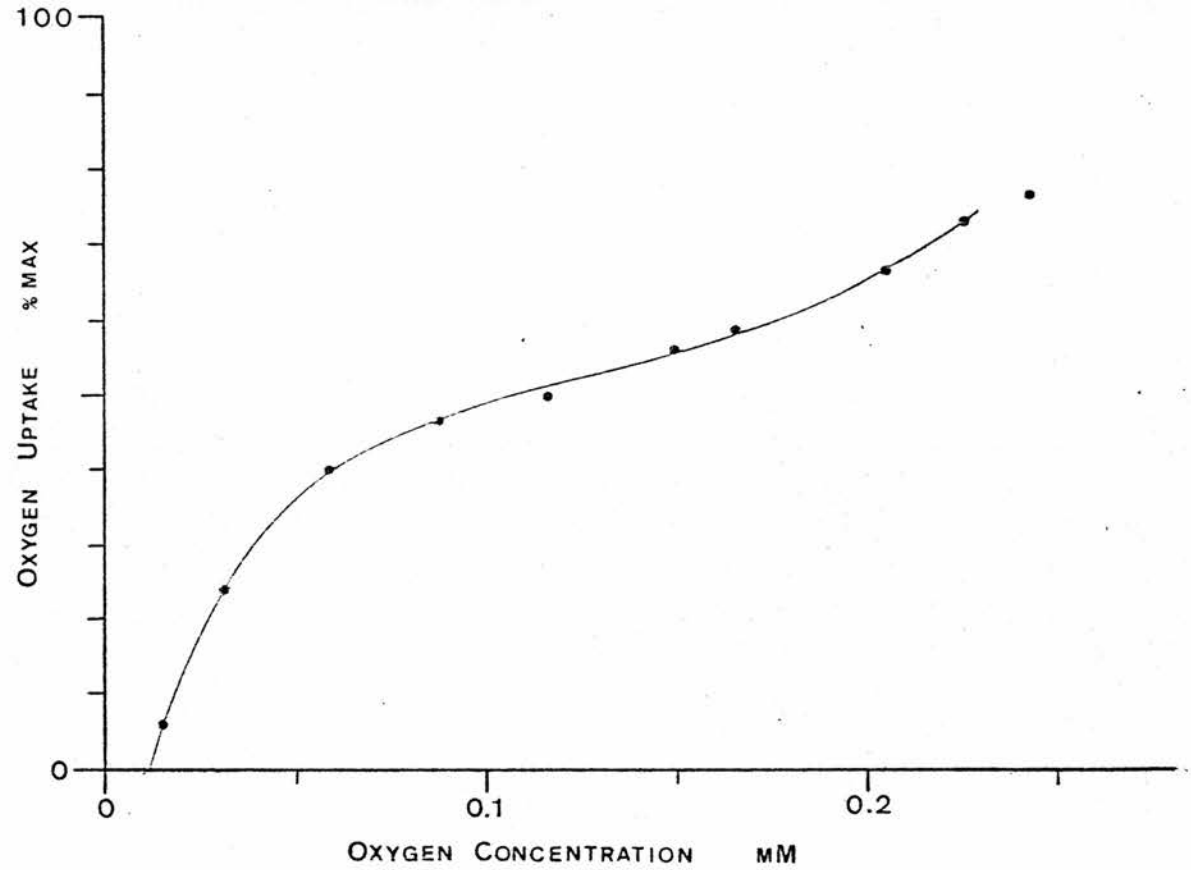

Fig 1.31 - Oxygen uptake vs oxygen concentration in Ammophila arenaria grown in flooded sand culture. Max uptake taken as that for Fig 1.30.

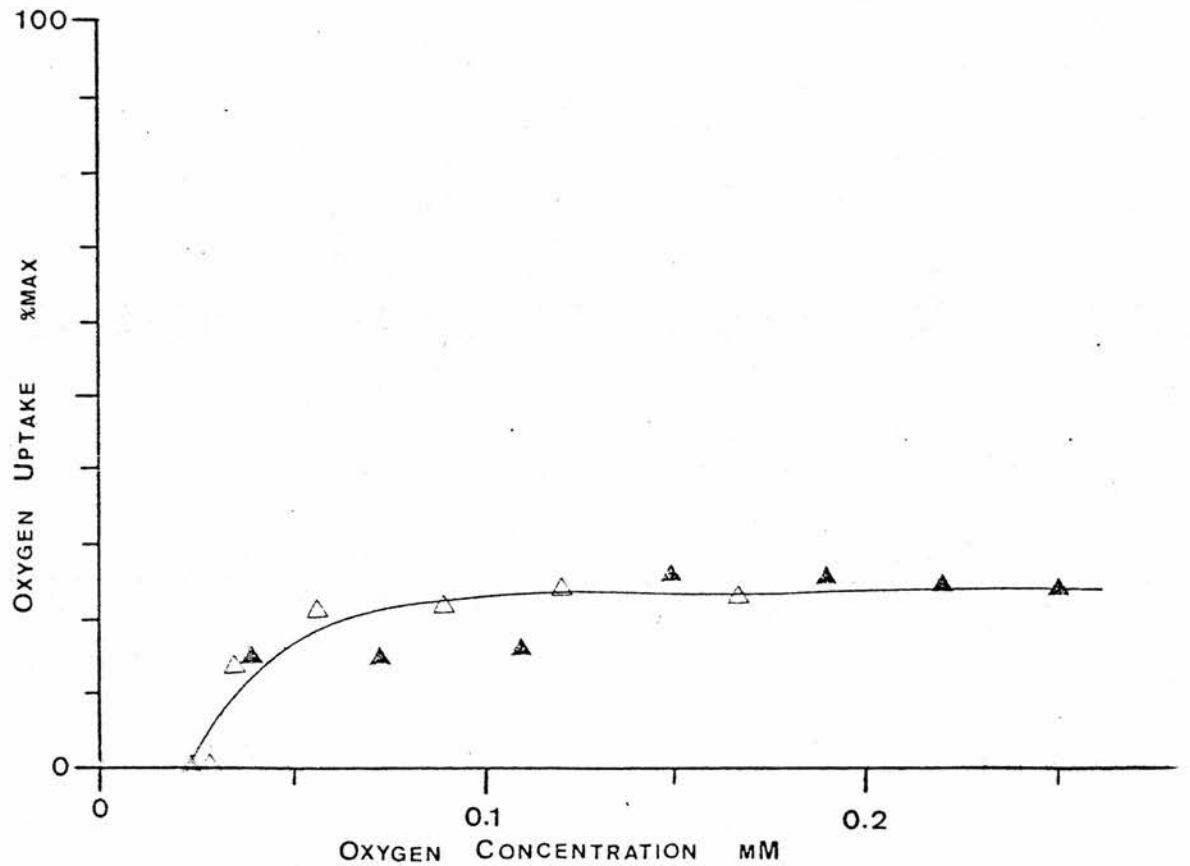

Fig 1.32 - Oxygen uptake vs oxygen concentration in Phalaris arundinacea (experiment started at zero 02 concentration) grown in flooded sand culture. Max uptake taken as that for Fig 1.35.

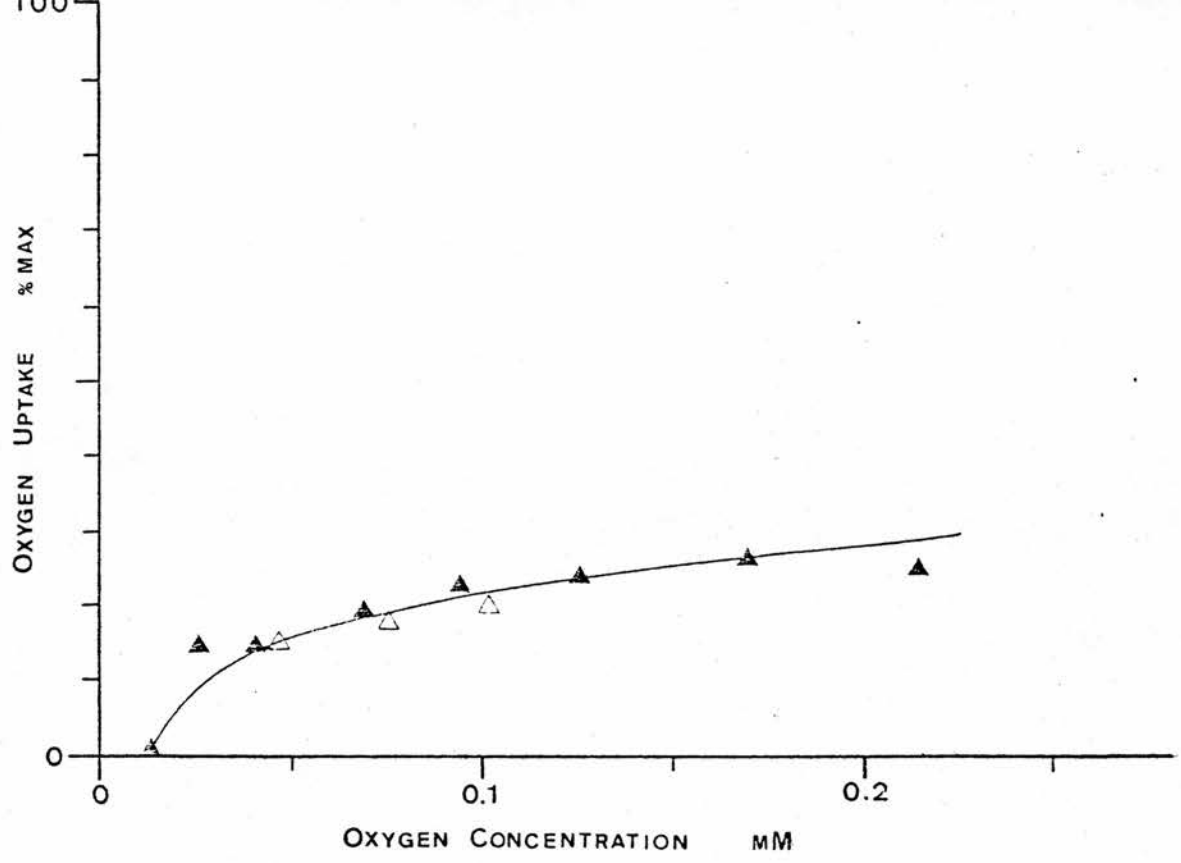

Fig 1.33 - Oxygen uptake vs oxygen concentration in Phalaris arundinacea (experiment started at zero O_2 concentration) grown in unflooded sand culture. Max uptake taken as that for fig 1.35.

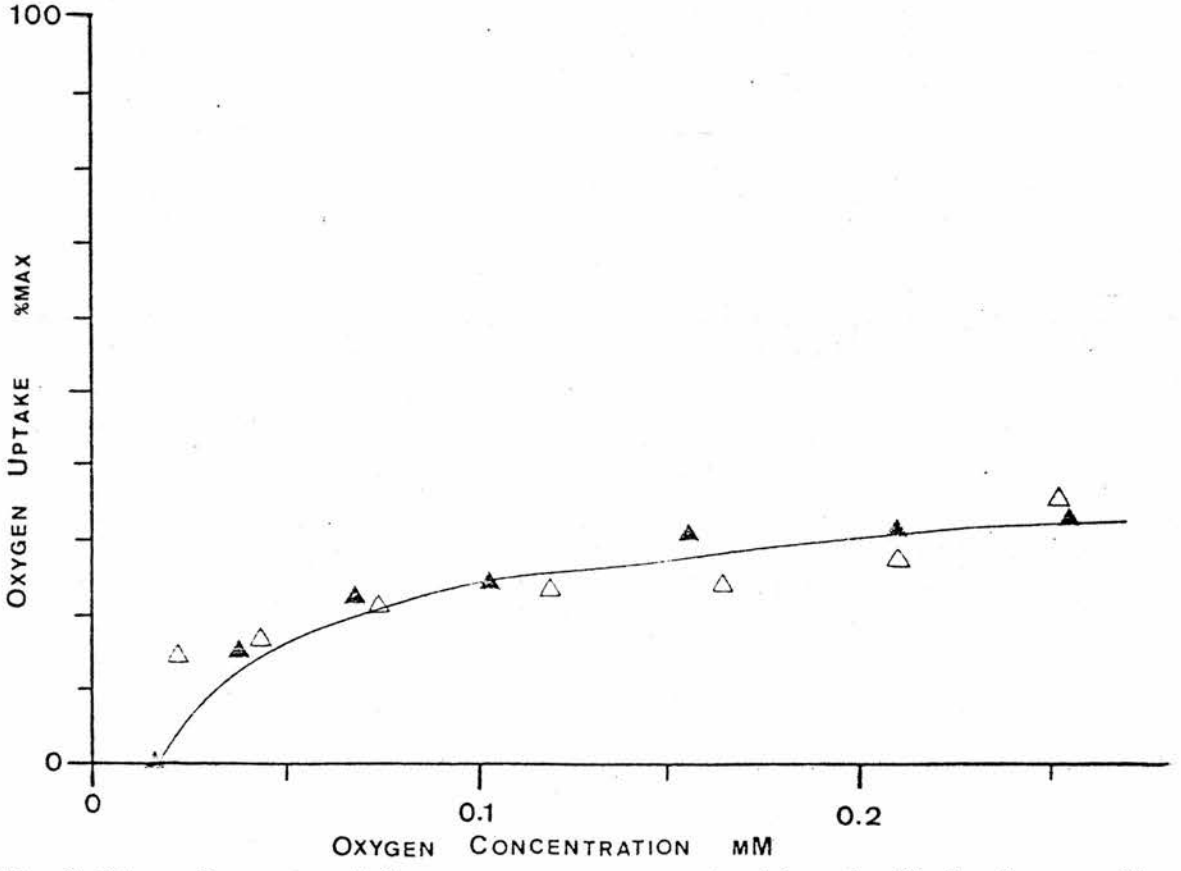

Fig 1.34 - Oxygen uptake vs oxygen concentration in Phalaris arundinacea grown in flooded sand culture. Max uptake taken as that for Fig 1.35.

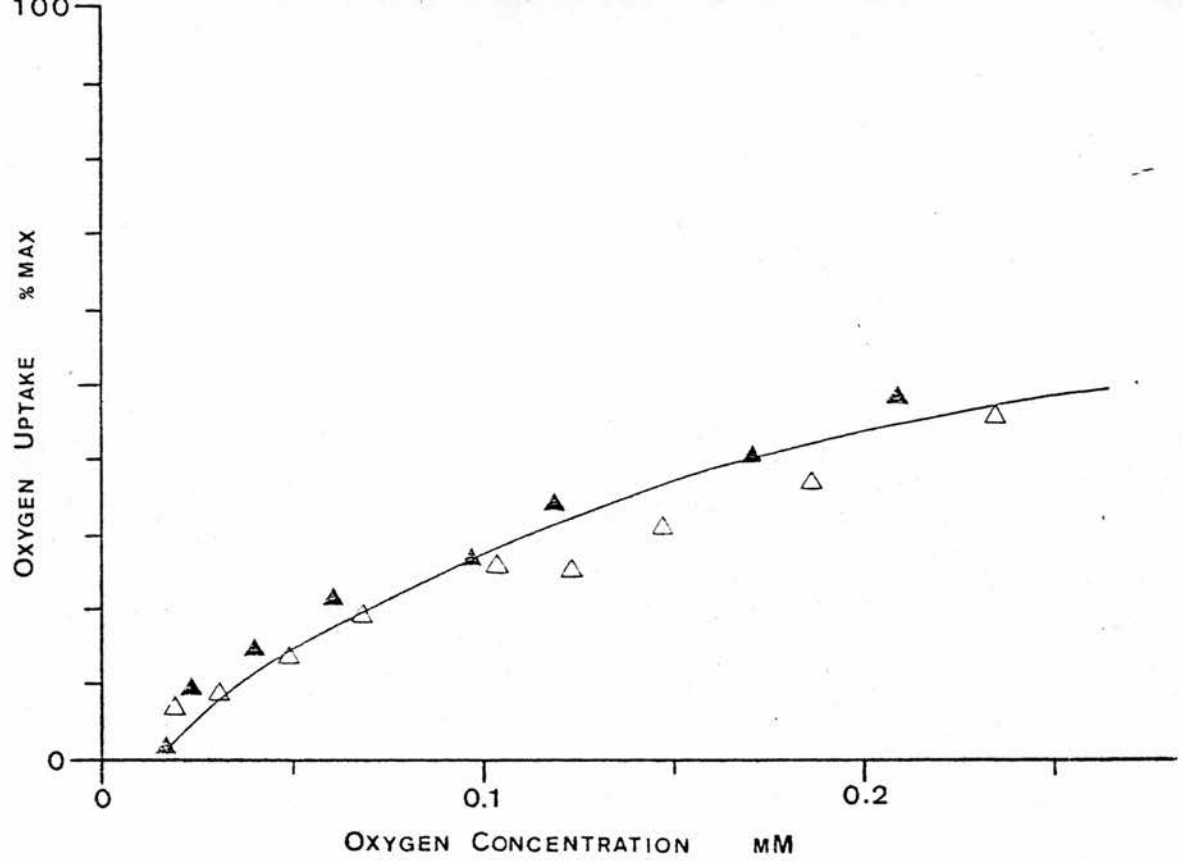

Fig 1.35 - Oxygen uptake vs oxygen concentration in Phalaris arundinacea grown in unflooded sand culture.

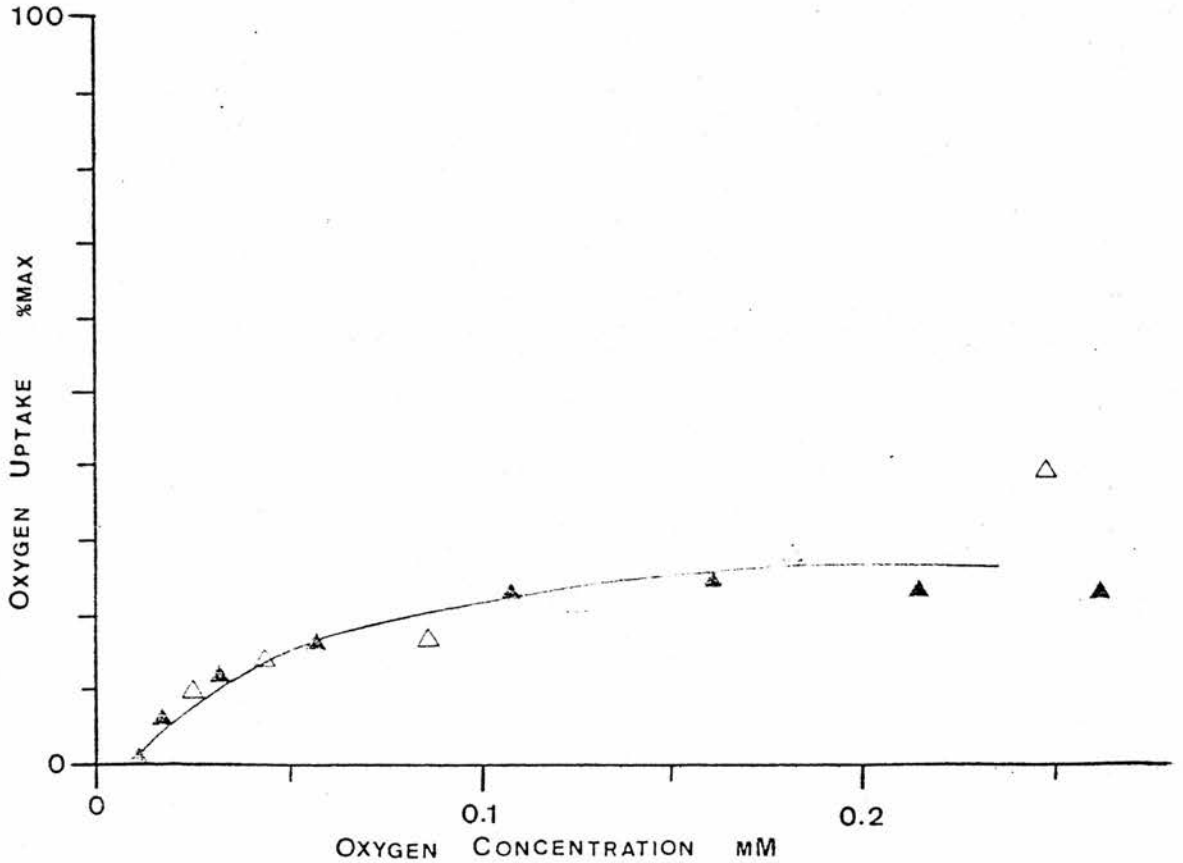

Fig 1.36 - Oxygen uptake vs oxygen concentration in Deschampsia caespitosa grown in flooded sand culture. Max uptake taken as that for fig 1.37.

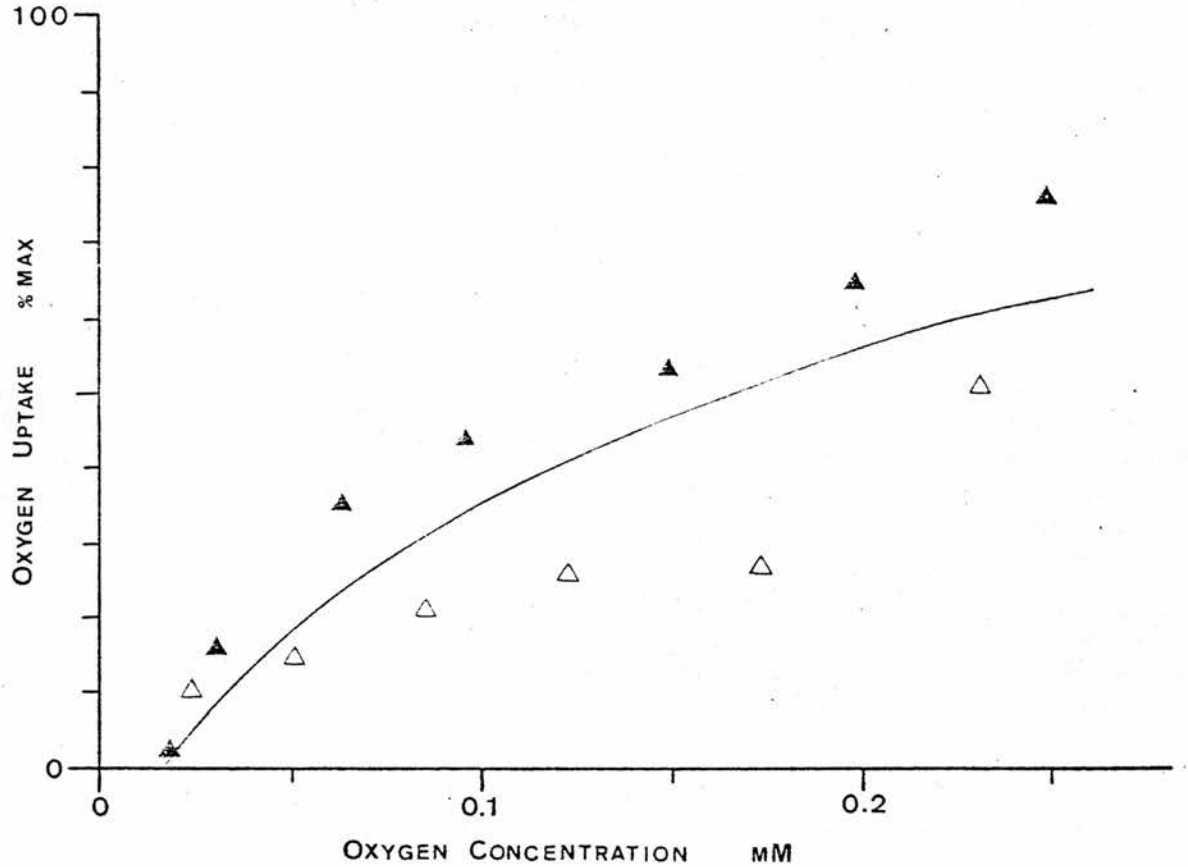

Fig 1.37 - Oxygen uptake vs oxygen concentration in Deschampsia caespitosa grown in unflooded sand culture.

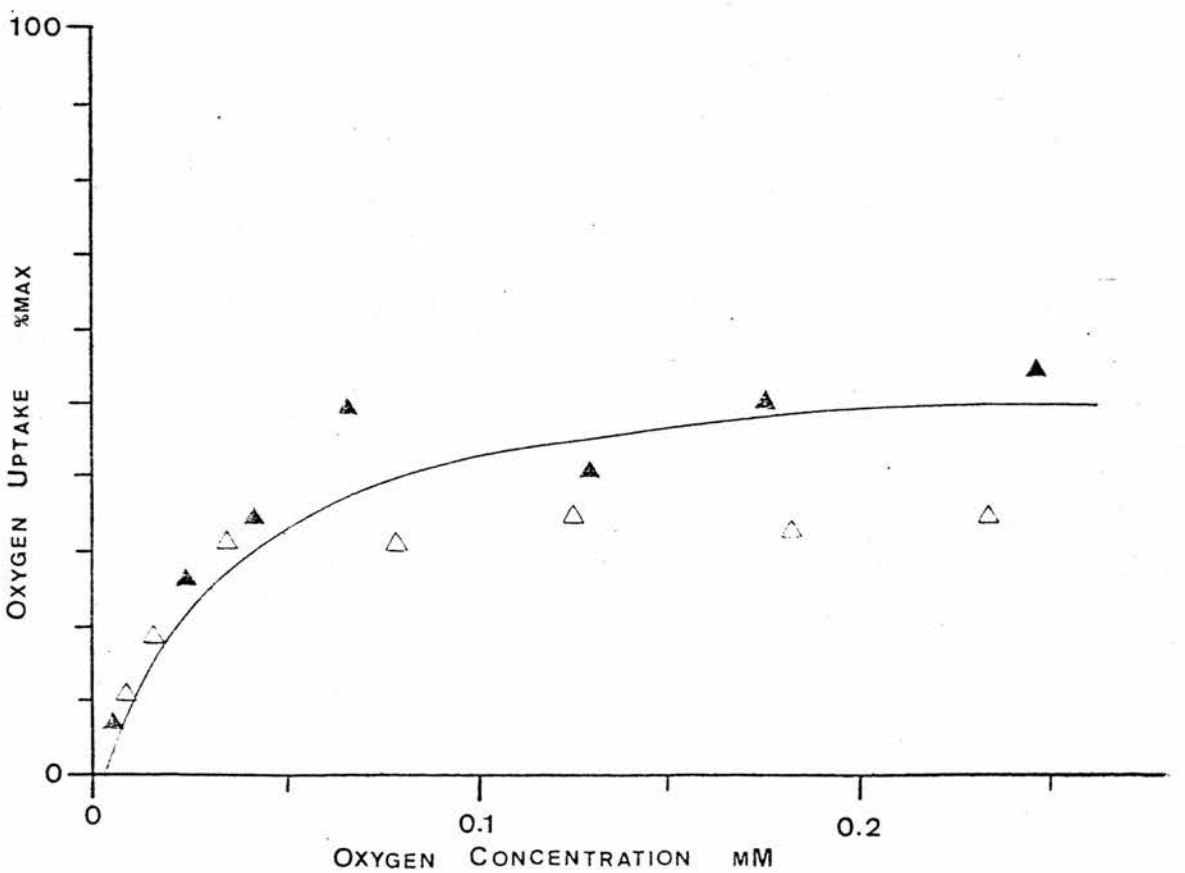

Fig 1.38 - Oxygen uptake vs oxygen concentration in Ammophila arenaria grown in flooded sand culture. Max uptake taken as that for Fig 1.39.

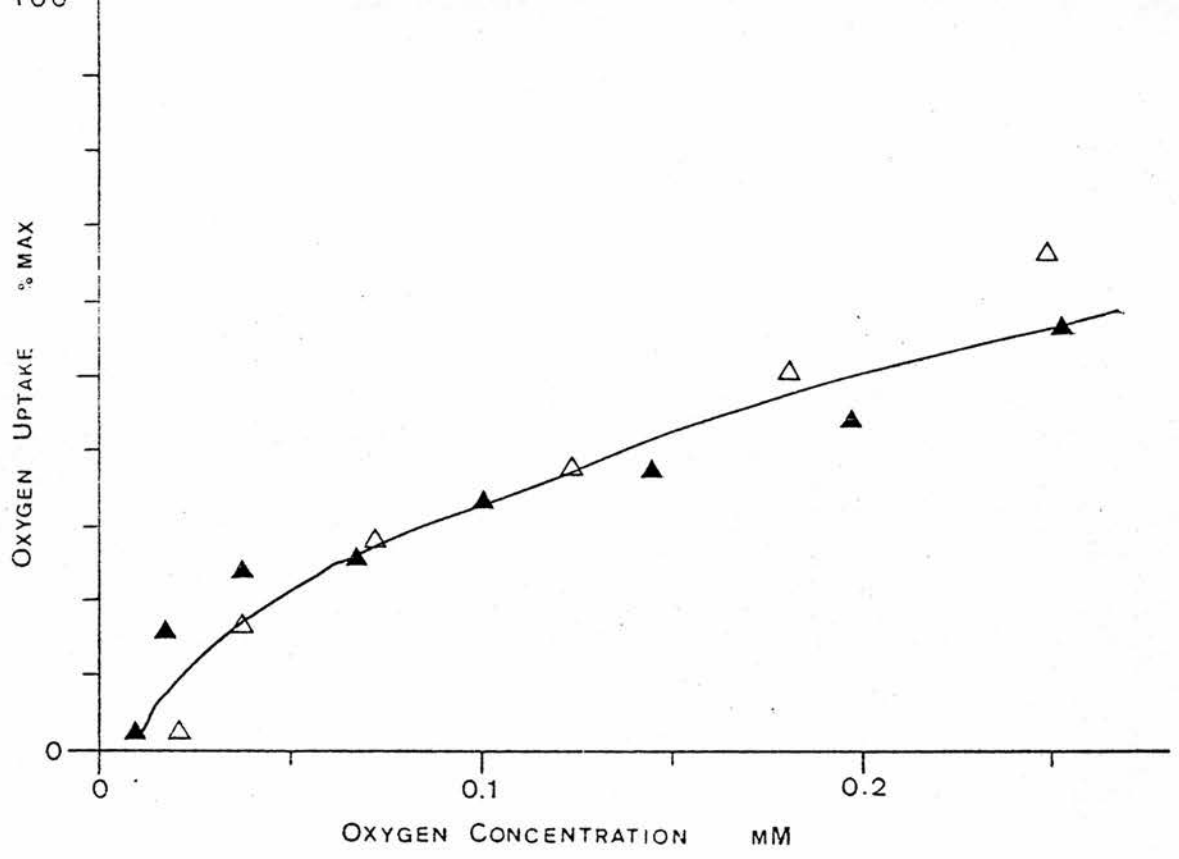

Fig 1.39 - Oxygen uptake vs oxygen concentration in Ammophila arenaria grown in unflooded sand culture.

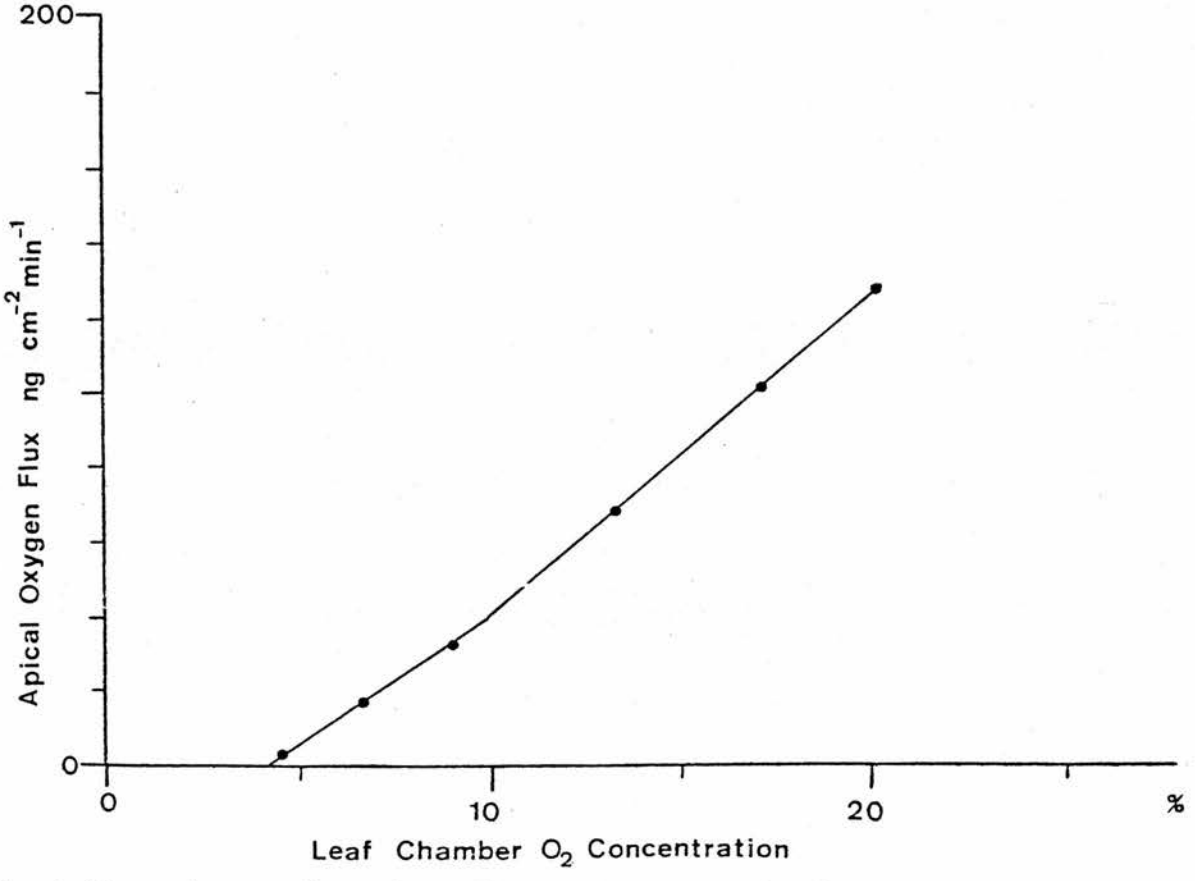

Fig 1.40 - Oxygen loss from the root apex vs leaf oxygen concentration, after Armstrong & Gaynard (1976) (see text).

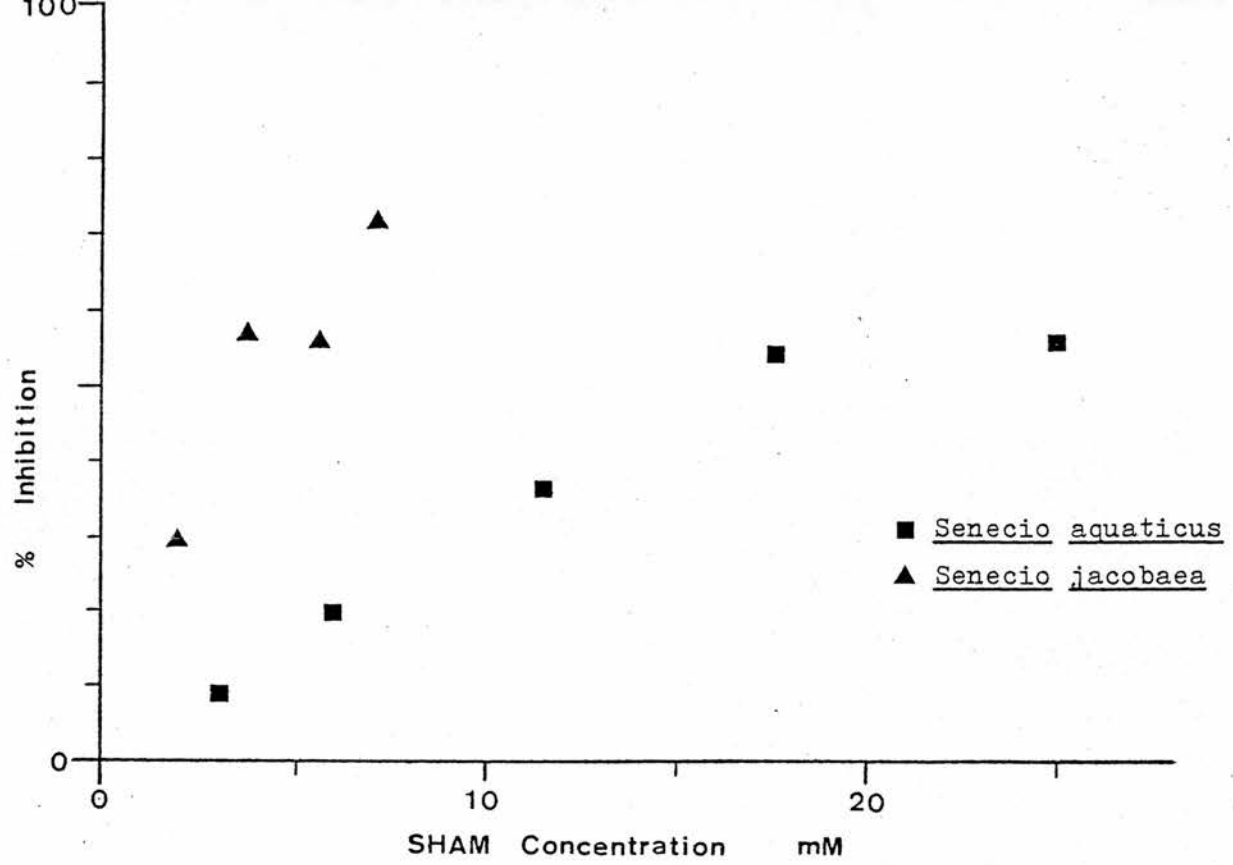

Fig 1.41 - Inhibition of oxygen uptake by Salicyl Hydroxamic Acid in two species of Senecio.

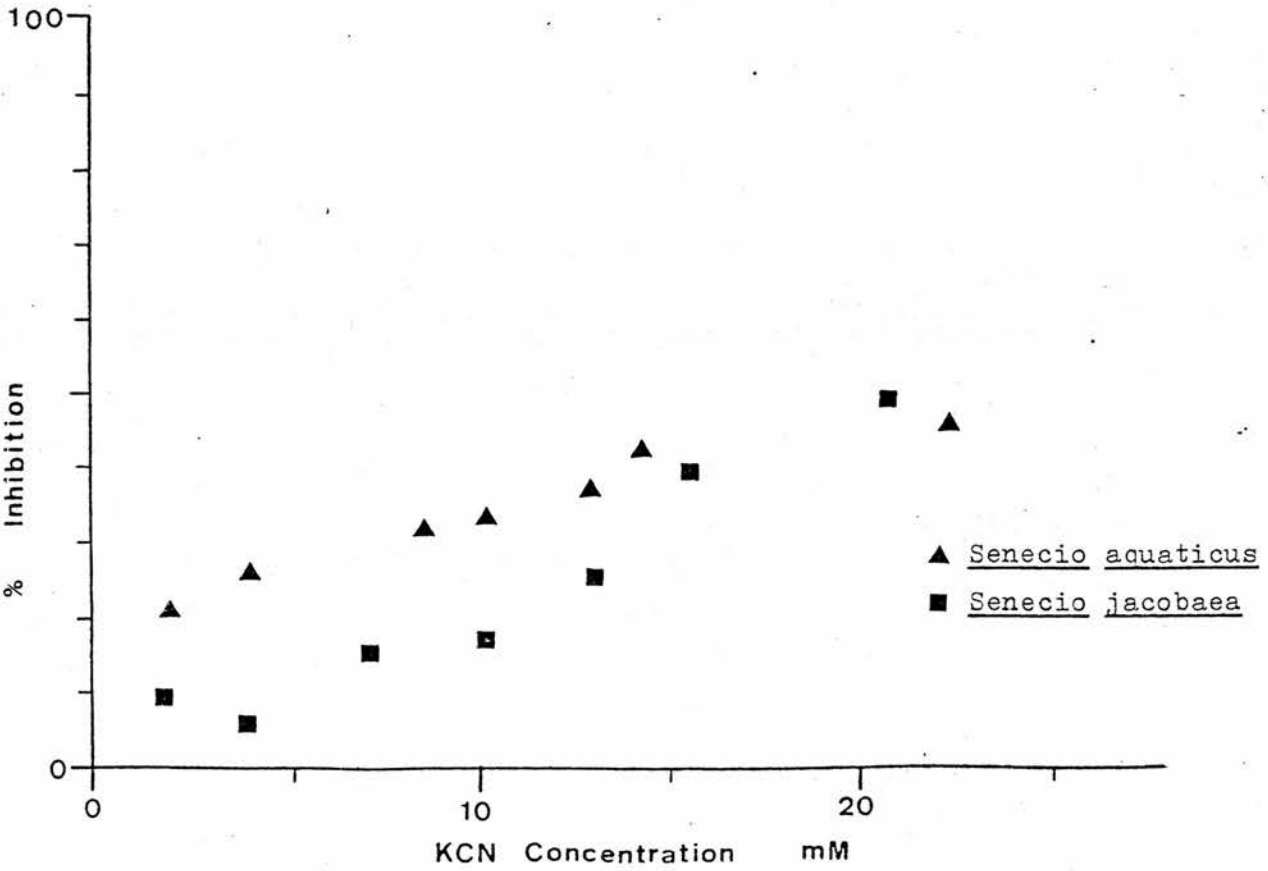

Fig 1.42 - Inhibition of oxygen uptake by Potassium Cyanide in two species of Senecio.

inhibition by SHAM in the two species can be explained by the fact that the SHAM added to the S. jacobaea sample had been dissolved in ethanol, and the presence of ethanol would have had an effect on the electrode reading, both from direct physical interaction and also as a result of its toxic effect on the root tissues. Apart from this, the response of the two species was similar and of the order of magnitude found by LAMBERS and SMAKMAN (1978).

b) Possible Explanations for the Hyperbolic Curves

As already outlined, the first experiments which were carried out to measure the rates of oxygen uptake used samples which had been collected directly from the wild, without any pre-treatment in the glasshouse. Some examples of the types of response obtained in such experiments are shown in figures 1.11 to 1.24. The fact that the plant material used had not been subjected to any controlled growth conditions was almost certainly responsible in part for some of the variation in the responses obtained. Nevertheless, although this makes it difficult to attribute any particular cause to the variation found, these experiments were useful simply by illustrating the variety of responses which could be expected, and in particular that the hyperbolic curve was the most typical.

Before analysing the possible reasons why this should be the case, some attention must be given to the fact that all the experiments were carried out in vitro using excised root tips. There are two main advantages in carrying out in vitro experiments with excised plant organs. Firstly, it is possible to carefully control the experimental conditions to which the material is subjected, and secondly, it is possible with great ease to study specific parts of the plant without having to consider influences from the rest of the plant. However, this second advantage immediately points to the great disadvantage of in vitro experiments - namely that one can never be quite sure

that the behaviour of the excised plant material accurately represents its behaviour as part of a whole, intact, plant. The first question to ask, therefore, is to what extent the *in vitro* arrangements used in the experiments presented here may have produced results which do not correspond to the *in vivo* situation.

One possibility is that the excised root apices were unable to retain their full viability for the duration of the experiment and that this was in part responsible for the reduction in oxygen uptake as the experiment progressed. Certainly, in those cases where the rate of uptake in air-saturated buffer was measured both at the beginning of the experiment and at the end, a slight reduction in uptake is apparent (compare figures 1.32 and 1.34). However, it is just as likely that this reduction was due to an increased amount of flooding of the air spaces at the end of the experiment (see below). Furthermore, depending on the amount and nature of the material used, the length of time it took to conduct each experiment varied from 0.5 to 6 hours, but the results from those experiments which took several hours (for example *Plantago lanceolata*, fig 1.25) did not differ markedly from those which took less than one hour (for example *Deschampsia caespitosa*, fig 1.23). It seems unlikely, therefore, that the shapes of the curves can be attributed to loss of viability during the course of the experiment.

A more likely possibility is that at low oxygen concentrations, the rate of oxygen diffusion is insufficient to maintain full aerobic respiration throughout the root (BERRY and NORRIS, 1949). It has already been mentioned in the General Introduction that this may be largely an artefact due to the much greater diffusional impedance which results from flooding of the intercellular air spaces under the *in vitro* conditions of the experiment. ARMSTRONG and GAYNARD (1976) describe an alternative method for measuring the COP in plant roots, which involves measuring the radial oxygen loss (ROL) from the root apex of an intact plant. They found that the ROL was related to the

oxygen concentration around the leaves as shown in figure 1.40. The internal oxygen concentration calculated from the ROL at the inflexion point is taken as the COP for root respiration, and turns out to be approximately an order of magnitude lower than corresponding estimates obtained by *in vitro* experiments.

An exploratory experiment carried out as part of this project showed directly that the amount of air space in an excised root does decline when it is immersed in aqueous solution. In this experiment, air space was measured in 1 cm lengths of root cut from a rice plant previously grown in an unflooded sand culture, before and after incubation under identical conditions to those used in oxygen uptake experiments. It was found that after 2 hours incubation, the air space content was 11% (volume per volume) while that of the untreated control was 27%. It is worth noting, however, that 40% of the original gas space volume remained unflooded even after 2 hours immersion.

It is possible, therefore, that the hyperbolic curves obtained are an exaggeration of the response which might be expected from the root tip of an intact plant. One would expect, however, that the difference between the *in vivo* and *in vitro* situations will be less in those plant species in which there is only a small amount of air space, even in the intact plant. Furthermore, CHEVILLOTE (1973) has shown that intracellular diffusion of oxygen may limit the rate of oxygen uptake in some plant tissues. These considerations will be discussed more fully later.

Another explanation which can also account for the hyperbolic curves obtained is a low affinity of the respiratory enzymes for oxygen. Although the cytochrome enzymes are known to have an extremely high affinity for oxygen, there has been some interest recently in the occurrence in a wide variety of plant tissues of an alternate oxidative pathway, with a somewhat lower affinity for oxygen (SOLOMOS, 1977). The behaviour of this alternate system has been studied in the genus *Senecio*. LAMBERS and SMAKMAN (1978) measured

the rate of oxygen uptake in intact root systems of Senecio aquaticus and found a hyperbolic relationship similar to those obtained in this project (fig 1.43). Because the root system was intact (although excised from the aerial portions), they claim that flooding of the intercellular air-spaces was highly improbable and that the hyperbolic shape could be more satisfactorily explained by the low affinity of the alternate system for oxygen (SOLOMOS, 1977). They estimated the apparent Km for whole root respiration to be 22μM, which compares favourably with estimates obtained by other workers for the Km of the alternate oxidase (SOLOMOS, 1977).

In the discussion which follows later, these possible explanations for the hyperbolic curves obtained will be discussed in relation to the experimental results and the model predictions.

c) Possible Explanations for the Non-Hyperbolic Curves

A number of experiments, notably those involving Chamaenerion angustifolium and Caltha palustris (figs 1.11 and 1.12), showed a much lower dependence of oxygen uptake on the external concentration of oxygen. In Chamaenerion, for example, the rate of uptake was unaffected by the external oxygen concentration until a very low oxygen concentration (about 0.02atm) was reached. This was in marked contrast to most of the other experiments. A similar situation can be seen in some of the 'paired' experiments, in which the flooded samples showed a much lower dependence on the supply of oxygen.

Such differences can be attributed to there either being a much lower diffusional impedance to oxygen movement, or to a much higher affinity of the respiratory enzymes for oxygen. The latter explanation would imply that the differences between the two types of response were metabolic in origin.

In a small number of experiments, a curious 'diphasic' response was obtained (for example, Senecio jacobaea, fig 1.28). The reasons

for this type of response remain obscure. Although it was found for Senecio jacobaea on some occasions, it was not on others (compare figures 1.28 and 1.16 for example). Possibly, there was some period of instability when the root tips were first placed in the electrode. Alternatively, a diphasic response may indicate the presence of two respiratory systems. Predictions from the model (see later), however, suggest that this would only lead to a diphasic response if the activity of one system was completely or largely reduced below a certain critical concentration of oxygen, and there is little evidence of such a respiratory system in plant tissues.

d) Model Predictions

It was impossible, other than by speculation, to deduce from the results of the experiments alone the influences responsible for the results obtained. The predictions made from the simple model designed as part of this project, however, can be compared with the observed results, thus assisting their interpretation.

The two main factors which will govern the behaviour of an excised root tip in the oxygen electrode are a) the affinity of the respiring tissues for oxygen and b) the diffusional resistance of the root tissue to oxygen. It should also be noted, however, that in a diffusion-limited system, the effect of the diffusional resistance will be greater in plant material which has a high respiration rate. Therefore, for a given diffusional impedance and affinity for oxygen, the potential maximum rate of oxygen uptake must also be considered as a factor which will influence the type of response obtained.

The model was also developed with the option of specifying a particular concentration of oxygen at which oxygen uptake fell completely to zero, as distinct from the concentration at which uptake fell to half its maximum value. The reason for including this option was that in many of the experiments carried out, oxygen uptake

fell to zero before the oxygen concentration became zero. This might occur, for example, because of the accumulation of toxic by-products such as ethanol. The inclusion of this option in the model assumes that a similar phenomenon will occur in specific regions of the root. Thus, when the inner regions of the root reach this critical oxygen concentration the model assumes that their oxygen uptake ceases completely, while the outer regions remain unaffected. This is obviously a simplification, as the diffusion of ethanol from the inner regions of the root will also affect the more peripheral regions, but the use of this option does lead to some interesting results.

The set of predictions obtained from the model were, then, obtained by varying four factors - a) the affinity of the root tissues for oxygen; b) the oxygen concentration at which oxygen uptake ceases completely; c) the diffusional impedance of the root tissues to the movement of oxygen; and d) the maximum potential rate of oxygen uptake. In addition, the model was used to simulate the behaviour of particular species. Unfortunately, the use of the model in this way was limited to only two species. This was because in the majority of experiments, the respiration rates were only calculated as μmoles/g dry weight/hour, whereas the model required that the respiration rates be given as μmoles/cm root/hour. Since only two species (Chamaenerion and Juncus) had their total root length as well as dry weight measured, only these two species could be directly simulated by the model. This situation arose because the model was developed after the experimental results had been obtained, and it was not anticipated at the time of conducting the experiments that total root length would be required as well as the dry weight.

i) The Effect of Varying Affinity for Oxygen

Fig 1.43 shows the predicted response of a hypothetical excised root, for different values of Km. In this example, there was only

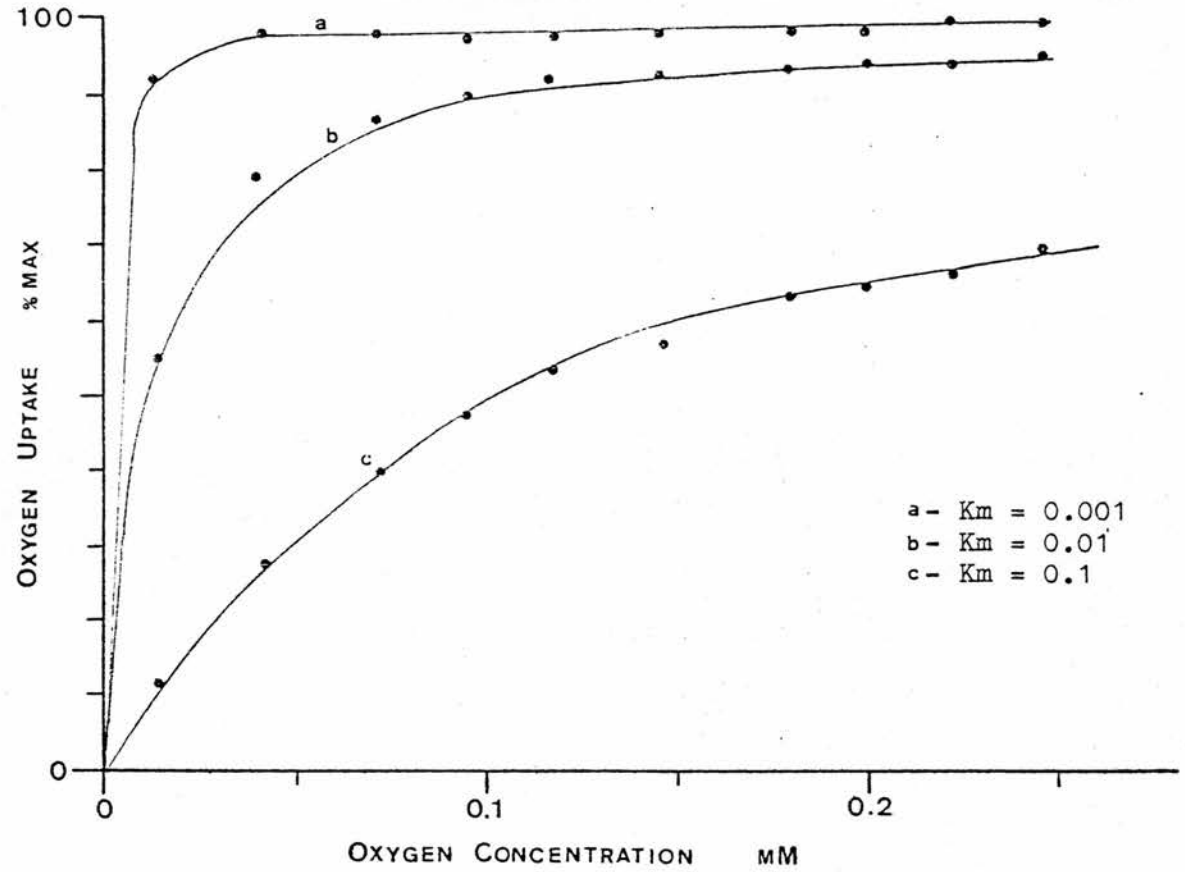

Fig 1.43 - Model prediction. Effect of varying affinity for oxygen (see text). Single respiratory system.

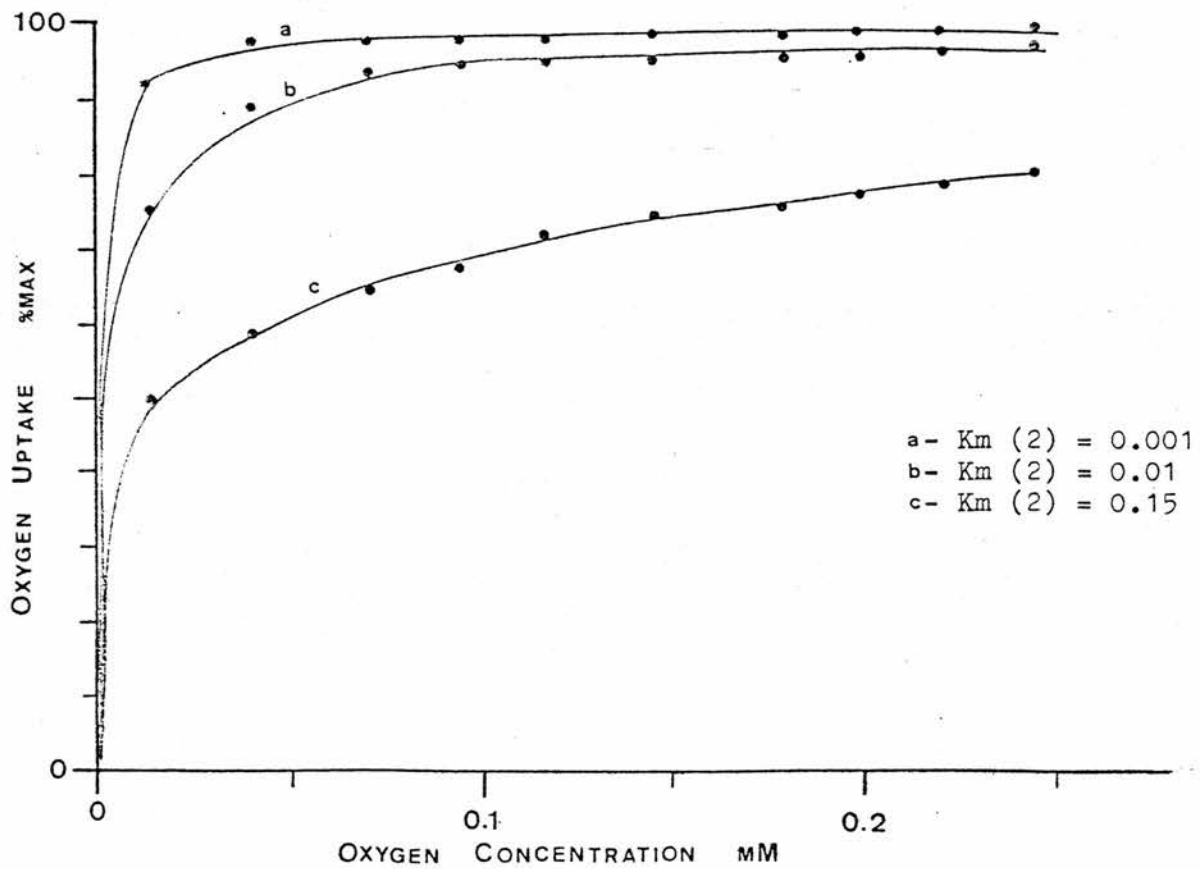

Fig 1.44 - Model prediction. Effect of varying affinity for oxygen (see text). Two respiratory systems.

considered to be one respiratory system, and the diffusion coefficient was set to a value of 1, so that there was no diffusional resistance to the movement of oxygen. The input data used were:

Rmax = 0.05
Km = 0.001 - 0.1
COP = 0
D = 1
b = 0.05
a = 0.0001
n = 10

(see Appendix III for definitions of paramters and units)

With this set of input data, the model is essentially predicting the behaviour of the respiratory enzymes rather than the root itself, and not surprisingly, therefore, the predicted curves correspond exactly to those predicted by the Michaelis-Menten kinetics. Figure 1.44 shows the predicted responses where there are two respiratory systems, each with the same maximal rate of oxygen uptake, but where the Km of one of the systems is varied. Again, the diffusion coefficient was set to 1 to eliminate the influence of diffusional resistance. The input data used were:

System 1
(Rmax = 0.05
(Km = 0.001
(COP = 0

System 2
(Rmax = 0.05
(Km = 0.001 - 0.15
(COP = 0

D = 1
b = 0.05
a = 0.0001
n = 10

The shapes of the predicted responses are very similar to those produced when only one respiratory system was present. In fact, from the shapes of the curves alone, there is nothing to suggest the presence of two independent systems.

ii) The Effect of Varying the COP

The use of the COP option in the model is meaningless unless there is some diffusional impedance to the flow of oxygen. If, for

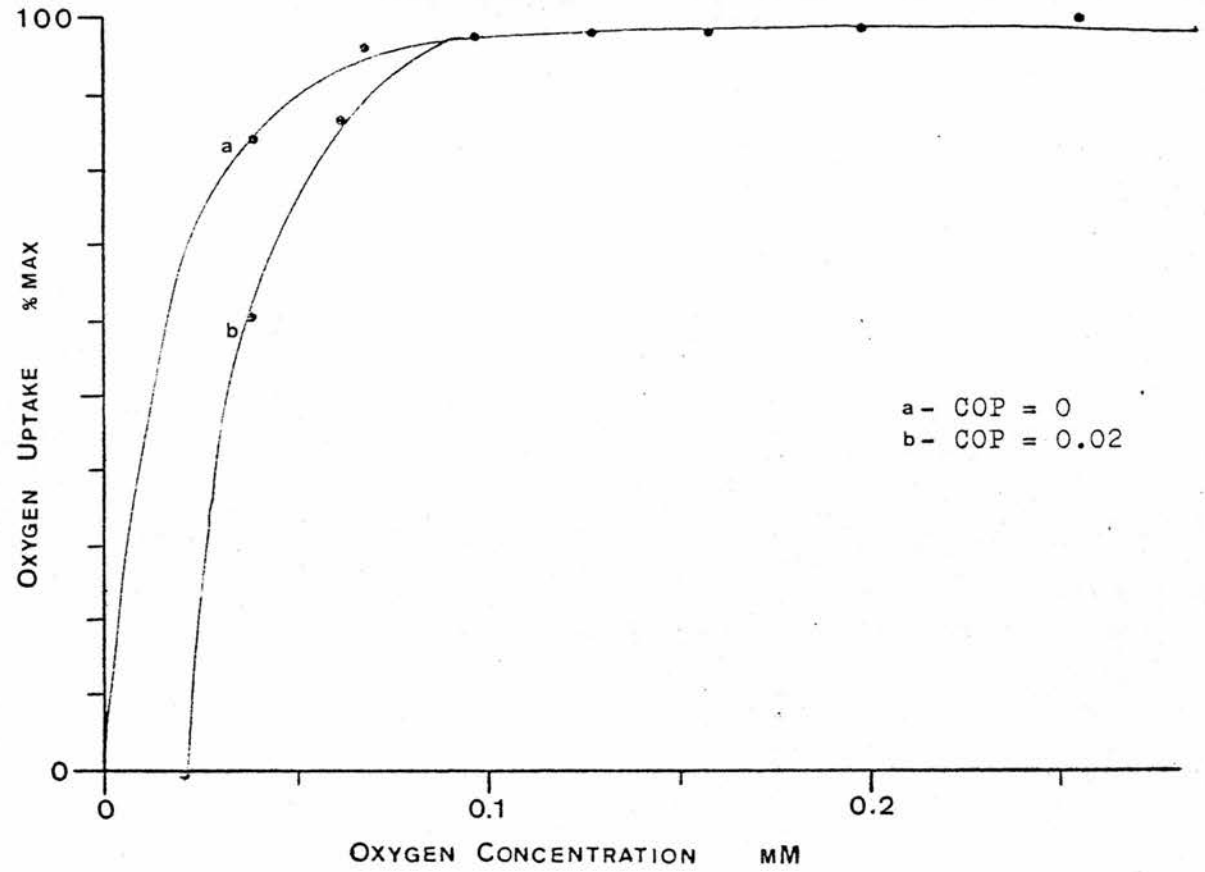

Fig 1.45 - Model Prediction. Effect of varying the critical oxygen concentration (see text). Single respiratory system.

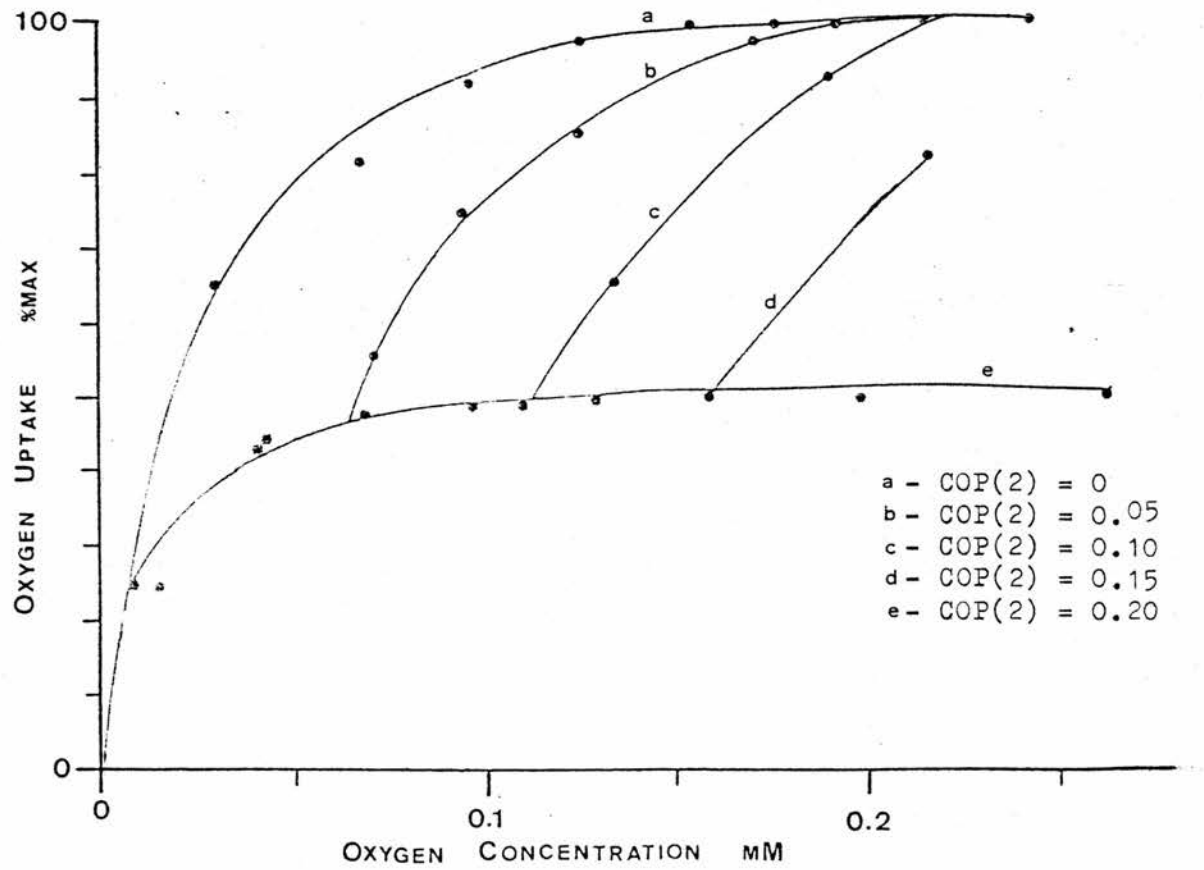

Fig 1.46 - Model prediction. Effect of varying the critical oxygen concentration in one of two systems (see text).

example, there was no diffusional resistance, then the predicted response would show a hyperbola with a sharp cutoff point at the critical oxygen concentration - a situation which was never found in any of the experiments. Therefore, the diffusional resistance was set arbitrarily as the diffusion coefficient for oxygen movement through water at 23°C (MILLINGTON, 1955). Fig 1.45 compares the predicted response of a hypothetical root with and without the COP option. The input data used were:

Without any COP:
Rmax = 0.05
Km = 0.001
COP = 0
D = 2.267×10^{-5}
b = 0.05
a = 0.0001
n = 10

With COP = 0.02
Rmax = 0.05
Km = 0.001
COP = 0.02
D = 2.267×10^{-5}
b = 0.05
a = 0.0001
n = 10

In this example, where there is only one respiratory system, the two curves are very similar except that the one with the COP drops off more sharply at low oxygen concentrations and finally falls to zero at a concentration of 0.02 mM.

In the case where there are two respiratory systems, some interesting effects can be observed. Figure 1.46 shows the predicted response of a hypothetical root in which there are two respiratory systems. The two systems are identical except that one has a COP of zero, while the COP of the other is varied from 0 to 0.2. The input data used were:

System 1
Rmax = 0.05
Km = 0.001
COP = 0

System 2
Rmax = 0.05
Km = 0.001
COP = 0 - 0.2

D = 2.267×10^{-5}
b = 0.05
a = 0.0001
n = 10

The graphs show clearly that as the COP of the second system is increased, the response becomes diphasic, with a sharp change at the COP of the second system. Initially, as the oxygen concentration declines, the rate of oxygen uptake by the second system drops steeply as the inner regions of the root will have an oxygen concentration below the COP for the second system. Oxygen uptake by the second system ceases completely when this inner zone expands to include the whole diameter of the root.

iii) The Effect of Varying the Diffusion Coefficient

Figure 1.47 shows the predicted response of a root with one respiratory system, in which the diffusion coefficient is varied. The input data used were:

$$
\begin{aligned}
\text{Rmax} &= 0.2 \\
\text{Km} &= 0.001 \\
\text{COP} &= 0 \\
\text{D} &= 1 \times 10^{-5} - 1 \times 10^{-4} \\
\text{b} &= 0.05 \\
\text{a} &= 0.0001 \\
\text{n} &= 10
\end{aligned}
$$

The effect of lowering the diffusion coefficient (i.e. making the root tissue less permeable to oxygen) is broadly similar to lowering the Km (see above). However, the curves in which diffusion is the limiting factor tend to slope off more steeply at low oxygen concentrations and reach the maximum rate of oxygen uptake at lower concentrations than comparable curves in which there is no diffusional resistance and where the curves therefore follow pure Michaelis-Menten kinetics.

The diffusional resistance of the root tissue will obviously affect equally all respiratory systems that may be present. For simplicity, therefore, the above model analysis was carried out assuming the presence of only one system.

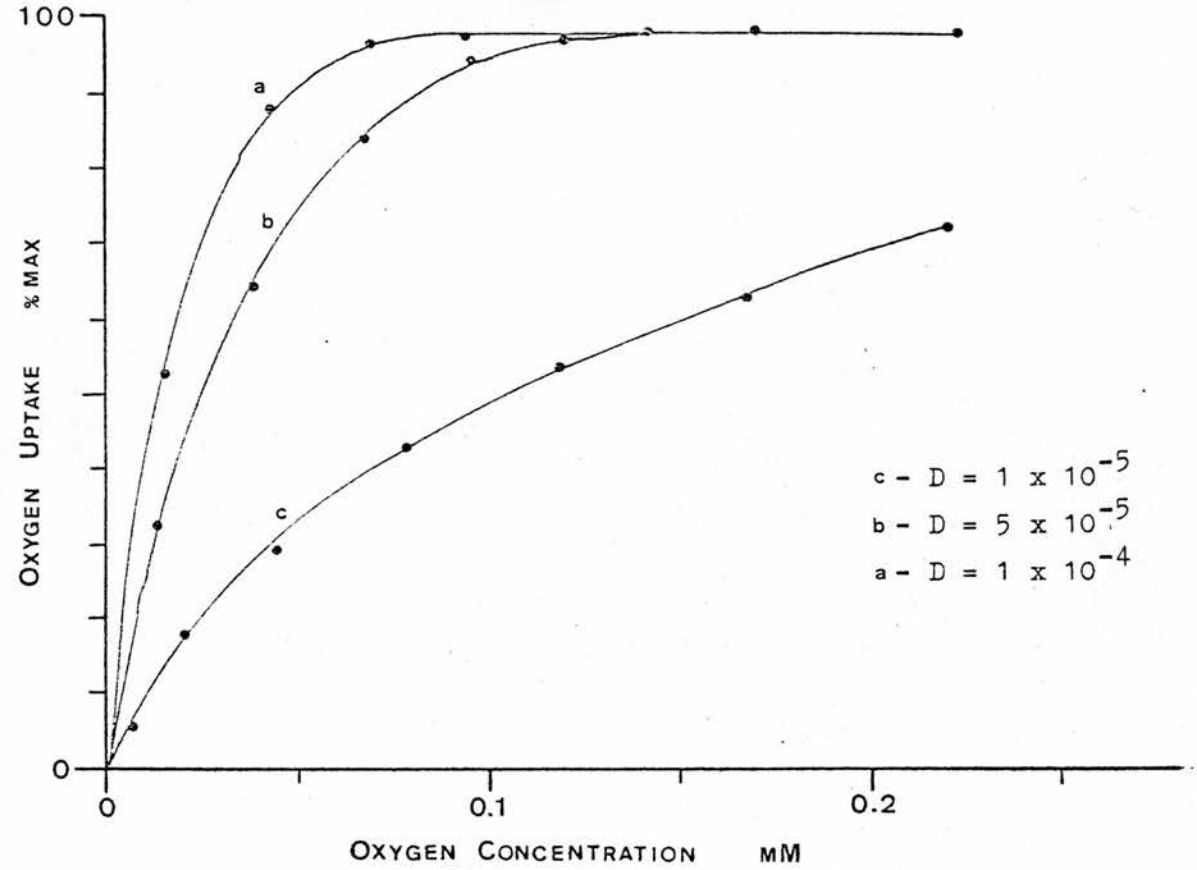

Fig 1.47 - Model prediction. Effect of varying the diffusion coefficient (see text). Single respiratory system.

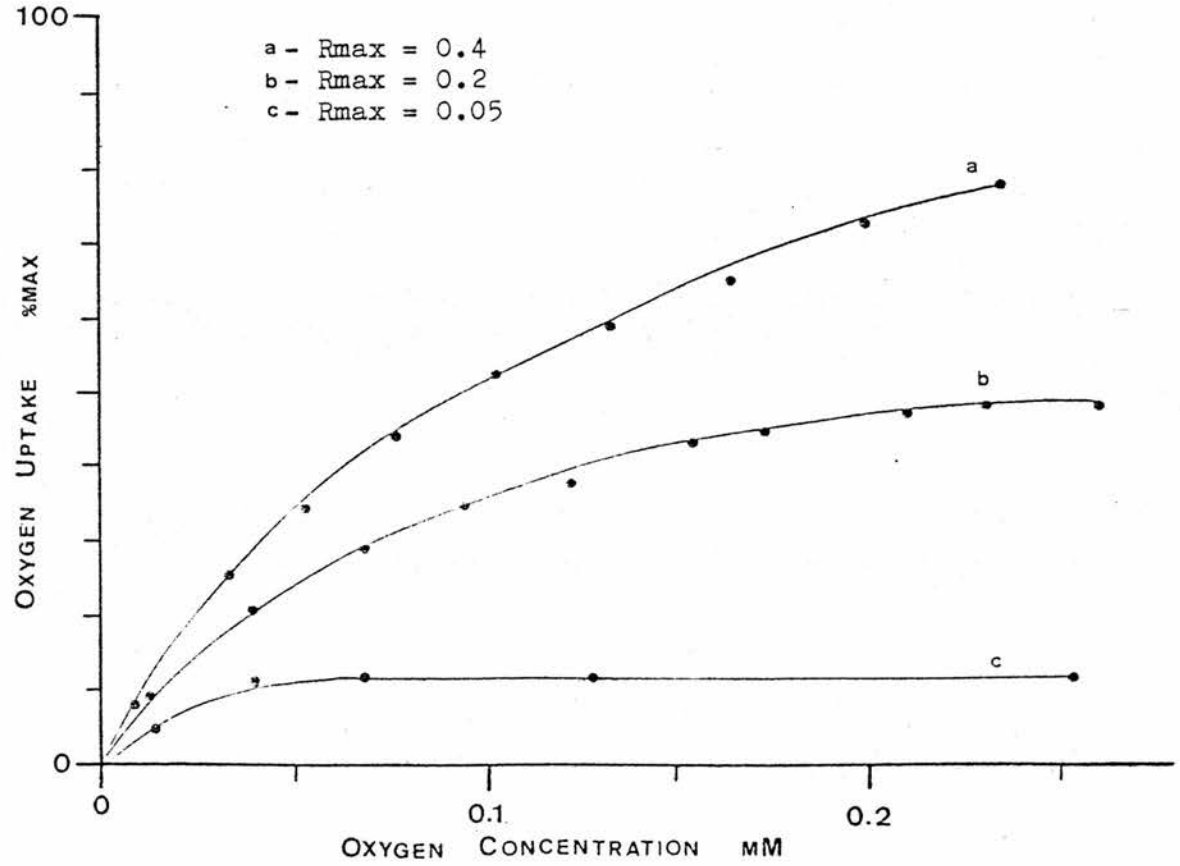

Fig 1.48 - Model prediction. Effect of varying the maximum rate of respiration (see text). Single respiratory system. All curves are plotted relative to the curve for Rmax = 0.4.

iv) The Effect of Varying the Maximum Rate of Oxygen Uptake

The maximum rate of oxygen uptake will only affect the response curve of a root section in which diffusion is a limiting factor. Clearly, if there was no diffusional resistance, the shape of the response would be the same regardless of the rate of oxygen uptake, and would depend only on the Km and the COP. However, in the case where diffusional resistance is limiting the supply of oxygen to the inner regions of the root, an increase in the rate of oxygen uptake would cause this supply to be further limited, and could be expected to alter the shape of the response curve.

Figure 1.48 shows the predicted response of an excised root in which the rate of oxygen uptake is limited by diffusional resistance, and in which the potential maximum rate of oxygen uptake is varied. The input data used were:

$$
\begin{aligned}
\text{Rmax} &= 0.05 - 0.4 \\
\text{Km} &= 0.001 \\
\text{COP} &= 0 \\
D &= 2.267 \times 10^{-5} \\
b &= 0.05 \\
a &= 0.0001 \\
n &= 10
\end{aligned}
$$

At the lowest respiration rate (0.05), the maximum rate of oxygen uptake is maintained over most of the range of oxygen concentrations. Only at low concentrations does the rate become limited. At the highest respiration rate (0.4), however, the effect of the diffusional impedance is very high and the root is unable to reach its maximum potential rate of oxygen uptake within the range studied (from zero oxygen concentration up to the concentration of oxygen in air-saturated water). Nevertheless, although this example did not reach its maximum rate at any point, the actual rate of uptake at any given oxygen concentration was always higher than that of any of the other curves.

v) The Effect of Varying Both the Maximum rate of Oxygen Uptake and the Diffusion Coefficient

So far, the factors which might influence the response of a root section have only been examined singly. Varying more than one of these factors at a time is obviously more complex and the number of possible combinations too great to study here. However, one interesting effect which came to light was the result of simultaneously lowering the maximum rate of oxygen uptake and increasing the diffusion coefficient. The input data used were:

a)
Rmax = 0.4
Km = 0.001
COP = 0
D = 2.3×10^{-5}
b = 0.05
a = 0.0001
n = 10

b)
Rmax = 0.2
Km = 0.001
COP = 0
D = 9.1×10^{-5}
b = 0.05
a = 0.0001
n = 10

Figure 1.49 shows the predicted responses of the two cases. Clearly visible is a 'crossover' point, below which the root with the lower maximum rate of respiration is able, because of its higher diffusion coefficient, to maintain a higher actual rate of oxygen uptake than the root with the higher maximum rate of respiration.

vi) Model Simulation of Chamaenerion and Juncus

Chamaenerion angustifolium (fig 1.12) and Juncus effusus (fig 1.15) behaved quite differently when their rates of oxygen uptake were examined with the oxygen electrode. Chamaenerion was able to maintain its respiration rate at a constant level until very low oxygen concentrations were reached, whereas the oxygen uptake of Juncus started to decline as soon as the oxygen concentration started to fall below the starting value of air-saturated buffer. On the other hand,

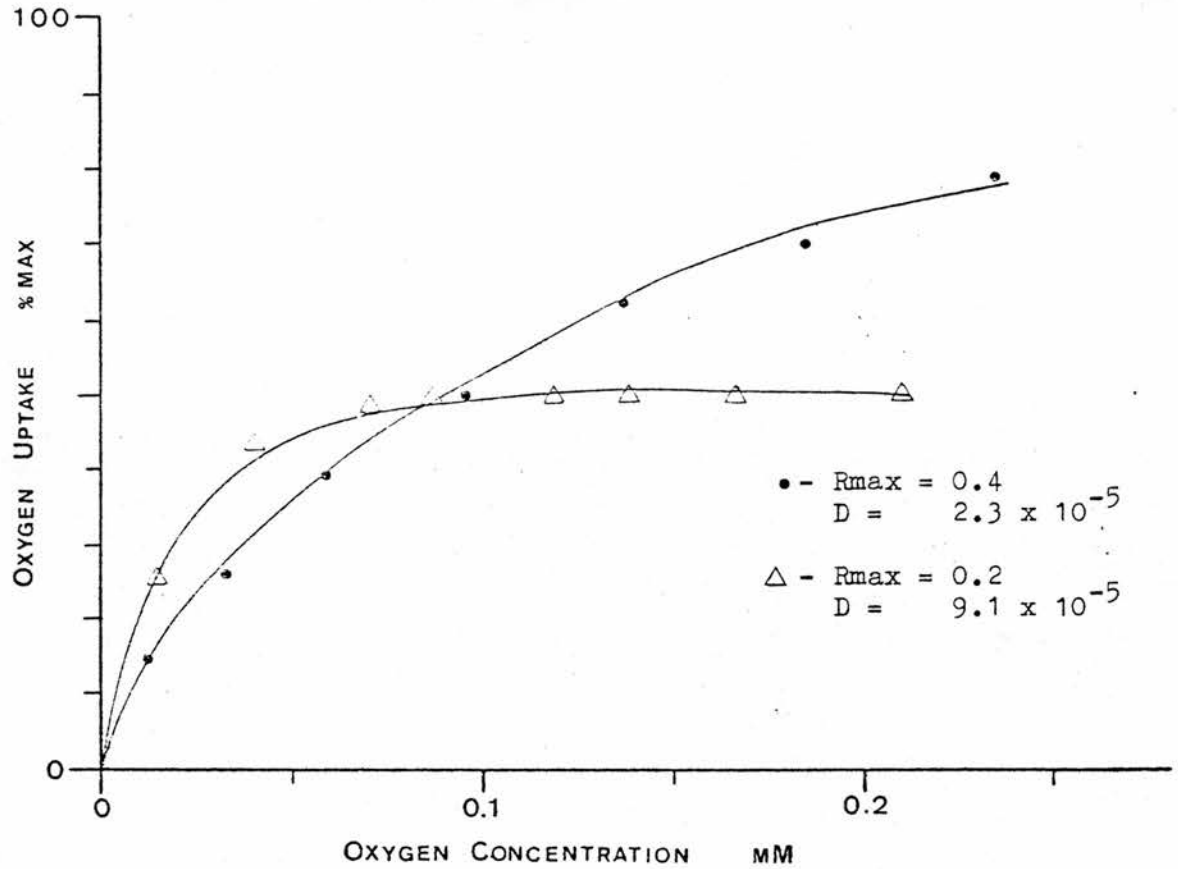

Fig 1.49 - Model prediction. Effect of varying both the diffusion coefficient and the maximum rate of respiration (see text). Both curves plotted relative to Rmax = 0.4.

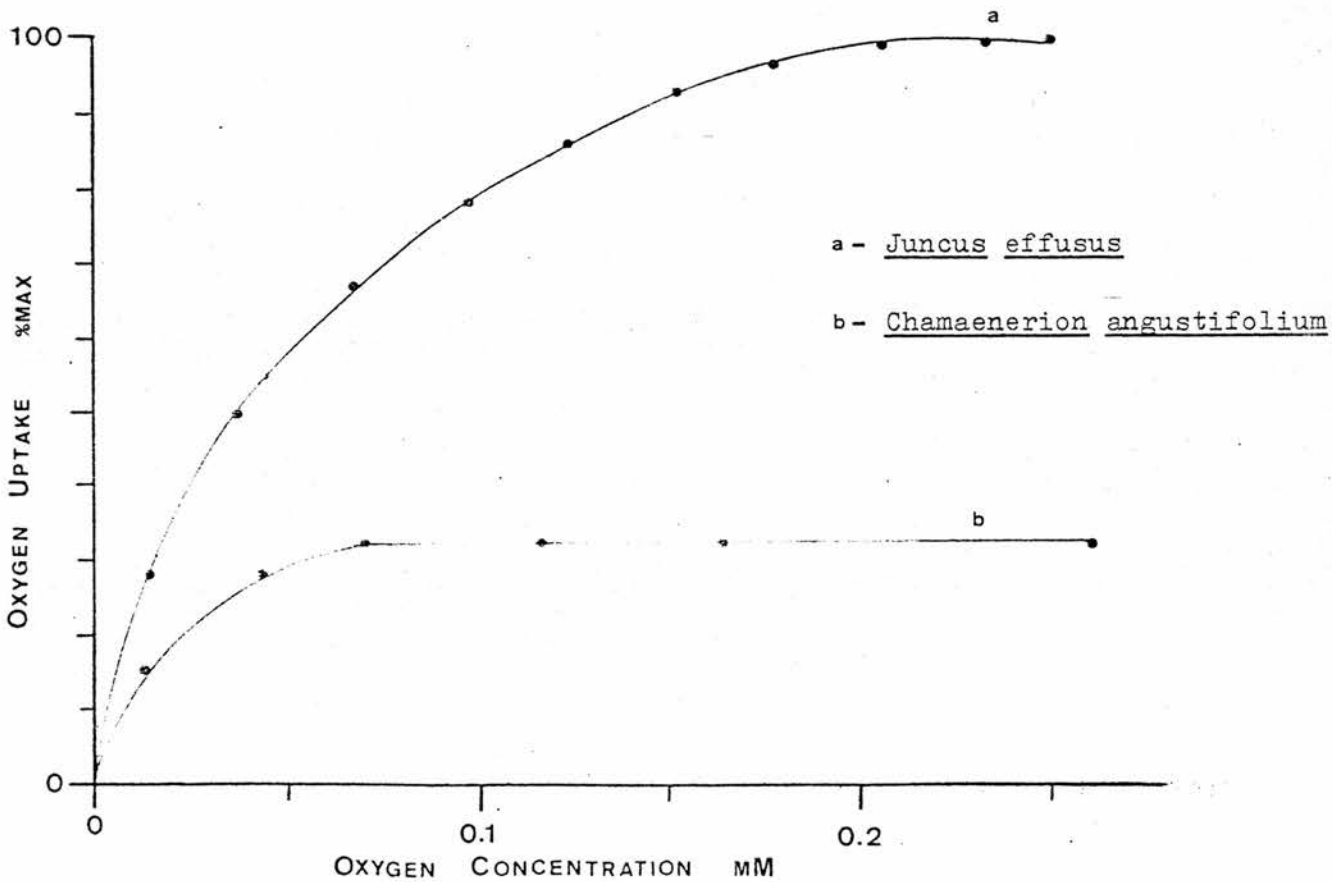

Fig 1.50 - Model prediction. Predicted responses of Chamaenerion angustifolium and Juncus effusus (see text).

the maximum rate of oxygen uptake in Juncus was three times higher than that of Chamaenerion , when expressed per unit length of root. It was decided to set up the model to simulate the response of Chamaenerion and then to see if the response of Juncus could be obtained simply by increasing the maximum rate of respiration.

It was assumed that oxygen uptake in Chamaenerion was due entirely to the cytochrome system, which is known to have an extremely high affinity for oxygen. The value chosen for the Km was therefore 1×10^{-5} mM, which is of the order of magnitude found for oxygen uptake by isolated mitochondria (CHEVILLOTTE, 1973). The response of whole root respiration in Chamaenerion showed a much higher oxygen concentration for half-maximal respiration, and it was therefore concluded that this was a diffusion-limited system. The value of the diffusion coefficient used in the model was calculated from equation 1.11, slightly modified from BERRY and NORRIS (1949).

$$D = \frac{Q}{4\pi C} \quad cm^2\ sec^{-1} \qquad (1.11)$$

where D is the diffusion coefficient, Q is the maximum rate of oxygen uptake (μmoles/cm/sec) and C is the external oxygen concentration at which oxygen uptake just starts to become limited (μM). (* see note on P. 39).

The input data used in the model simulation were:

Rmax = 0.05
Km = 1×10^{-5}
COP = 0
D = 2.09×10^{-5}
b = 0.05
a = 0.0001
n = 10

The response curve predicted by the model is shown in figure 1.50. Comparing this with figure 1.12 shows that the predicted behaviour according to the calculator model corresponds very closely to the results which were obtained in the actual experiment. The rate of oxygen uptake remains unaffected by oxygen concentration until a low concentration of oxygen is reached.

The maximum rate of oxygen uptake in Juncus was 0.155 μmoles/cm/hr. If the only difference between the two species is in their rate of respiration, then substitution of this value into the input data used for Chamaenerion should produce a response curve similar to that obtained in the actual experiment on Juncus. Figure 1.50a shows the model prediction such a substitution produces. Clearly, the result of the original experiment showed a much higher dependence of oxygen uptake on external oxygen concentration than is predicted by the model. This strongly suggests that the diffusional resistance to oxygen movement was higher in the Juncus root tips than in those from Chamaenerion, unless one is to postulate some difference in the affinity of the tissues for oxygen.

* Footnote: Both equations 1.11 and 1.12 assume that the external oxygen concentration at which respiration is just limited corresponds to a zero oxygen concentration at the centre of the respiring tissue. In other words, they assume that the rate of respiration is independent of oxygen concentration. This is not strictly true, but because of the extremely high affinity of the cytochrome system for oxygen, the error involved is likely to be small.

e) Discussion

The purpose of the preceeding introductory discussion was to outline those factors which will determine the behaviour of the root tip zone under hypoxia. It is now necessary to examine closely the experimental results to interpret them in the light of what has been said so far and also to assess their ecological significance.

The first conclusion which can be drawn is that in those samples in which root oxygen uptake shows a low affinity for oxygen, diffusion is the limiting factor. Two observations lead to this conclusion. Firstly, in the majority of the experiments, oxygen concentrations for half-maximal respiration are well in excess of those recorded for both cytochrome oxidase and the alternate oxidase (SOLOMOS, 1977). Secondly, the shape of many of the curves is more suggestive of a diffusion-limited system rather than a pure enzyme-substrate reaction. BERRY and NORRIS (1949) conducted a similar series of experiments to investigate the effect of oxygen partial pressure on respiration in the onion root tip. They concluded that the inhibition of oxygen uptake at low oxygen concentrations was due to diffusion, and in support of this conclusion they found that the activation energies for their calculated diffusion coefficients agreed closely with those predicted for diffusion-limited reactions.

It has been pointed out in the General Introduction, however, that there has been recent criticism of such in vitro measurements of oxygen uptake and diffusion coefficients on the grounds that immersion of an excised root segment in aqueous solution may lead to some flooding of the intercellular air spaces (ARMSTRONG and GAYNARD, 1976). PRADET (1978), however, has pointed out that such criticism would not apply to experiments on young seedlings in which respiration also shows a hyperbolic relationship to declining oxygen concentration. A detailed consideration of the diffusion of oxygen within the root tip may help to clarify the situation.

In its path through the root tissue, oxygen must diffuse through the intercellular spaces, across the cell wall and plasmalemma, through the cytoplasm and finally across the mitochondrial membranes before it can combine with cytochrome oxidase. Each of these stages will be characterised by a specific diffusion coefficient and experimental data on each separate coefficient is obviously difficult to obtain. However, it is possible to simplify the situation and consider the movement of oxygen as occurring in two stages, namely intercellular and intracellular diffusion.

If it is assumed that the epidermis is freely permeable to oxygen (ARMSTRONG and WRIGHT, 1975) and that diffusion through the intercellular spaces is adequate, then a hyperbolic response of respiration to oxygen concentration would have to be attributed to a low rate of intracellular diffusion. For a spherical cell with a uniform internal distribution of mitochondria, the intracellular diffusion coefficient can be calculated from equation 1.12 (CHEVILLOTTE, 1973).

$$D = \frac{Vm\ R^2}{6Cr} \qquad (1.12)$$

where Vm is the maximum rate of oxygen uptake ($g/cm^3/sec$), R is the radius of the cell (cm), Cr is the external oxygen concentration at which respiration is just limited (g/cm^3), and D is the diffusion coefficient (cm^2/sec). (* see P.39)

Using the data from BERRY and NORRIS (1949), estimates can be given for the apparent intracellular diffusion coefficient, assuming that intercellular diffusion is not limiting. The calculated values were obtained (Table 1.6) assuming a mean cell radius of 20μ and 50μ, to cover the range of cell size likely to occur in the young root tip (ESAU, 1960). The calculated values obtained by this method are between two to three orders of magnitude lower than the diffusion coefficient for oxygen in water. CHEVILLOTTE (1973) calculated the intracellular diffusion coefficient for oxygen in potato tuber cells

ROOT ZONE	TEMP °C	Vm g/ml/sec x 10^{-7}	Cr g/ml x 10^{-5}	D (cm^2/sec) r = 20μ x 10^{-9}	D (cm^2/sec) r = 50μ x 10^{-9}
0 - 5mm	15	1.529	0.720	14.2	88.5
	20	2.192	0.910	16.1	100
	30	4.751	1.606	19.7	123
5 - 10mm	15	0.719	0.480	9.99	62.4
	20	0.990	0.650	10.2	63.5
	30	2.478	0.750	22.0	138

Table 1.6 - Apparent Intracellular Diffusion Coefficient in the Onion Root Tip.

This table shows the calculated intracellular diffusion coefficients required to produce the critical oxygen pressures found in the onion root tip by Berry and Norris (1949b) (see text). The figures were calculated assuming that intracellular diffusion was the only factor responsible for the observed critical oxygen pressures. Calculated coefficients are shown for a mean cell radius of 20μ and 50μ .

Vm - maximum rate of oxygen uptake

Cr - observed critical oxygen pressure

D - calculated intracellular diffusion coefficient

ROOT ZONE	TEMP °C	Vm g/ml/sec x 10^{-7}	Cr (g/ml) r = 20μ x 10^{-7}	r = 50μ x 10^{-7}
0 - 5mm	15	1.529	1.79	11.2
	20	2.192	2.56	16.0
	30	4.751	5.56	34.7
5 - 10mm	15	0.719	.841	5.26
	20	0.990	1.16	7.24
	30	2.478	2.90	18.1

Table 1.7 - Calculated Critical Oxygen Pressures of the Onion Root Tip.

This table shows the predicted critical oxygen pressures of the onion root tip, assuming that intracellular diffusion was the only factor responsible for such critical pressures, and that the intracellular diffusion coefficient is 5.7 x 10^{-7} cm^2/sec (Chevillotte, 1973). These values are calculated using the data of Berry and Norris (1949b), for a mean cell radius of 20μ and 50μ .

Vm - maximum rate of oxygen uptake

Cr - calculated critical oxygen pressure (note - 1 atm = 9.1 x 10^{-6} g/ml)

to be 5.7×10^{-7} cm^2 sec^{-1}, which is approximately an order of magnitude higher than the values shown in Table 1.6. KROGH (1919) investigated the movement of oxygen across sheets of muscle and connective tissue and estimated the diffusion coefficient to be between 6.2 and 7.5×10^{-6}. The assumption that intracellular diffusion is responsible for the hyperbolic curves so widely reported, therefore, implies values for the intracellular diffusion coefficient which are much lower than those generally accepted for plant and animal tissues. Furthermore, it must be pointed out that the values shown in Table 1.6 must be regarded as maxima, since equation 1.12 is only valid for a cell in which there is a uniform distribution of respiratory sites (i.e. mitochondria). CHEVILLOTTE (1973) provides some evidence for such a cell structure in higher plants, but this is in direct contradiction to the widely held view that mature plant cells are generally characterised by a peripheral distribution of cytoplasm around a large, central vacuole. For a cell in which most of the cytoplasm was distributed peripherally, a hyperbolic response to declining oxygen uptake such as that found by BERRY and NORRIS (1949) would only occur if the diffusion coefficient within the cell was substantially lower than the values shown in Table 1.6.

If the diffusion coefficient of CHEVILLOTTE (1973) is regarded as a more accurate measure of intracellular diffusion, then, using this value and rearranging equation 1.12 enables the critical oxygen concentration for an individual root cell to be predicted. The values calculated in this manner, using again the data for the onion root tip (BERRY and NORRIS, 1949), are shown in Table 1.7. These values are consistent with the results of other experiments on plant tissues in which intercellular diffusion is not a limiting factor (YOCUM and HACKETT, 1957; FORRESTER *et al*, 1966; CHEVILLOTTE , 1973).

Although the above discussion is somewhat tentative due to the scarcity of relevant data, the strong suggestion is that intracellular diffusion in the plant cell is adequate to maintain unrestricted

aerobic respiration even at low extracellular concentrations of oxygen. The hyperbolic curves reported by BERRY and NORRIS (1949) and those obtained in this project, therefore, must be largely due to an intercellular impedance to oxygen movement.

The model predictions presented earlier showed that in a root with a respiration rate of 0.2µmoles/cm/hour (four times that of Chamaenerion, and three times that of the apical 5mm of an onion root at 20°C (BERRY and NORRIS, 1949)), the rate of oxygen uptake will be largely unaffected by external oxygen concentration provided that the apparent diffusion coefficient of the root is above 1×10^{-4}. For a root segment in which the intercellular air space system occupies 1% of the total volume, and in which the tortuous pathway between the air spaces can be represented by a tortuousity factor of 0.4 (JENSEN et al, 1967), the effective diffusion coefficient for diffusion in the gas phase alone, calculated from equation 1.13, will be 8.2×10^{-4}.

$$De = Do\ t\ P \qquad \text{(ARMSTRONG and WRIGHT, 1975)} \qquad (1.13)$$

where De is the effective diffusion coefficient, Do is the diffusion coefficient for oxygen in air, t is the tortuousity factor and P is the fractional porosity of the root.

From the model prediction, therefore, it is clear that even a very small volume of intercellular air space should allow sufficient diffusion of oxygen within the root for uninhibited aerobic respiration, even at low external oxygen concentrations. Experimental results which show a hyperbolic relationship, therefore, would suggest, as predicted by ARMSTRONG and GAYNARD (1976), that under the in vitro conditions of the experiment, there is a substantial amount of flooding of the intercellular gas space system. This conclusion is supported by the finding, presented earlier, that two hours immersion in buffer reduced the air space content of rice root segments to 40% of its original value. From what has been said above, it might be thought that the remaining air space might still be sufficient to

allow adequate diffusion of oxygen. However, it is unlikely that this remaining air space is distributed uniformly throughout the root. More likely, after a period of immersion, the intercellular air spaces in the region near the excision will be totally flooded, while those further away will be largely intact. Consequently, oxygen uptake in the 'flooded zone' will be limited by diffusion, even if other areas within the root are unaffected.

The hyperbolic responses obtained in this project can therefore be explained as follows: As the experiment progresses, the root tip will be subjected to a progressive flooding of the intercellular air space system and a declining oxygen concentration in the external solution. These two factors, acting together, will tend to reduce the rate of oxygen uptake measured for the whole root tip. The extent of this reduction and the shape of the response will depend on the rapidity of flooding , the oxygen demand of the root tissues, and other factors such as the sensitivity of individual cells to low extracellular oxygen concentrations. The results of other workers (YOCUM and HACKETT, 1957; FORRESTER et al, 1966; ARMSTRONG and GAYNARD, 1976) and the model predictions presented earlier strongly suggest that in the intact root tip, oxygen uptake from the external medium (as well as from internal aeration) will only become restricted at relatively low oxygen concentrations.

The experiment in which air space was measured in rice root segments showed that even after two hours immersion, there was a substantial amount of remaining air space. Therefore, while the initial decline in oxygen uptake can be attributed largely to flooding of the air space system, one might expect there to be, at low oxygen concentrations, a sharp turn in the curve as the 'unflooded' tissues remaining in the root experience their critical oxygen pressure. This is indeed found in a number of the graphs. In Deschampsia caespitosa (fig 1.23) and Phalaris arundinacea (fig 1.34), for example, a sharp decline can be seen at an oxygen concentration of approximately

25uM (0.02 atm). This is close to the critical oxygen pressures calculated for intact plant roots by ARMSTRONG and GAYNARD (1967).

The above analysis still leaves a number of questions unanswered. In particular, one must ask why, even under the *in vitro* conditions of the experiment, *Chamaenerion* (fig 1.12) and *Caltha palustris* (fig 1.11) showed a remarkable insensitivity to a lowering of the external oxygen concentration. The experiment with *Chamaenerion* was repeated, using the apical 0.5 cm of the root instead of the apical 1 cm (fig 1.13), and a different response was obtained. A response such as that shown by *Caltha* could be explained if the root oxygen demand was so low that, even with flooding of the air space system, diffusion only became limiting at low oxygen concentrations. However, this would not explain the difference between the two *Chamaenerion* experiments, especially since the rate of oxygen uptake in the second experiment was actually lower than in the first one. Since diffusion of oxygen through water is more rapid than through a plant cell (see the above discussion on intracellular diffusion), differences in porosity should still be apparent from *in vitro* experiments, even if considerable flooding of the air spaces occurs. Thus, the difference between the two *Chamaenerion* experiments could be due to a lower porosity in the apical 5 mm. In the first experiment (fig 1.12), one must assume that the more apical regions had remained largely unflooded. The assumption of a lower porosity in the apical region is consistent with observations made by other workers (ARMSTRONG, 1978; ESAU, 1960).

The observation that the root tip zone, and in particular the meristematic regions, is a region of high respiratory activity and low porosity has lead some authors to propose that, even in well-aerated conditions, some degree of anaerobiosis is likely (CRAWFORD, 1976). Evidence that ethanol can be detected in root tips even under aerobic conditions certainly supports such a hypothesis. However, the fact that even under the adverse experimental conditions used, species such as

Caltha were able to maintain unrestricted oxygen uptake down to very low oxygen concentrations suggests that, at least in some instances, not even the apical meristem is subjected to an oxygen stress at normal oxygen levels. Results from the other species studied in this project give little indication as to whether or not this is a general phenomenon. Clearly, more experimental work is required, but some conclusions can be drawn from the model predictions presented earlier. If, for example, the meristematic region consists of closely packed cells with high respiratory activity and few intercellular air spaces, then, because of the low diffusion coefficient for intracellular oxygen diffusion, the model would suggest (fig 1.47) that oxygen uptake would be strongly limited by diffusion. However, over the short length of the meristematic region, there will be a significant longditudinal diffusion component, and no account is made for this by the model. Moreover, ESAU (1960) reports that the intercellular air spaces start to develop close to the promeristem and EVANS and HOWARD (1961) suggest, from studies on Vicia faba that the internal air space system may be continuous with fine channels extending into the meristematic tissue. It is possible, therefore, that the aeration of the meristem is much greater than has previously been supposed.

A description has already been given of an attempt to use the model to directly compare the responses of Juncus and Chamaenerion. The surprising conclusion from this comparison was that the root tip of Juncus was less permeable to oxygen than that of Chamaenerion. It has already been pointed out that differences in permeability due either to different air space contents or to other factors should be apparent from in vitro studies, so that it is unlikely that the difference between these two species is an artefact. The difference is surprising since Juncus, a wetland plant, almost certainly has a higher air space content than Chamaenerion. Although it would be unwise to make any generalisation on the basis of this single comparison,

there is a suggestion that the differences might be accounted for by a lower permeability of the root wall, or even of the root cells. Such differences are exaggerated by the use of *in vitro* techniques and are therefore easier to detect. Since they would be much less apparent in the *in vivo* situation, however, their ecological significance is questionable.

Similar differences in permeability can also be seen between flooded and unflooded samples of the same species. In the experiment on *Ammophila arenaria* for example (figs 1.38 and 1.39), the effect of flooding is to induce a lowering of the respiration rate and an increase in the root permeability. The increase in permeability can be deduced from the fact that at oxygen concentrations below approximately 0.13 mM, the actual rate of oxygen uptake was higher in the flooded samples, whereas the maximum rate of oxygen uptake, at high oxygen concentrations, was lower than in the unflooded sample. Reference to the model predictions (fig 1.49) indicate that this situation will occur where the drop in the maximum rate of oxygen uptake is accompanied by an increase in the permeability of the root tissue. From observations made by other workers (YU *et al*, 1969), it would seem likely that this increase in permeability is due to the greater development of the gas space system in flooded plants.

This decline in the respiratory oxygen demand of the root along with an increase in porosity has been interpreted as a mechanism for increasing the internal supply of oxygen to the root system under conditions of soil waterlogging (ARMSTRONG, 1978). It is tempting to suggest, from the experiments on *Ammophila* (figs 1.38 and 1.39) and *Phalaris* (figs 1.34 and 1.35), that an additional effect will be to increase the efficiency of oxygen uptake at low oxygen concentrations. From what has been said regarding the use of *in vitro* experiments, however, it is more likely that in the intact plant, where the response of oxygen uptake would be more like that shown by *Caltha* (fig 1.11), such an effect will be barely apparent.

It can be seen from the results of the experiments, that in some cases oxygen uptake ceased completely before the oxygen concentration in the buffer had reached zero. This effect did not appear to be correlated with any pre-treatment, and was most pronounced in Senecio jacobaea where, in one experiment, oxygen uptake ceased when the external oxygen concentration was as high as 0.05 mM (fig 1.16). The most likely explanation for this phenomenon is that the development of anaerobic centres within the root tissues leads to the production of toxic by-products, such as ethanol, and that the cessation of oxygen uptake is due to the presence of these metabolites rather than to the low oxygen concentration per se. Again, this effect would probably not occur in vivo until extremely low oxygen concentrations were reached.

The exact role of the alternate oxidase and its possible effects on the oxygen relations of plant root tips are still not clear. LAMBERS and SMAKMAN (1978) have suggested that, in the genus Senecio, the presence of an alternate oxidase with a low affinity for oxygen may lead to a genuine hyperbolic response, even in the intact plant. YOCUM and HACKETT (1957), however, found that in the aroid spadix, a tissue known to have a high percentage of cyanide-resistant respiration, oxygen uptake was unaffected by lowering of the external oxygen concentration until a partial pressure of about 0.02 atm was reached. Certainly, not even the highest estimates for the apparent Km of the alternate oxidase can account for the hyperbolic curves obtained here (SOLOMOS, 1977). However, the half-saturation oxygen concentration calculated by LAMBERS and SMAKMAN (1978) for Senecio aquaticus (22 uM) agrees closely with experiments on microorganisms (SOLOMOS, 1977). The inhibition experiments carried out in this project confirmed the existence of a cyanide-insensitive pathway in the genus Senecio, though it is not possible to make any generalisations from the results on this genus alone. Oxygen uptake behaviour of Senecio did not differ markedly from that of other species, apart from a pronounced diphasic

response in some cases (fig 1.28). Predictions from the model, however, indicate that such a response could not be attributed to the presence of two respiratory systems with different affinities for oxygen (fig 1.44), so that the precise reasons for the diphasic response are obscure. One would expect, however, that the presence of an alternate oxidase with a half-saturation oxygen concentration of 22 μM would substantially affect oxygen uptake behaviour, but this does not appear to be the case. More experimental work is required to find the extent to which the alternate oxidase system is present in higher plants and to obtain further information on its affinity for oxygen, preferably using intact plants. It is possible, for example, that the hyperbolic responses obtained by LAMBERS and SMAKMAN (1978) were due to a low root wall permeability in the sub-apical regions of the root system (ARMSTRONG, 1978), and not to the presence of the alternate system.

1.4 CONCLUSIONS

Since the onset of waterlogging results in the rapid development of anaerobic conditions in the soil, it is clear that the oxygen relations of the plant root system will be of prime importance in determining an ability to withstand waterlogged conditions. From the results of experiments such as those carried out by BERRY and NORRIS (1949) and LUXMOORE *et al* (1970), it has generally been believed in the past that the rate of aerobic respiration in a plant root was closely dependent on the concentration of oxygen in the external medium. Thus, the observations of BOYNTON *et al* (1938) that apple tree roots required at least 12% oxygen in the soil air for the growth of new roots could be explained as a direct effect of concentrations lower than this on root respiration. It was originally hoped, therefore, that the experiments carried out in this project would reveal a higher affinity for oxygen in species tolerant of waterlogging. From the facts which have emerged in the preceding discussion, however, one can conclude that it is unlikely that major differences in affinity for oxygen exist between plant species.

This conclusion can be drawn from the results of experiments on intact plants (ARMSTRONG and GAYNARD, 1976) and also from the model predictions presented earlier. Trials with the model have revealed that for a root tip with only a small percentage of air space, the radial diffusion of oxygen will still be adequate to meet the full respiratory requirements of the root even at low oxygen concentrations in the external medium. It is well known from anatomical studies that intercellular air spaces are characteristic in the cortical tissues of most, if not all, higher plant roots (ESAU, 1960). Consequently, the indication is that in the majority of plant species, root respiration in the intact plant will be largely independent of the external concentration of oxygen. Such a conclusion is supported by the findings of ARMSTRONG and GAYNARD (1976), YOCUM and HACKETT (1957) and

VARTAPETIAN et al (1978), who have all conducted experiments which show a high affinity of plant tissues for oxygen. It is clear that an affinity for oxygen which is already extremely high even in flood-sensitive species cannot be substantially improved upon.

A consideration of the soil environment also leads to the conclusion that affinity for oxygen cannot form a basis for flooding tolerance. MEEK and STOLZY (1978) and BOYNTON (1938) suggest that, generally speaking, a soil oxygen level of less than 10% will tend to limit root growth. This would appear to contradict what has been said above regarding the affinity of plant roots for oxygen. However, it is now generally accepted that the oxygen diffusion rate (ODR) is a better measure of the available oxygen than measurements of the average soil oxygen concentration (BRADY, 1974). The ODR is a measure of the rate at which oxygen consumed by plant roots can be replaced by diffusion from other regions of the soil. It is obvious that if the oxygen demand of a plant root exceeds the rate at which the supply can be replenished, an anaerobic zone will develop around the root. Therefore, the observed decline in root growth at oxygen levels below 10% is probably due to the development of depletion zones around the root system rather than to a direct concentration effect. Since the affinity for oxygen is high even in flood-sensitive species, it is clear that the rate of oxygen diffusion through the soil to the root will only increase marginally following an improvement in the affinity of the root for oxygen. The conclusion is, therefore, that the supply of oxygen to the root through the soil will depend on the properties of the soil rather than on those of the root.

Under conditions of prolonged waterlogging, the soil will become completely anaerobic. Aerobic respiration in such conditions will therefore depend on an oxygen supply from the aerial parts of the plant. Along the length of the root, some of this oxygen will be lost to the surrounding soil, depending on the permeability of the root

wall. A number of authors have shown that this loss of oxygen, in flood-tolerant species, tends to be greatest towards the root tip (PHILIPSON and COUTTS, 1978; LUXMOORE et al, 1970; ARMSTRONG, 1964), so that the soil immediately surrounding the root apex will be partially aerobic. Since internal aeration of the meristematic region may be restricted due to a lower development of the gas space system, this loss of oxygen into the surrounding soil may function as an additional means of aerating the meristematic tissues. The exact relation of oxygen uptake to external oxygen concentration in the meristem is not clear from the experiments carried out here. From the predictions of the model, however, it seems likely that the existence of small air spaces within the meristem, such as those reported by McPHERSON (1939) and EVANS and HOWARD (1961), would allow adequate diffusion of oxygen into the meristem from the surrounding medium. The combination of internal aeration and oxygen diffusion into the surrounding soil may, therefore, be sufficient to allow full aerobic respiration within the meristem in a well-adapted species growing in a waterlogged soil.

SECTION 2

Measurement of Energy Charge in Plant Roots Under Anoxia.

2.1 INTRODUCTION

Attention has been drawn recently to the concept of 'energy charge' and its role as a regulatory parameter in almost every metabolic activity in the cell (PRADET, 1978; ATKINSON, 1968). Energy charge has been defined as the number of anhydride-bound phosphates per adenosine moiety (ATKINSON and WALTON, 1967), as shown in equation 2.1.

$$\text{Energy Charge} = \frac{(ATP) + \frac{1}{2}(ADP)}{(ATP) + (ADP) + (AMP)} \qquad (2.1)$$

ATKINSON (1968) outlines how different types of metabolic reaction will respond to changes in the energy charge of the cell. These responses are summarised in figure 2.1. The argument is that enzymes involved in the regulation of ATP-regenerating sequences will tend to be inhibited by a high energy charge within the cell, whereas those involved in ATP-utilising sequences will tend to be stimulated by a high energy charge. Although somewhat simplified, this argument shows how the adenylate system can play a central role in the regulation of all energy-coupling processes in the cell.

The intersection of the two curves in figure 2.1 can be taken to represent a metabolic steady-state, corresponding to a relatively high energy charge. From experiments on a variety of plant tissues, PRADET and BOMSEL (1978) suggest that under aerobic conditions the energy charge will lie between 0.8 and 0.95. Should the energy charge fall for any reason, figure 2.1 shows that this would tend to increase the rate of ATP regeneration and reduce the rate of utilisation, and *vice versa* should the energy charge rise.

The question arises as to what happens in a situation in which the plant is subjected to some stress, such as anoxia. If, for example, the ATP-regenerating reactions within the plant were inhibited as a result of lack of oxygen, the energy charge would fall, and the

biosynthetic and other ATP-utilising reactions within the cell would be inhibited as a result. Thus, there would be a general 'slowing down' of metabolism within the cell. On the other hand, ATP-regenerating reactions which did not require oxygen (i.e. those involved in anaerobic respiration) might be stimulated, restoring the energy charge and enabling energy-consuming reactions to continue.

Either of these responses might be expected if a plant root system was subjected to anoxia. In the first case, where there is a fall in the energy charge and hence a drop in the energy-consuming processes in the cell, there are two ways of looking at the situation. The general slowing-down of metabolism can be thought of as a conservation measure, reducing the demands made on the cell's metabolism and enabling it to survive an otherwise adverse situation. On the other hand, the reduction in biosynthetic would almost certainly limit the potential for growth.

In the case in which anaerobic reactions are stepped-up to maintain the energy charge of the cell, growth and other energy-consuming reactions will be able to continue unhindered, but the cost will be a much less efficient respiratory system requiring a greater input of respiratory substrates. There is a danger, in other words, that the cell may 'burn itself out' in trying to maintain a high energy charge.

In the following experiments, attempts were made to measure energy charge levels in a number of species incubated under both aerobic and anoxic conditions. It was hoped that different patterns of response would emerge which could be correlated with the ability of the species concerned to withstand flooding.

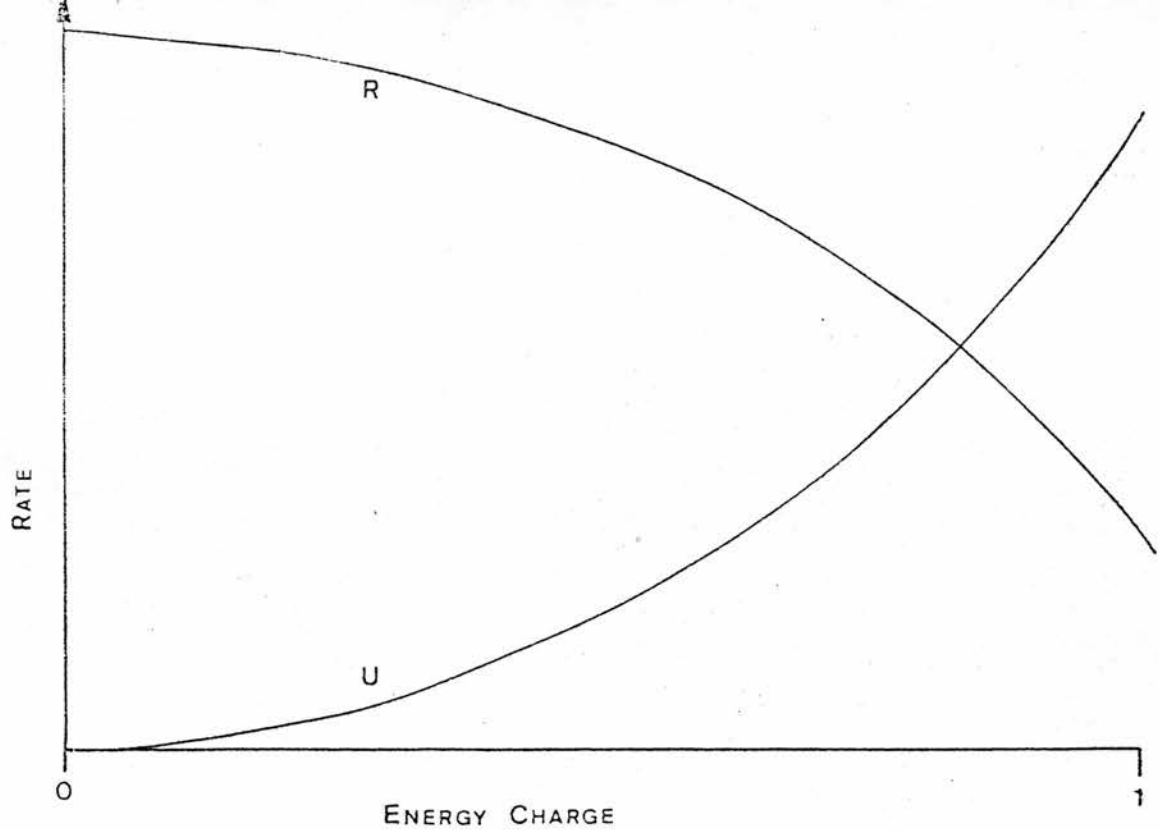

Fig 2.1 - Generalised response of ATP regenerating reactions (R) and ATP utilising reactions (U) to the energy charge of the cell. After Atkinson (1968).

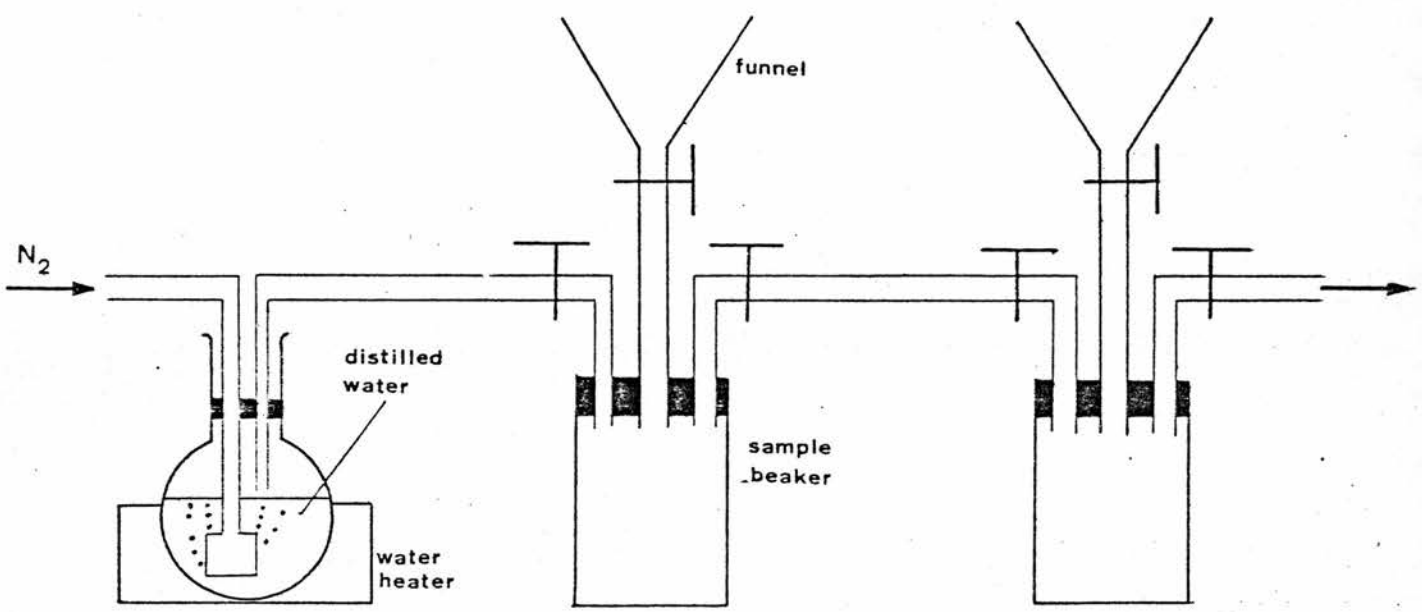

Fig 2.2 - Diagram of the gassing apparatus used in measurements of ATP/ADP ratios (see text).

2.2 MATERIALS AND METHODS

a) Plant Material

Plant species were grown in the glasshouse, either in flooded or unflooded sand culture as described in Section 1. It had originally been planned to follow energy charge in excised root apices alone, but it quickly became apparent during trial experiments that the concentration of adenine nucleotides in the root tissues was so low that a large number of root tips would be required for each experiment, far in excess of the amount of material actually available. Accordingly, energy charge was followed in portions of the whole root system.

b) Measurement of Energy Charge

Prior to each experiment, the whole root system of the plant to be investigated was removed, washed in distilled water, and then placed in 0.02% Mercuric Chloride for several minutes for surface sterilization. The root system was then divided into the number of required samples and each sample washed in distilled water before being transferred to the gassing apparataus.

The gassing apparataus (figure 2.2) was used to subject the root samples to anoxic conditions for varying lengths of time. Each root sample was placed in 10ml deoxygenated phosphate buffer (see Section 1) in a 50ml beaker which was then attached to the apparataus as illustrated. A stream of nitrogen gas, humidified by passage through warm water, was used to maintain the anoxic conditions throughout the system. Once a particular sample had been under anoxia for the required length of time, the tap below the funnel was opened and a thin piece of plastic tubing passed into the beaker to siphon off the buffer in which the root sample had been immersed. Since there was a positive pressure of nitrogen gas within each beaker, it is unlikely that any air entered during this process. Once the buffer had been

drawn off, the chamber was completely sealed by closing all three taps. In the funnel above the chamber, was placed 30ml 0.6N trichloroacetic acid (TCA) in diethyl ether, which had previously been frozen solid by immersion in liquid nitrogen. This was just allowed to thaw, and then the tap was opened, thus flooding the sample chamber with extremely cold TCA in ether and stopping all metabolic reactions within the sample. The sample beaker was then removed from the gassing apparataus and the sample immediately homogenized by means of an 'Ultra-Turrax' homogeniser. At all following stages, each sample was kept in an ice bath, until the assay stage was reached.

After the sample had been homogenized, the homogenate was poured off, and the tubes rinsed with cold 0.1N TCA in water which was then added to the homogenate. The extract was then centrifuged at 18,000 rpm for 15 mins to remove all particles and the supernatant poured off. The remaining precipitate was re-extracted with 0.1N TCA, homogenised, and centrifuged again as before. The two supernatants were then collected together and the TCA removed by washing with cold diethyl ether three times. All remaining traces of ether were removed by bubbling air through the sample. Finally, the sample was neutralised by adding drops of 0.2N sodium hydroxide. As this sometimes caused a precipitate to form, the sample was re-centrifuged for 2 mins at 10,000 rpm in a small 'Microfuge'. The sample was then assayed for adenine nucleotides immediately, or else stored in the deep freeze at -20 C for not more than a few days until it could be assayed.

As energy charge is a ratio, it was not necessary to determine actual quantities of each nucleotide per unit weight of tissue, but merely to determine their relative proportions in each sample.

The assay method was based on the firefly lantern principle (BERGMEYER, 1963), which provides a simple and sensitive method for measuring ATP. The addition of a sample containing ATP to a solution containing firefly lantern extract (FLE) leads to an enzymatic reaction

with the emission of light:

$$1)\quad \text{ATP + luciferin} \underset{\text{luciferase}}{\overset{\text{Mg}}{\rightleftharpoons}} \text{adenyl-luciferin + pyrophosphate}$$

$$2)\quad \text{adenyl-luciferin} \xrightarrow{O_2} \text{adenyl-oxyluciferin + } H_2O \text{ + light}$$

At low ATP concentrations, the degree of luminescence is directly proportional to the concentration of ATP in the sample. ADP and AMP can also be measured after enzymatic conversion to ATP. The principle of the assay to measure energy charge is therefore as follows:

The sample is divided into three portions, which are used to measure ATP, ADP, and AMP respectively. The first portion is used to directly determine the amount of ATP present in the sample, using the FLE method outlined above. The second portion is incubated with pyruvate kinase (PK) and phosphoenol pyruvate (PEP) to convert all the ADP present to ATP:

$$2\ \text{ADP} + 2\ \text{PEP} \overset{\text{PK,Mg,K}}{\rightleftharpoons} 2\ \text{ATP} + 2\ \text{pyruvate}$$

An assay of this sample therefore gives a measure of the amount of ATP + ADP present in the original sample. The third portion is incubated with pyruvate kinase, myokinase and phosphoenol pyruvate to convert all the ADP and AMP present to ATP:

$$\text{AMP + ATP} \overset{\text{MK, Mg}}{\rightleftharpoons} 2\ \text{ADP}$$

$$2\ \text{ADP} + 2\ \text{PEP} \overset{\text{PK, Mg, K}}{\rightleftharpoons} 2\ \text{ATP} + 2\ \text{pyruvate}$$

An assay of this portion therefore gives an estimate of the amount of AMP + ADP + ATP present in the original sample. By appropriate subtraction, therefore, the relative amount of each nucleotide in the original sample can be calculated.

For the assay, the following standard reagents were prepared as given in BERGMEYER (1963):

1) Triethanolamine Buffer (.05M, pH 7.55)

1.865g triethanolamine was dissolved in approximately 200ml distilled water, heated to 30°C (the temperature for incubation of the samples) and adjusted to pH 7.55 with 1M sulphuric acid. This was then made up to 250ml with distilled water and stored in the refrigerator.

2) 0.5M Magnesium Sulphate

3) 2M Potassium Chloride

4) EDTA (100mg/ml)

10g EDTA (disodium salt) were dissolved in water, neutralised with 2N NaOH and made up to 100ml with distilled water.

5) PEP (approximately 0.04M)

100mg PEP were dissolved in distilled water and made up to 5ml. This solution was prepared freshly every few days.

From these standard solutions, the following reagents were prepared for incubation of the samples:

i) ATP Reagent

$MgSO_4$	-	3.3ml	)
KCl	-	6.9ml	) made up to 250ml with triethanolamine
EDTA	-	0.36ml	) buffer.
PEP	-	3.6ml	)

ii) ADP Reagent

0.08ml pyruvate kinase suspension ('Sigma', 9.6mg/ml protein) was dissolved in 2.2 M ammonium sulphate (1.5ml, pH 6.0) and centrifuged for 1 minute at 4000 rpm in a 'Microfuge'. The supernatant was then discarded, and 1.5ml 'ATP Reagent' added to the precipitate and shaken. This was then poured into a flask and made up to 160ml with 'ATP Reagent'. The final concentration of pyruvate kinase in this solution was approximately 0.005mg protein/ml.

iii) AMP Reagent

0.04 ml myokinase suspension ('Sigma', 5mg protein/ml) was dissolved in 1.5ml 3.2M ammonium sulphate (pH 6.0) and centrifuged for 1 minute at 4000 rpm. The supernatant was then discarded and 1.5ml 'ADP reagent' added to the precipitate and shaken. This was then poured into a flask and made up to 80ml with 'ADP Reagent'. The resulting solution contained approximately 0.005 mg protein/ml pyruvate kinase, and 0.0025 mg protein/ml myokinase.

Firefly lantern extract (FLE) was made up according to the maker's instructions (Sigma) by adding the appropriate amount of distilled water to the powdered extract. This solution was then centrifuged

for one minute on a small bench centrifuge to remove major particles which would otherwise interfere with the assay. The extract was kept in ice during the course of the experiment, and in the deep freeze at -20°C when not in use (at this temperature it is extremely stable).

As a check on the assay, a set of standard solutions of ATP, ADP and AMP were also prepared:

ATP -)
ADP -) all 1×10^{-3}M, made up with distilled water and kept at -20°C when not in use.
AMP -)

The ATP standard was used to prepare a series of dilute solutions between 1×10^{-7} M and 1×10^{-8} M - the range of concentrations found in the plant extracts. This series of solutions was used to check that the degree of luminescence produced by the firefly extract was in fact directly proportional to the concentration of ATP in the sample. The standard solutions were also used to prepare a test solution of known 'energy charge', to check the remaining stages of the assay:

ATP - 5×10^{-7}M)
ADP - 2×10^{-7}M) corresponding to an 'energy charge' of 0.8.
AMP - $.5 \times 10^{-7}$M)

Each extract, prepared as described above, was then assayed as follows (all solutions and samples, except at the incubation stage, were kept in ice throughout the experiment):

Three test tubes were taken; to the first one was added 3.5ml 'ATP Reagent', to the second 3.5ml 'ADP Reagent' and to the third 3.5ml 'AMP Reagent'. To each test tube was then added 0.5ml of the extract from the root sample, and all three test tubes were shaken and transfered to a water bath kept at 30°C, for two hours. After the two hour incubation period, the test tubes were removed from the water bath and transfered to an ice bath.

The solution in each test tube was then assayed for ATP. 1.5ml FLE prepared as described was placed in a plastic semi-microcuvette in a fluorimeter ('MSE Spectro Plus'). The top of the cuvette chamber

was covered with a piece of black cardboard, sealed round the edges with 'Blu-Tack' to exclude all traces of light. A hole had been previously pierced in the cardboard, directly above the cuvette, and covered with a small piece of 'Blu-Tack'. 0.2ml of the reagent to be assayed was drawn into a small syringe, and the needle was then inserted through the hole in the cardboard so that it was lined up above the cuvette, the 'Blu-Tack' round the hole acting as a seal to prevent the entry of light. The fluorimeter was then set to maximum gain and the chart recorder started up. The reagent sample was then injected quickly into the cuvette by means of the syringe and the luminescence from the firefly extract was followed on the chart recorder. A typical trace is shown on figure 2.3. The height of the peak on such a trace was taken as a measure of the concentration of ATP in the sample. During trials , it was found that repeated assays of the same solution gave excellent reproducibility, the height of the peak varying by rarely more than +/- 10%, and usually by much less. A calibration curve (figure 2.4) prepared using the standard series of ATP solutions shows that over the concentration range studied, the height of the luminescence peak was directly proportional to the concentration of ATP.

Figure 2.5 shows an example of the three different peaks obtained when each of the three test tubes was assayed. The three peaks have heights h1, h2 and h3 corresponding to the tubes containing ATP, ADP and AMP reagents respectively. The amount of ATP present in the sample is represented by h1, (h2 - h1) represents the amount of ADP present, and h3 represents the total amount of adenine nucleotides present. The energy charge is therefore given as:

$$\text{Energy Charge} = \frac{h1 + \frac{1}{2}(h2 - h1)}{h3}$$

Trial experiments with the test solution having an 'energy charge' of 0.8 revealed considerable difficulty in estimating the amount of

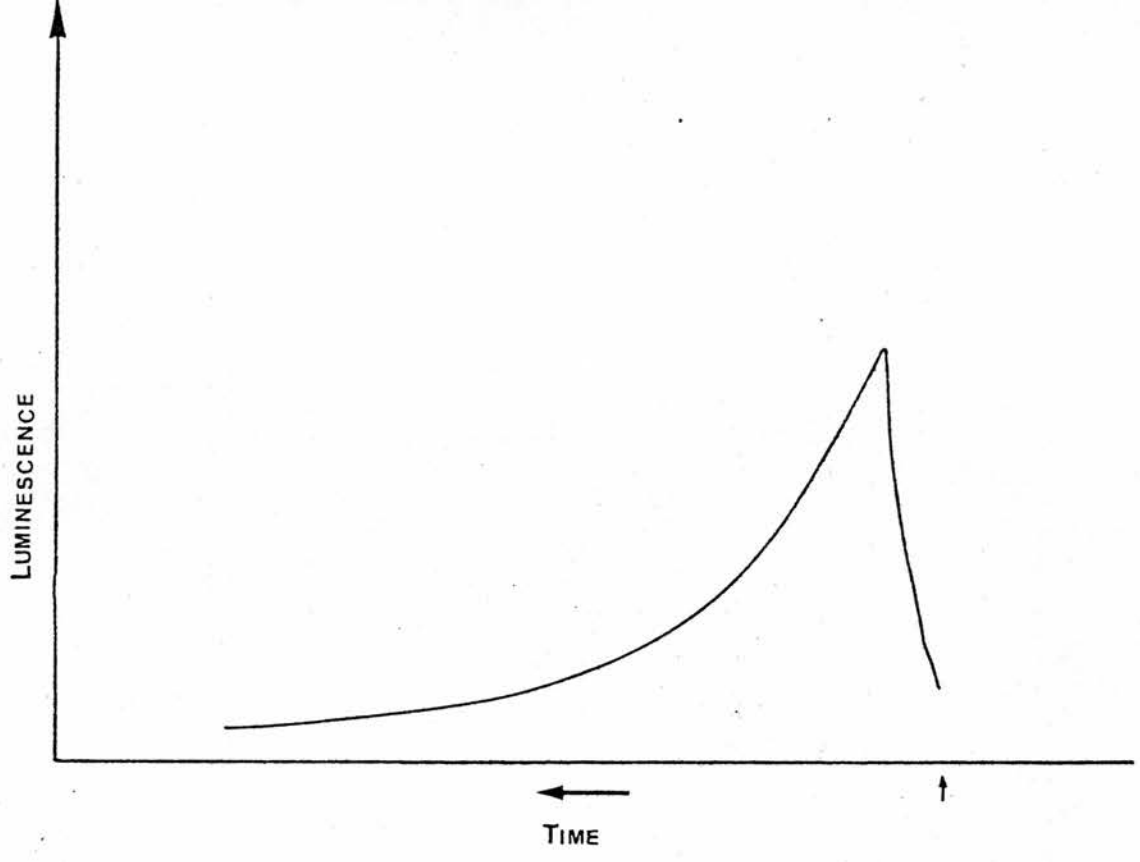

Fig 2.3 - Typical trace on the recorder chart following the injection of an ATP sample into a cuvette containing firefly lantern extract (see text).

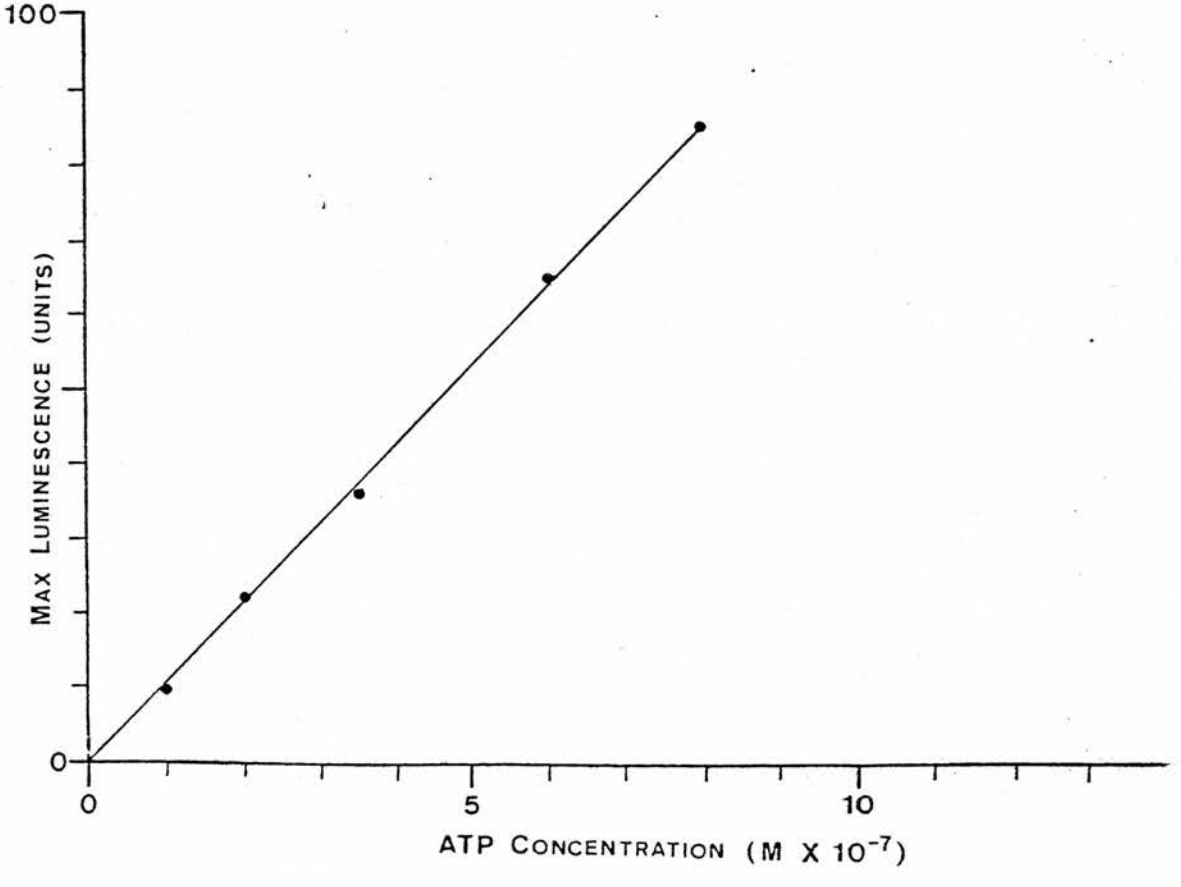

Fig 2.4 - Relation between the concentration of ATP in a sample injected into a cuvette containing firefly lantern extract, and the resulting luminescence.

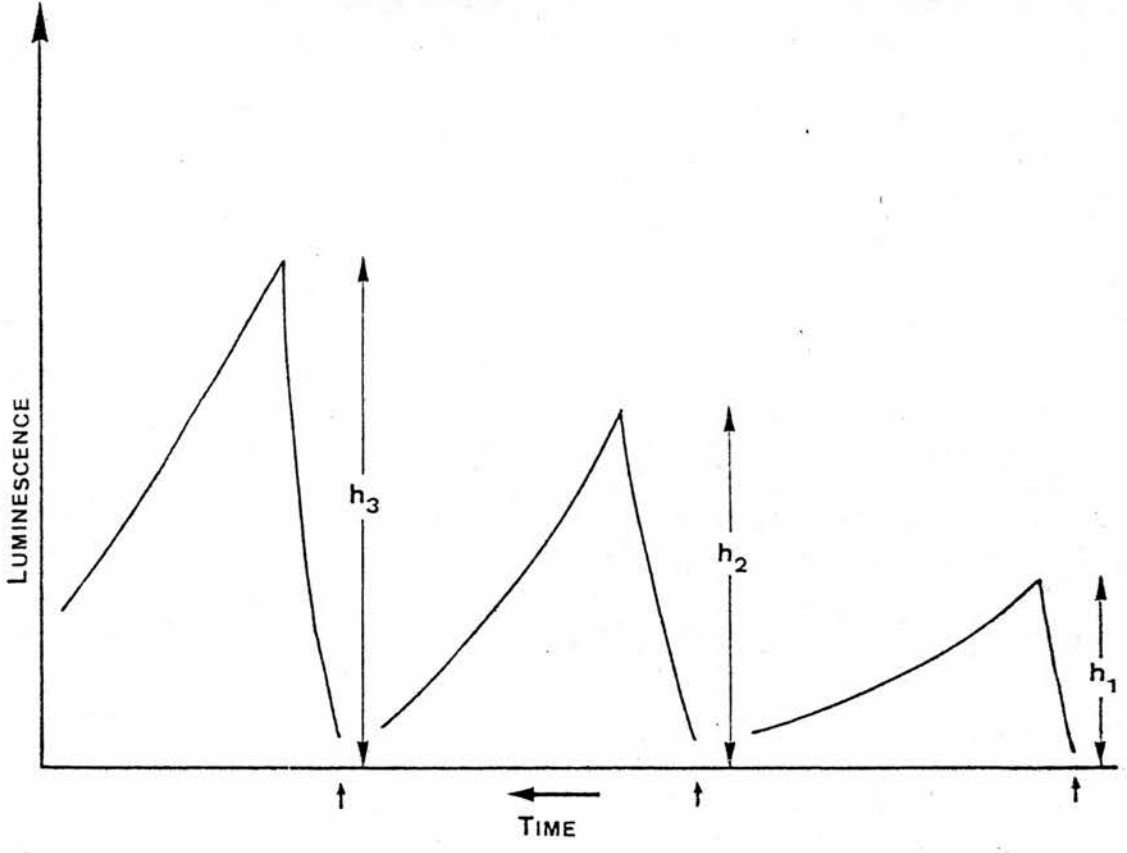

Fig 2.5 - Typical trace on the chart recorder following the injection of samples incubated with ATP, ADP and AMP reagents (see text).

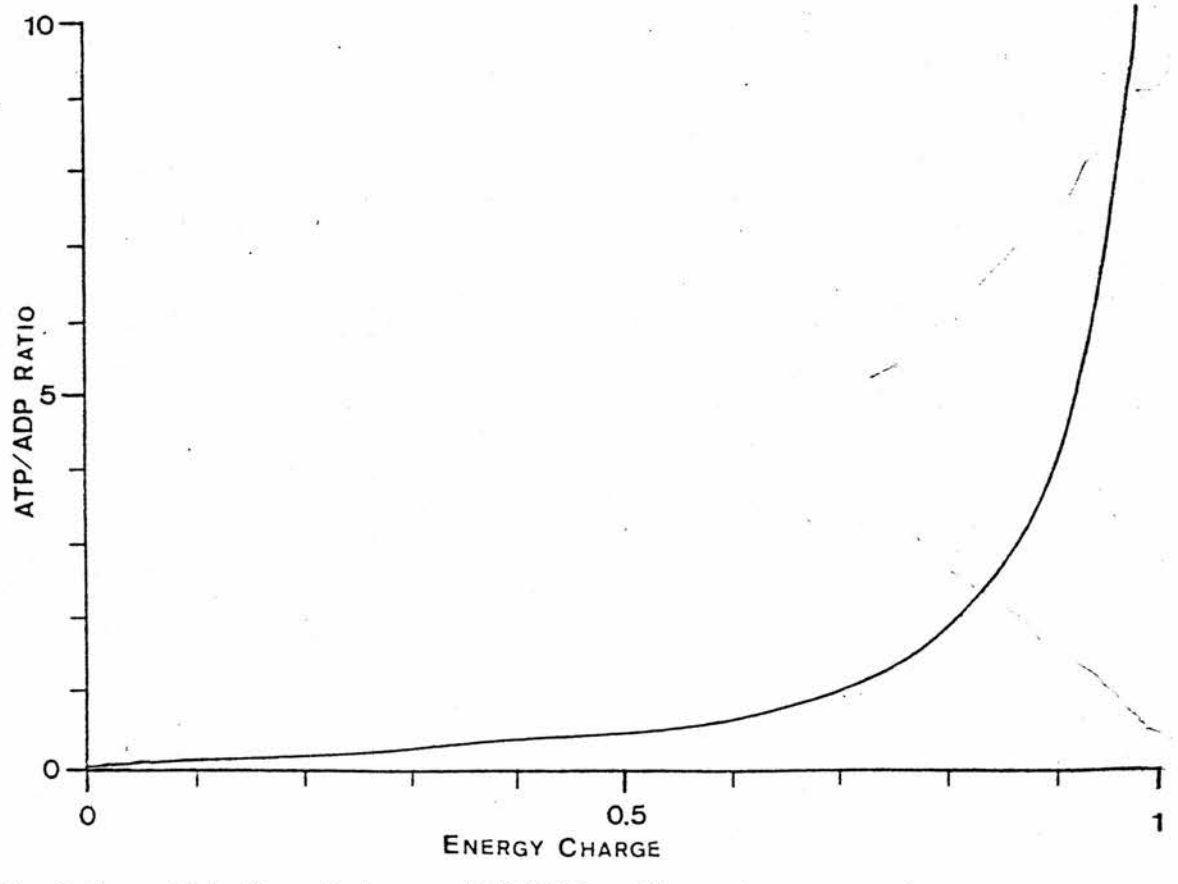

Fig 2.6 - Relation between ATP/ADP ratio and energy charge. After Atkinson and Walton (1967).

AMP present. The exact cause of this difficulty, which involved the enzymatic conversion of AMP to ADP, was never established, but PRADET (personal communication) has reported similar difficulties. Since measurements of AMP could not be relied upon, therefore, it was decided instead to measure ATP/ADP ratios.

Assays of each plant extract were replicated twice, replicates invariably coming within 5% of each other. Where there was sufficient material, control experiments were conducted with a stream of air, supplied from a small aquarium pump, passed through the gassing apparataus instead of nitrogen.

2.3 RESULTS AND DISCUSSION

a) Summary of Results

The results from this series of experiments are presented in Table 2.1. These results were somewhat more varied than had been hoped, but some trends can be distinguished. In the two control experiments, the ATP/ADP ratios were generally higher than in the corresponding samples kept under nitrogen. In the two experiments on Phalaris arundinacea, there is some indication that the samples which had previously been grown under a 'flooded' regime maintained a higher level of ATP than those which had been grown unflooded.

In a number of cases, the initial ATP ratio was somewhat low, possibly as a result of the root system being excised from the plant, but this was not apparent in all cases. Generally speaking, the ATP/ADP ratios obtained were relatively high, apart from an isolated measurement on Phalaris.

b) Discussion

Unlike energy charge, the measurement of ATP/ADP ratios takes no account of the relative amount of AMP present, so that, in theory, a large change in the amount of AMP present might not be reflected in the ATP/ADP ratios measured. ATKINSON and WALTON (1967), however, suggest that the ATP/ADP ratio will, in fact, rise with increasing energy charge, as shown in figure 2.6. Although not perhaps as satisfactory as energy charge, therefore, the ATP/ADP ratio is probably a good indication of the energy balance within the cell. The numerical values of the ATP/ADP ratio and its corresponding energy charge will not, of course, be the same, and it should be particularly noted (see fig 2.6) that at high energy charge levels, a small change in the energy charge will lead to a much larger change in the ATP/ADP ratio.

EXPERIMENT NO	SPECIES	TIME IN O_2 (min)	TIME IN N_2 (min)	ATP/ADP RATIO
1	Pisium sativum		4	0.39
			17	2.58
			25	3.07
2	Phalaris arundinacea*		0	0.53
			32	1.56
3	Phalaris arundinacea*		0	4.44
			32	∞
			62	2.44
			118	1.77
4	Phalaris arundinacea		0	0.92
			35	0.36
			75	0.04
			105	0.32
5	Phalaris arundinacea		0	2.28
			33	3.46
			65	1.26
			125	1.92
6	Phalaris arundinacea	35		31.57
		60		7.38
		122		9.8
7	Dactylis glomerata	0		2.31
		32		3.07
		60		3.83
		125		3.39
8	Dactylis glomerata		34	4.83
			60	2.56
			120	2.10
9	Holcus lanatus		138	1.41
			250	1.78
10	Juncus effusus*		0	1.98
			34	2.14
			68	2.94
			125	0.62

Table 2.1 - ATP/ADP Ratios Obtained From Experiments on the Gassing Apparatus.

This table shows the calculated ATP/ADP ratios obtained in the experiments described in Section 2.2. Species marked with an asterisk were grown in flooded sand culture. All other species were grown in unflooded sand culture.

PRADET and BOMSEL (1978) have summarised research into the energy relations of plant tissues, with particular reference to the effect of anoxia. Their findings suggest that in all plant material, a transfer from air to anaerobic conditions results in an immediate drop in the energy charge. Subsequent behaviour, however, will depend on the plant material involved. After about 15 minutes, a new equilibrium energy charge is established as a result of fermentative processes. This energy charge tends to be low (approximately 0.1 to 0.2) in seeds but can be very high in, for example maize seedlings (0.7). After a more prolonged period of several hours or days under anaerobic conditions, three different types of response can be distinguished. SELLAMI and BOMSEL (1975) found that in wheat leaves, there was a gradual decline in the energy charge followed by death after 24 hours. In rice coleoptiles, however, growth continues under anoxia and the energy charge remains between 0.75 and 0.85. Germinating lettuce seeds are also able to survive prolonged periods of anoxia, but in contrast to rice coleoptiles, they do not grow and the energy charge remains low at around 0.05 (PRADET and BOMSEL, 1978).

These findings suggest that survival of a plant organ under conditions of anoxia may be achieved in two ways. Firstly, as in the case of lettuce seeds, survival may entail a much reduced energy charge and correspondingly low metabolic activity. Secondly, as in the rice coleoptile, energy charge and metabolic activity may remain high, enabling the plant not only to survive, but also to grow.

Due to lack of material, only two experiments in this project had a control in which the sample was maintained in an aerobic environment. In these two experiments (Phalaris arundinacea and Dactylis glomerata), the anaerobic samples showed a lower ATP/ADP ratio than the corresponding control samples, although the difference was only slight in Dactylis. These results support the findings of PRADET and BOMSEL (1978), that in all plant material energy charge drops on transfer to an anaerobic environment. However, in all the

experiments conducted in this project, the actual ATP/ADP ratios, even after two hours under anoxia, were surprisingly high. Reference to figure 2.6 shows that an ATP/ADP ratio of greater than 1.0 indicates an energy charge in excess of 0.7. The normal energy charge in an aerobic plant cell is probably between 0.8 and 0.9 (PRADET and BOMSEL, 1978). Since many of the calculated ATP/ADP ratios in this project were greater than 1, the suggestion is that over the first few hours under anoxia, the energy charge is only slightly lower than under aerobic conditions. Only in one sample of Phalaris did the ATP/ADP ratio remain consistently below a value of 1.

PRADET and BOMSEL (1978) have summarised the results of similar experiments carried out by a number of authors on a variety of plant material. They report that when a plant tissue is subjected to anoxia, there is an immediate drop in the energy charge, which recovers within 1 to 15 minutes to reach a new stable value, which may be low or high depending on the plant material in question. As far as long-term survival is concerned, these authors suggest two possible strategies. On the one hand, there is the Rice coleoptile, unique in being able to grow actively under anoxic conditions. This organ is able to survive without oxygen for several weeks, during which time the energy charge remains high. Thus, the Rice coleoptile survives under anoxia by maintaining a high energy charge and active metabolism. Lettuce seeds, on the other hand, are also able to survive under anoxia for up to two weeks, but only with a very reduced metabolic activity and a low energy charge. When restored to aerobic conditions, the energy charge quickly recovers and normal growth resumes.

Most plant tissues, however, are unable to withstand prolonged periods without oxygen. In wheat leaves, for example, the energy charge stabalises at approximately 0.5 after the initial onset of anoxia, but this value exhibits a gradual decline over 24 hours, until the cells die (SELLAMI and BOMSEL, 1975).

Under anaerobic conditions, the production of energy-rich bonds will depend entirely on glycolysis. However, the amount of ATP which can be produced by glycolysis from one mole of glucose is considerably lower than that which can be produced by the Krebs cycle. Under anoxia, therefore, an increased rate of glycolysis is required to maintain the level of ATP production which is found in aerobic conditions. Thus, in most plant tissues, the onset of anaerobic conditions leads to a rapid acceleration in the glycolytic rate, known as the Pasteur effect.

As a mechanism for survival under anoxia, the value of the Pasteur effect is limited for two reasons. Firstly, the much lower efficiency of glycolysis in producing ATP will lead to a rapid depletion of food reserves. Secondly, there will be an accumulation of toxic by-products such as ethanol which the plant tissue will be unable to oxidise and which will ultimately lead to death. The behaviour of wheat leaves under anoxia may therefore be explained by assuming that the initial high value of the energy charge was maintained by an increased glycolytic rate, which started to decline after a few hours as food reserves became depleted and toxic by-products accumulated. Thus, while an acceleration of glycolysis may enable a plant organ to survive a short period of anoxia, survival for longer periods must necessitate the use of other mechanisms.

CRAWFORD (1966, 1967) has shown that in plant species tolerant of soil waterlogging, there is a control of metabolism in the root tissues so that, by contrast with mesophytic species, there is no acceleration of glycolysis when the plants are grown in flooded, anaerobic soil. As a result, there is a much lower accumulation of ethanol than is found in the roots of unadapted species and the plants are capable of prolonged survival on waterlogged soils. Clearly, however, a reduction in the rate of glycolysis will also lead to a reduction in the rate of ATP production and hence, one might

expect, in the energy charge of the plant tissue. In animals and microorganisms, however, adverse conditions can result in the reduction in the size of the adenylate pool (CHAPMAN et al, 1973, 1976). Thus, under anaerobic conditions, a relatively high energy charge can be maintained with the production of fewer energy-rich bonds. A similar effect is found in some plant tissues, such as wheat leaves and rice seedlings (PRADET and BOMSEL, 1978). The maintenance of a high energy charge by reduction of the pool size will not in itself allow a high metabolic rate to continue in adverse conditions, since the supply of ATP will be limited, but in view of the regulatory importance of the energy charge (ATKINSON, 1968) there may be an advantage in sustaining this at a high value.

From the foregoing discussion, one would expect that the response of the energy charge, or ATP/ADP ratio to a shortage of oxygen will vary according to the plant species involved. In particular, one would expect differences between the root tissues of those plants which are tolerant of soil waterlogging and those which are not. From the response of wheat leaves to anoxia, it can tentatively be predicted that in the case of a flood-intolerant species, the subjection of the roots to anoxia will result in the maintenance of a relatively high energy charge initially, followed by a gradual decline as toxic by-products build up. It is more difficult to predict a generalised response for a plant species which is tolerant of soil waterlogging. From the behaviour of the rice coleoptile, outlined above, one might expect that flood-tolerant species will maintain a high energy charge even under anaerobic conditions. On the other hand, the response of germinating lettuce seeds would suggest that survival could be achieved through the maintenance of a low energy charge, with correspondingly low metabolic activity.

From the experiments carried out in this project, however, such differences failed to emerge. In all cases, the measured ATP/ADP

ratios declined during the course of the experiment. The two control experiments also indicate that the ATP/ADP ratios under anoxia, although relatively high, are still lower than in an atmosphere of air. Interpretation of these results is difficult because of the short periods of time during which the excised root tissues were subjected to anoxia, but a number of possibilities are likely.

The response of Dactylis, a flood-intolerant species, is exactly as predicted above, with a high initial ATP/ADP ratio followed by a gradual decline. If the high initial value is due to the production of energy-rich bonds by fermentative respiration, then it is clear that the capacity of this system for maintaining a high energy charge is very limited. The response of the flooded sample of Phalaris, on the other hand, is virtually indistinguishable from that of Dactylis. This is difficult to explain if it is assumed, as suggested by the experiments of CRAWFORD (1977), that the Pasteur effect in flood-tolerant species is very low. It is possible, however, that even a very low Pasteur effect is sufficient to maintain a high energy charge initially, if the metabolic energy-consuming processes are also very low in activity. From the experiments carried out in Section 1, which showed a low rate of respiration in plant species grown under flooded conditions, this is quite possible. In that case, the difference between flood-tolerant and flood-intolerant species, with regard to energy charge behaviour, would be one of degree rather than something more fundamental.

These experiments do not directly reveal the long-term responses of the species used, but the indications are that the decline in energy charge (or ATP/ADP ratio) would continue and eventually stabalise at a low value, provided the tissue was able to survive. Certainly, none of the species studied showed any response like that of the Rice coleoptile, which maintains a high energy charge for several weeks while under total anoxia (PRADET and BOMSEL, 1978).

2.4 CONCLUSIONS

There have been two approaches to the study of energy charge in plant tissues. The first approach has been to use the energy charge as a measurement of the general metabolic activity of the tissue in question (RAYMOND et al, 1978). The second approach, however, has attempted to link the ability of the plant tissue to control the value of the energy charge with its ability to withstand adverse conditions, such as the anaerobic environment characteristic of waterlogged soils (PRADET and BOMSEL, 1978). Thus, for example, PRADET and BOMSEL (1978) suggest that one survival mechanism for anaerobic conditions may be the maintenance of a low energy charge which in turn leads to a low rate of metabolic activity and thus a conservation of resources. The implication is that in plant organs unable to survive under anoxia, attempts to maintain a high energy charge through accelerated glycolysis lead to a rapid depletion of food reserves and an accumulation of toxic by-products.

From the experiments which have been carried out in this project, however, it would appear that there is no difference between the responses of excised roots from flood-tolerant and flood-intolerant species. This apparent anomaly can be explained if it is remembered that the metabolic changes occurring in each case are probably not the same. Thus, in intolerant species, the initial period of rapid glycolytic respiration will be followed by a period in which, as a result of the depletion of resources and accumulation of ethanol, glycolysis slows down and the energy charge drops. In tolerant species, there is a much lower acceleration of glycolysis (CRAWFORD, 1977) and the decline in energy charge is due simply to the drop in ATP production in the absence of aerobic respiration.

In each case, the end result is an energy charge (or ATP/ADP ratio) lower than that found in an organ which has been allowed to grow under aerobic conditions. The important difference is that in the

flood-tolerant species, a low energy charge is reached without being preceded by a period of rapid glycolysis and consequent stress of the cell's metabolism. The conclusion which one might draw therefore is that the low energy charge reported, for example, for lettuce seeds under anoxia (PRADET and BOMSEL, 1978), is not in itself a mechanism for survival under anoxia, but rather a consequence of the control of metabolic rate.

The behaviour of the rice coleoptile, in which energy charge remains high under anoxia, should be regarded as an exception. Experiments by VARTAPETIAN et al (1978) suggest that the high metabolic activity of the rice coleoptile under anoxia is due to a high rate of glycolysis, maintained by the transport of organic compounds from the seed to the growing coleoptile. Because this organ grows in contact with free water, ethanol can readily diffuse out of the plant and does not accumulate in the tissues. Thus, the high rate of glycolysis is not associated with the fatal side effects normally found in other species.

In general, therefore, root survival in waterlogged conditions will depend on the control of glycolysis in situations where the supply of oxygen from the aerial parts is not sufficient to maintain aerobic respiration. This in turn will lead to a decline in the energy charge, so that all metabolic activities in the tissue will slow down. In such a situation, a plant root may survive for a period of months in a dormant state, and resume growth once the water table is lowered (COUTTS and PHILIPSON, 1977a). The primary adaptation, however, would appear to be the control of the glycolytic rate rather than any direct control over the value of the energy charge.

SECTION 3

Final Conclusions

The main original aim of this project was to explore the possibility of further metabolic adaptations in plant species tolerant of soil waterlogging. Two main lines of investigation have been carried out - one on the oxygen relations of plant root tips, and the other on energy relations within whole root systems.

From the investigation into the oxygen relations in the root tip it has been shown, particularly with the aid of the calculator model, that tolerant and intolerant species are not distinguished by different affinities for oxygen. In both groups of plants, full aerobic respiration can be maintained at very low concentrations of oxygen. Only in flood-tolerant species, however, is the transport of oxygen to the root system sufficient to maintain aerobic respiration. This transport of oxygen enables many flood-tolerant species to avoid the development of anaerobic centres within the root system, and hence to maintain active growth and nutrient uptake.

A number of authors, however, have demonstrated the existence of metabolic adaptations to anaerobiosis in the roots of flood-tolerant species, which would seem to contradict the conclusion that aerobic respiration is able to continue at an unrestricted rate. It is probably more realistic to regard such metabolic adaptations as complimentary to the transport of oxygen, rather than as an alternative. Even in a plant with an extensive internal gas system, there will be periods during which the root system is subjected to oxygen stress. At night, for example, when the stomata close, there will be little entry of oxygen into the root system from the aerial parts of the plant. In such circumstances, CRAWFORD and SMIRNOFF (unpublished data) have shown that the residual oxygen in the air spaces will not support aerobic respiration for more than two hours, so that anaerobic regions will develop quite quickly.

Some authors have suggested recently that the control of energy charge may represent another form of metabolic adaptation to soil waterlogging. While the energy charge is certainly a closely regulated

parameter under normal conditions, there is no direct evidence that plant root cells are able to maintain a high energy charge under anaerobic conditions. On the contrary, the experiments in this project would seem to indicate that a fall in energy charge is characteristic in the root tissues of both flood-tolerant and flood-intolerant species under anaerobic conditions. Research in this field is still in the early stages, however, and it is possible that more detailed measurements may reveal certain adaptations. It may be, for example, that control of the size of the adenylate pool may enable some species to maintain a higher energy charge than would otherwise be possible in the absence of oxygen, as suggested by PRADET and BOMSEL (1978). It may be more useful, however, to use energy charge measurements as an indication of the overall metabolic activity in plant tissues. This would provide an accurate method of assessing the overall contribution of oxygen transport to enabling a plant to grow under waterlogged conditions. One would expect, for example, that if oxygen transport is able to fully satisfy the root demand for oxygen, then the energy charge in the root system would be the same irrespective of whether the plant was grown in an aerobic or anaerobic medium. Such direct evidence would be a welcome verification of the predictions made by the various mathematical and other models which have been used.

REFERENCES

ATKINSON, D.E (1968) The Energy Charge of the Adenylate Pool as a Regulatory Parameter. Interaction with Feedback Modifiers. Biochemistry 7: 4030.

ATKINSON, D.E. & WALTON, G.M. (1967) Adenosine Triphosphate Conservation in Metabolic Regulation. Rat Citrate Cleavage Enzyme. J. Biol. Chem. 242: 3239.

ARMSTRONG, W. (1964) Oxygen Diffusion from the Roots of some British Bog Plants. Nature, London 204: 801.

ARMSTRONG, W. (1967) The Use of Polarography in the Assay of Oxygen Diffusing from Roots in Anaerobic Media. Physiol. Plant. 20: 540.

ARMSTRONG, W. (1971) Oxygen Diffusion from the Roots of Rice Grown Under Non-waterlogged Conditions. Physiol. Plant. 24: 242.

ARMSTRONG, W. (1978) Root Aeration in the Wetland Condition. In Plant Life in Anaerobic Environments, Hook, D.D., & Crawford, R.M.M. (Ed). Ann Arbor Science.

ARMSTRONG, W. & GAYNARD, T.J. (1976) The Critical Oxygen Pressures for Respiration in Intact Plants. Physiol. Plant. 37: 200.

ARMSTRONG, W. & WRIGHT, E.J. (1975) Radial Oxygen Loss from Roots: The Theoretical Basis for the Manipulation of Flux Data Obtained by the Cylindrical Platinum Electrode Technique. Physiol. Plant. 35: 21

BARTLETT, R.J. (1961) Iron Oxidation Proximate to Plant Roots. Soil Sci. 92: 372.

BENAC, R. (1976) Effect of Manganese Concentration in the Nutrient Solution on Groundnuts (Arachis hypogea L.). Oleagineaux 31: 539.

BERGMEYER, H.U. (1963) Methods of Enzymatic Analysis. London.

BERRY, L.J. & NORRIS, W.E. (1949a) Studies of Onion Root Respiration. I. Velocity of Oxygen Consumption in Different Segments of Root at Different Temperatures as a Function of Partial Pressure of Oxygen. Biochim. Biophys. Acta 3: 593.

BERRY, L.J. & NORRIS, W.E. (1949b) Studies of Onion Root Respiration. II. The Effect of Temperature on the Apparent Diffusion Coefficient in Different Segments of the Root Tip. Biochim. Biophys. Acta 3: 607.

BETZ, A. (1957) Zur Atmung wachsender Wurzelspitzen. Planta 50: 122.

BOYNTON, D. et al (1938) Are There Different Critical Oxygen Concentrations for the Different Phases of Root Activity? Science 88: 569.

BRADY, N.C. (1974) The Nature and Properties of Soils. MacMillan Publishing Co., Inc.

CHAPMAN, A.G. & ATKINSON, D.E. (1973) Stabilization of Adenylate Energy Charge by the Adenylate Deaminase Reaction. J. Biol. Chem. 248: 8309.

CHAPMAN, A.G., MILLER, A.L. & ATKINSON, D.E. (1976) Role of the Adenylate Deaminase Reaction in Regulation of Adenine Nucleotide Metabolism in Ehrlich Ascites Tumor Cells. Cancer Res. 36(3): 1144.

CHEVILLOTTE, P. (1973) Relation Between the Reaction Cytochrome Oxidase-Oxygen and Oxygen Uptake in Cells in vivo. J. Theor. Biol. 39: 277.

COUTTS, M.P. & PHILIPSON, J.J. (1978) Tolerance of Tree Roots to Waterlogging. I. Survival of Sitka Spruce and Lodgepole Pine. New Phytol. 80: 63.

COUTTS, M.P. & PHILIPSON, J.J. (1978) Tolerance of Tree Roots to Waterlogging. II. Adaptation of Sitka Spruce and Lodgepole Pine to Waterlogged Soil. New Phytol. 80: 71.

CRANK (1956) The Mathematics of Diffusion.

CRAWFORD, R.M.M. (1966) The Control of anaerobic Respiration as a Determining Factor in the Distribution of the genus Senecio. J. Ecol. 54: 403.

CRAWFORD, R.M.M. (1967) Alcohol Dehydrogenase Activity in Relation to Flooding Tolerance in Roots. J. Ecol. 18: 458.

CRAWFORD, R.M.M. (1976) Tolerance of Anoxia and the Regulation of Glycolysis in Tree Roots. In Tree Physiology and Yield Improvement, Cannell, M.G.R., & Last, F.T. (Eds). New York: Academic Press.

CRAWFORD, R.M.M. (1977) Tolerance of Anoxia and Ethanol Metabolism in Germinating Seeds. New Phytol. 79: 511.

CRAWFORD, R.M.M. & BAINES, M.A. (1977) Tolerance of Anoxia and the Metabolism of Ethanol in Tree Roots. New Phytol. 79: 519.

CRAWFORD, R.M.M. & McMANMON, M. (1968) Inductive Responses of Alcohol and Malic Dehydrogenases in Relation to Flooding Tolerance in Roots. J. Exp. Bot. 19: 435.

CRAWFORD, R.M.M. & TYLER, P.D. (1969) Organic Acid Metabolism in Relation to Flooding Tolerance in Roots. J. Ecol. 57:237.

DIONNE, J.L. & PESANT, A.R. (1976) Effects of pH and Water Regime on the Yield and Mineral Content of Lucerne and Birdsfoot Trefoil Grown in the Glasshouse. Can. J. Plant. Sci. 56: 919.

EISENTHAL, R. & CORNISH-BOWDEN, A. (1974) The Direct Linear Plot. A New Graphical Procedure for Estimating Enzyme Kinetic Parameters. Biochem. J. 139:715.

ESAU, K. (1960) Anatomy of Seed Plants. New York - London, John Wiley & Sons, Inc.

EVANS, M. & HOWARD, A. (1961) Relative Radiation Sensitivity in the Study of the Oxygen Supply to Root Meristems. Int. J. Rad. Biol. 3:619.

EVANS, D.D. & SCOTT, A.D. (1955) A Polarographic Method of Measuring Dissolved Oxygen in Saturated Soil. Soil Sci. Soc. Am. Proc. 19:12.

FORRESTER, M.L., KROTKOV, G. & Nelson, C.D. (1966) Effect of Oxygen on Photosynthesis, photorespiration and Respiration in Detached Leaves. I. Soybean. Plant Physiol. 41: 422.

GREENWOOD, D.J. (1967a). Studies on the Transport of Oxygen Through the Stems and Roots of Vegetable Seedlings. New Phytol. 66: 337.

GREENWOOD, D.J. (1967b) Studies on Oxygen Transport Through Mustard Seedlings (Sinapsis alba L.). New Phytol. 66: 597.

HENRY, M.F. & NYNS, E.J. (1975) Subcell. Biochem. 4: 1.

JENSEN, C.R., STOLZY, L.H. & LETEY, J. (1967) Tracer Studies of Oxygen Diffusion Through the Roots of Barley, Corn and Rice. Soil Sci. 103: 23.

LAMBERS, H. (1976) Respiration and NADH-Oxidation of the Roots of Flood-Tolerant and Flood-Intolerant Senecio species as Affected by Anaerobiosis. Physiol. Plant. 37: 117.

LAMBERS, H. & SMAKMAN, G. (1978) Respiration of the Roots of Flood-Tolerant and Flood-Intolerant Senecio Species: Affinity for Oxygen and Resistance to Cyanide. Physiol. Plant. 42: 163.

LAMBERS, H. & STEINGROVER, E. (1978) Efficiency of Root Respiration of a Flood-Tolerant and a Flood-Intolerant Senecio Species as Affected by Low Oxygen Tension. Physiol. Plant. 42: 179.

LINHART, Y.B. & BAKER, G. (1973) Intra-Population Differentiation of Physiological Responses to Flooding in a population of Veronica peregrina L. Nature London 242: 275.

LUXMOORE, R.J., STOLZY, L.H. & LETEY, J. (1970) Oxygen Diffusion in the Soil-Plant System. I - IV. Agron. J. 62: 317.

LUXMOORE, R.J. & STOLZY, L.H. (1972) Oxygen Diffusion in the Soil-Plant System. V & VI. Agron. J. 64

McPHERSON, D.C. (1939) Cortical Gas Spaces in the Roots of Zea mays. New Phytol. 38: 190.

MARKUS, M., HESS, B., OTTAWAY, J.H. & CORNISH-BOWDEN, A. (1976) The Analysis of Kinetic Data in Biochemistry. A Critical Evaluation of Methods. FEBS Letters 63(2): 225.

MEEK, B.D. & STOLZY, L.H. (1978) Short-Term Flooding. In Plant Life in Anaerobic Environments, Hook, D.D. & Crawford, R.M.M. (Eds). Ann Arbor Science.

MILLINGTON, R.J. (1955) Diffusion Constant and Diffusion Coefficient. Science 122: 1090.

PHILIPSON, J.J. & COUTTS, M.P. (1978) The Tolerance of Tree Roots to Waterlogging. III. Oxygen Transport in Lodgepole Pine and Sitka Spruce Roots of Primary Structure. New Phytol. 80: 341.

PRADET, A. & BOMSEL, J.L. (1978) Energy Metabolism in Plants Under Hypoxia and Anoxia. In Plant Life in Anaerobic Environments, Hook, D.D. & Crawford, R.M.M. (Eds). Ann Arbor Science.

RAYMOND, P., BRUZAU, F. & PRADET, A. (1978) Etude du Transport d'oxygene des Parties Aeriennes aux Racines a l'aide d'un parametre du metabolisme: la Charge Energetique. C.R.Acad. Sc. Paris 286(D): 1061.

RUHLAND, W., & RAMSHORN, K. (1938) Aerobe Garung in Aktiven Pflanzlichen Meristemen. Planta 28: 471.

ROBSON, A.D. & LONERAGAN, J.F. (1970) Effects of Waterlogging on Giberellin Content & Growth of Tomato Plants. J. Exp. Bot. 22: 39.

SELLAMI, A. & BOMSEL, J.L. (1975) Evolution de la Charge Energetique du Pool Adenylique des Feuilles de Ble au cours de l'Anoxie. Etude de la Reversibilite des Phenomenes Observes. Physiol. Veg. 13(3): 611.

SOLOMOS, T. (1977) Cyanide-Resistant Respiration in Higher Plants. Ann. Rev. Plant Physiol. 28: 279.

SCHONBAUM, G.R., BONNER, W.D., STOREY, B.T. & BAHR, J.T. (1971) Specific Inhibition of the Cyanide-Insensitive Respiratory Pathway in Plant Mitochondria by Hyroxamic Acids. Plant Physiol. 47: 124.

TURNER, F.T. & PATRICK, W.H. (1968) Chemical Changes in Waterlogged Soils as a Result of Oxygen Depletion. Trans. 9th Internat. Cong. Soil Sci. 4: 53.

VALLANCE, K.B. & COULT, D.A. (1951) Observations on the gaseous Exchanges Which Take Place between Menyanthes Trifoliata L. and its Environment. I. The Composition of the Internal Gas of the Plant. J. Exp. Bot. 17: 355.

VARTAPETIAN, B.B., ANDREEVA, I.N. & NURITDINOV, N. (1978) Plant Cells Under Oxygen Stress. In Plant Life in Anaerobic Environments, Hook, D.D. & Crawford, R.M.M. (Eds). Ann Arbor Science.

WINZLER, R.J. (1941) The Respiration of Baker's Yeast at Low Oxygen Tension. J. Cell. Comp. Physiol. 17: 263.

YOCUM, C.S. & HACKETT, D.P. (1957) Participation of Cytochromes in the Respiration of the Aroid Spadix. Plant Physiol. 32: 186.

YU, P.T., STOLZY, L.H. & LETEY, J. (1969) Survival of Plants under Prolonged Flooded Conditions. Agron. J. 61: 844.

APPENDICES

APPENDIX I - Composition of the Hoagland's Solution used in Sand Cultures.

The nutrient solution used in the sand cultures was prepared from a set of stock solutions as shown in the following table:

Nutrient	g/l in stock solution	Volume of stock solution in final solution (ml)
KNO_3	101.1	6
$Ca(NO_3)_2.4H_2O$	236.16	4
$NH_4H_2PO_4$	115.08	2
$MgSO_4.7H_2O$	246.49	1
KCl	3.728	1
H_3BO_4	1.546	
$MnSO_4.4H_2O$	0.446	
$ZnSO_4.7H_2O$	0.575	
$CuSO_4.5H_2O$	0.125	
H_2MoO_4	0.018	
Fe-EDTA	6.922	1

The final solution was made up to 1 litre with distilled water and adjusted to a pH of 6.0 with 1N Hydrochloric Acid.

APPENDIX II - Direct Linear Plot Program

II.1 Description

This program is designed to estimate Vmax, the maximum rate of reaction, and Km, the substrate concentration at which the rate of reaction is $\frac{1}{2}$ Vmax, given the rate of reaction at several different substrate concentrations. The method employed is that of the Direct Linear Plot, the theory of which is described in Section 1.2 (b).

For each pair of observations (V1, S1), (V2, S2), the intersection (Km, Vmax) of the two lines plotted as shown in figure 1.6 is given by the formulae:

$$Km = \frac{V2 - V1}{\frac{V1}{S1} - \frac{V2}{S2}} \qquad Vmax = \frac{V1\ Km}{S1} + V1$$

If there are n observations, then there will be $\frac{1}{2}n(n - 1)$ intersections, and hence $\frac{1}{2}n(n - 1)$ estimates for Km and Vmax. The best estimate for each parameter is given by the median value of each series.

The program operates in the following manner: The number of intersections, NI, is calculated as $\frac{1}{2}n(n - 1)$. If NI is an odd number, then the value NI' is calculated as NI + 1, otherwise NI' is calculated as NI + 2. The program then calculates all the Km estimates, storing the lowest $\frac{1}{2}$NI' values. The best estimate for Km is then given as the mean of the two highest values stored if NI is even, or the highest value stored if NI is odd. For example, if n is 5, then NI is 10 and the lowest 6 estimates of Km will be calculated and stored. The best estimate of Km, the median, is then calculated as the mean of the 5th and 6th highest values stored. The whole process is then repeated, calculating Vmax instead of Km.

The intersection of any pair of parallel lines is ignored, and median estimates are only calculated on the basis of the remaining points. The user may also specify that any intersection which gives a negative estimate for either Km or Vmax is to be ignored.

II.2 Input Data

The user must enter a value for Vi, the rate of reaction, and Si, the corresponding substrate concentration, for each observation. A minimum of 2 and a maximum of 10 observations may be entered.

II.3 User Instructions

This program has been developed specifically for use with the Texas Instruments TI-59 Programmable Calculator and Printer, and the user is referred to the Manufacturer's Instruction Manual for full details of the operation of the calculator.

STEP	PROCEDURE	ENTER	PRESS	DISPLAY
1	Switch on Calculator & Printer			
2	Enter program manually, or from card (see II.7)			
	Initialise			
3	Initialise program		A	1
	Options			
4	To print all intermediate estimates of Km and Vmax (see II.4)		E'	Unchanged
5	To omit negative estimates		E	Unchanged
	Enter Data			
6	Enter Vi, the rate of reaction of the ith observation	Vi	B	-i
7	Enter Si, the substrate concentration of the ith observation	Si	C	i + 1
	Repeat steps 6 & 7 for all observations to be entered. If the maximum of 10 observations is entered, then Km and Vmax calculations start automatically (i.e. step 8 is not required).			
	Calculate Km and Vmax			
8	Execute calculation routine		D	(see II.4)
	Once calculations are complete, the program will re-initialise automatically, and a new set of data can be entered starting at step (4).			

II.4 Output

The output from the program is a printout showing the median estimates for Km and Vmax, and, if specified, all the intermediate estimates as well. An asterisk will be printed each time the program encounters an intersection of two parallel lines. An asterisk will also be printed if a negative estimate for Km or Vmax is encountered, and the user has specified that negative estimates are to be omitted.

As each estimate for Vmax or Km is calculated, the program will pause momentarily and display the calculated value, whether or not the print option has been specified.

A sample printout is shown below. The Km estimate is printed under the heading 'K=' and the Vmax estimate under the heading 'V='.

```
          K=
12.97198724
          V=
128.1676318
 END
```

II.5 Diagnostics

The following information is intended to assist the user in the event of any difficulty being encountered when attempting to run the program.

i) Program terminates with a flashing display.

   a) A zero substrate concentration has been entered.
   b) Program entered incorrectly.
   c) Memory incorrectly partitioned (refer to II.6).
   d) Calculator malfunction.

ii) Program terminates without printing estimates for Km or Vmax.

   a) No data entered, or only 1 observation entered.
   b) All intersections calculated lay at infinity (parallel lines).
   c) All intersections calculated had a negative value for Km or Vmax, and the user specified that negative values were to be omitted.

II.6 Program Requirements

i) Memory. The calculator memory must be correctly partitioned to allow space for the 447 program locations and 60 data registers. The partition set when the calculator is first switched on meets these requirements. If in doubt, the following key sequence will establish the correct partition:

6 2^{nd} OP 1 7

ii) Data Registers. The number of data registers used will depend on the number of observations entered as input data. The following table shows the data registers used when the maximum number of 10 observations is entered:

REGISTERS	CONTENTS
00-09	Used
10-29	Input data entered by user
30-36	Not used
37-59	Storage registers for intermediate estimates of Km and Vmax

iii) Flags. The following flags are used by the program:

Flag 1 - Indicates that $\frac{1}{2}n(n - 1)$ is even
Flag 2 - Negative values are to be omitted
Flag 3 - Print all intermediate estimates
Flag 4 - Storage registers for intermediate estimates are full
Flag 6 - Calculate Vmax values instead of Km
Flag 7 - Indicates parallel line intersection

iv) Labels. The following labels are used by the program:

A - Initialise routine
B - Vi entry routine
C - Si entry routine
D - Calculate Km and Vmax routine
E - Set flag 2 to omit negative estimates
E'- Set flag 3 to print intermediate estimates

All branches within the program use 'absolute addressing', or specific program locations rather than labels. For this reason, insertions and deletions should not be made to the program unless all branches are updated accordingly.

II.7 Program listing

The listing of all program steps, as printed on the calculator printer, is shown on the following pages. The user is referred to the Manufacturer's Instruction Manual for a full description of all the functions used and a translation of the key-codes and abbreviations.

The listing is shown in the following format:

LOCATION	KEY-CODE	INSTRUCTION
XXX	YY	ZZZ

```
000  92 RTN
001  76 LBL
002  11  A
003  01  1
004  00  0
005  42 STO
006  01  01
007  01  1
008  42 STO
009  00  00
010  81 RST
011  76 LBL
012  12  B
013  72 ST*
014  01  01
015  69 OP
016  21  21
017  72 ST*
018  01  01
019  43 RCL
020  00  00
021  94 +/-
022  92 RTN
023  76 LBL
024  13  C
025  22 INV
026  64 PD*
027  01  01
028  69 OP
029  21  21
030  69 OP
031  20  20
032  01  1
033  01  1
034  32 X:T
035  43 RCL
036  00  00
037  77  GE
038  14  D
039  92 RTN
040  76 LBL
041  15  E
042  86 STF
043  02  02
044  92 RTN
045  76 LBL
046  10 E'
047  86 STF
048  03  03
049  92 RTN
050  76 LBL
051  14  D
052  43 RCL
053  00  00
054  32 X:T
055  02  2
056  77  GE
057  02  02
058  90  90
059  69 OP
060  30  30
061  43 RCL
062  00  00
063  42 STO
064  07  07
065  53  (
066  43 RCL
067  00  00
068  75  -
069  01  1
070  54  )
071  65  ×
072  43 RCL
073  00  00
074  55  ÷
075  02  2
076  95  =
077  42 STO
078  03  03
079  55  ÷
080  02  2
081  95  =
082  22 INV
083  59 INT
084  29 CP
085  22 INV
086  67  EQ
087  00  00
088  93  93
089  69 OP
090  23  23
091  86 STF
092  01  01
093  69 OP
094  23  23
095  02  2
096  94 +/-
097  22 INV
098  49 PRD
099  03  03
100  06  6
101  00  0
102  44 SUM
103  03  03
104  42 STO
105  09  09
106  43 RCL
107  03  03
108  42 STO
109  06  06
110  43 RCL
111  07  07
112  65  ×
113  02  2
114  85  +
115  08  8
116  95  =
117  42 STO
118  01  01
119  42 STO
120  02  02
121  42 STO
122  04  04
123  42 STO
124  05  05
125  69 OP
126  22  22
127  69 OP
128  34  34
129  69 OP
130  34  34
131  69 OP
132  35  35
133  53  (
134  73 RC*
135  04  04
136  75  -
137  73 RC*
138  01  01
139  54  )
140  55  ÷
141  53  (
142  73 RC*
143  02  02
144  75  -
145  73 RC*
146  05  05
147  54  )
148  95  =
149  69 OP
150  19  19
151  42 STO
152  08  08
153  87 IFF
154  07  07
155  02  02
156  28  28
157  87 IFF
158  02  02
159  02  02
160  47  47
161  87 IFF
162  06  06
163  02  02
164  14  14
165  22 INV
166  87 IFF
167  03  03
168  01  01
169  71  71
170  99 PRT
171  66 PAU
172  87 IFF
173  04  04
174  01  01
175  98  98
176  43 RCL
177  09  09
178  32 X:T
179  43 RCL
```

```
180  06  06
181  77  GE
182  01  01
183  93  93
184  69  OP
185  39  39
186  43  RCL
187  08  08
188  72  ST*
189  09  09
190  61  GTO
191  03  03
192  36  36
193  71  SBR
194  03  03
195  03  03
196  86  STF
197  04  04
198  73  RC*
199  06  06
200  32  X:T
201  43  RCL
202  08  08
203  77  GE
204  03  03
205  36  36
206  72  ST*
207  06  06
208  71  SBR
209  03  03
210  03  03
211  61  GTO
212  03  03
213  36  36
214  43  RCL
215  08  08
216  65  ×
217  73  RC*
218  02  02
219  85  +
220  73  RC*
221  01  01
222  95  =
223  42  STO
224  08  08
225  61  GTO
226  01  01
227  65  65
228  25  CLR
229  22  INV
230  86  STF
231  07  07
232  87  IFF
233  06  06
234  02  02
235  56  56
236  01  1
237  00  0
238  69  OP
239  07  07
240  87  IFF
241  06  06
242  03  03
243  36  36
244  61  GTO
245  02  02
246  63  63
247  29  CP
248  32  X:T
249  77  GE
250  02  02
251  32  32
252  32  X:T
253  61  GTO
254  01  01
255  61  61
256  87  IFF
257  03  03
258  02  02
259  36  36
260  61  GTO
261  03  03
262  36  36
263  87  IFF
264  01  01
265  02  02
266  80  80
267  86  STF
268  01  01
269  05  5
270  09  9
271  32  X:T
272  43  RCL
273  03  03
274  77  GE
275  02  02
276  90  90
277  61  GTO
278  03  03
279  36  36
280  22  INV
281  86  STF
282  01  01
283  69  OP
284  23  23
285  06  6
286  00  0
287  61  GTO
288  02  02
289  71  71
290  69  OP
291  00  00
292  01  1
293  07  7
294  03  3
295  01  1
296  01  1
297  06  6
298  69  OP
299  01  01
300  69  OP
301  05  05
302  11  A
303  43  RCL
304  06  06
305  42  STO
306  09  09
307  05  5
308  09  9
309  32  X:T
310  43  RCL
311  09  09
312  22  INV
313  67  EQ
314  03  03
315  17  17
316  92  RTN
317  69  OP
318  29  29
319  73  RC*
320  06  06
321  32  X:T
322  73  RC*
323  09  09
324  22  INV
325  77  GE
326  03  03
327  07  07
328  72  ST*
329  06  06
330  32  X:T
331  72  ST*
332  09  09
333  61  GTO
334  03  03
335  07  07
336  02  2
337  94  +/-
338  44  SUM
339  04  04
340  44  SUM
341  05  05
342  09  9
343  32  X:T
344  43  RCL
345  05  05
346  22  INV
347  67  EQ
348  01  01
349  33  33
350  69  OP
351  37  37
352  43  RCL
353  07  07
354  32  X:T
355  01  1
356  22  INV
357  67  EQ
358  01  01
359  10  10
```

```
360  71 SBR
361  03  03
362  03  03
363  43 RCL
364  03  03
365  32 X:T
366  43 RCL
367  06  06
368  67  EQ
369  03  03
370  76  76
371  69 □P
372  26  26
373  61 GT□
374  03  03
375  60 .60
376  98 ADV
377  69 □P
378  00  00
379  87 IFF
380  06  06
381  03  03
382  90  90
383  02  2
384  06  6
385  06  6
386  04  4
387  61 GT□
388  03  03
389  94  94
390  04  4
391  02  2
392  06  6
393  04  4
394  69 □P
395  02  02
396  69 □P
397  05  05
398  87 IFF
399  01  01
400  04  04
401  08  08
402  73 RC*
403  06  06
404  99 PRT
405  61 GT□
406  04  04
407  26  26
408  69 □P
409  26  26
410  71 SBR
411  03  03
412  03  03
413  53  (
414  73 RC*
415  06  06
416  69 □P
417  36  36
418  85  +
419  73 RC*
420  06  06
421  54  )
422  55  ÷
423  02  2
424  95  =
425  99 PRT
426  98 ADV
427  87 IFF
428  06  06
429  02  02
430  90  90
431  86 STF
432  06  06
433  22 INV
434  86 STF
435  04  04
436  43 RCL
437  00  00
438  42 STO
439  07  07
440  06  6
441  00  0
442  42 STO
443  09  09
444  61 GT□
445  01  01
446  10  10
447  00  0
448  00  0
449  00  0
450  00  0
451  00  0
452  00  0
453  00  0
454  00  0
455  00  0
456  00  0
457  00  0
458  00  0
459  00  0
460  00  0
461  00  0
462  00  0
463  00  0
464  00  0
465  00  0
466  00  0
467  00  0
468  00  0
469  00  0
470  00  0
471  00  0
472  00  0
473  00  0
474  00  0
475  00  0
476  00  0
477  00  0
478  00  0
479  00  0
```

APPENDIX III - Root Oxygen Uptake Model

III.1 Description

The theory behind this model has already been described in Section 1.2 (e), and this Appendix is intended to provide details of the actual program used to obtin a plot of root oxygen uptake *versus* external oxygen concentration.

The principle of operation is as follows: The cross-section of the root is divided into a number of 'cylinders' (see Section 1.2 (e)) defined by the user. The oxygen concentration in the innermost cylinder is set to a concentration initially defined by the user. The rate of oxygen uptake is then calculated for this cylinder. Using this rate of oxygen uptake, a 'concentration increment' is calculated, and addition of this increment to the initial oxygen concentration gives the oxygen concentration in the next cylinder outwards. This oxygen concentration is then used to calculate the rate of oxygen uptake in the second cylinder, and this is added to the rate of uptake in the first cylinder to give the combined rate of oxygen uptake of the first two cylinders. This combined oxygen uptake rate is then used to calculate the next concentration increment, and addition of this to the oxygen concentration of the second cylinder gives the oxygen concentration in the third cylinder. This process is repeated until calculations have been completed for all cylinders. The addition of all the rates of oxygen uptake for all cylinders represents the total oxygen uptake of the root, and the addition of all the concentration increments to the initial oxygen concentration at the root centre represents the external oxygen concentration. These two values are then plotted on the printer.

The initial oxygen concentration at the centre of the root is then reduced by an amount specified by the user and the whole process repeated to give a new point on the plot.

The Program is designed to plot the respiratory behaviour of a root segment with two respiratory systems. This is achieved by calculating the rate of oxygen uptake separately for each system, and adding the two rates together to give the total uptake for the cylinder in question.

Provision is also given for defining a 'critical oxygen concentration' (COC) below which oxygen uptake ceases completely. Thus, in calculating the oxygen uptake for a particular cylinder, if the oxygen concentration is less then the COC of one of the respiratory systems, then the program calculates a zero rate of oxygen uptake for that system.

The initial oxygen concentration at the innermost cylinder is decreased each time in order to provide a range of values for the plot. If a critical oxygen concentration has been defined for each respiratory system, then there will come a point when the initial oxygen concentration is lower than the COC of each system. When this occurs, the innermost cylinder is considered to be inactive and is not considered in any further calculations. Instead, the program starts calculations at the next cylinder, using as its initial oxygen concentration the lower of the two COC's. Clearly, this cylinder too will become inactive the next time the initial concentration is decreased, and calculations will then proceed from the next cylinder outwards, again using the lower of the two COC's as an initial oxygen concentration. Calculations cease altogether when all cylinders become inactive. This will occur at an external oxygen concentration equal to the lower of the two COC's

III.2 Input Data

The following data must be entered before the graph is plotted:

Item	Units	Abbreviation
Max. rate of oxygen uptake (System 1)	µmoles/cm/hour	RA
Max. rate of oxygen uptake (System 2)	µmoles/cm/hour	RC
Km (System 1)	mM	KA
Km (System 2)	mM	KC
COC (System 1)	mM	CA
COC (System 2)	mM	CC
Diffusion Coefficient	cm^2/sec	D
Outer radius of root	cm	B
Inner radius of root	cm	A
Number of cylinders	integer	NR
Base oxygen concentration	mM	CB
Number of plot positions (x-axis)	integer	NCB
Decrement factor	$0 < x < 1$	O.X
Initial internal O_2 concentration	mM	CI

Careful consideration must be given to the choice of the above data in order to obtain an accurate plot and avoid an excessive run-time. The following items in particular have a large effect on the performance of the program:

i) NR: This specifies the number of 'cylinders' into which the root is divided for the purpose of calculation. If this number is too small, then the resulting plot will be inaccurate. If this number is too large, then the run-time of the program will increase substantially and rounding errors will affect the accuracy of the results. In practice, a value of 10 should give satisfactory results.

ii) NCB: The choice of this value will depend on the accuracy desired. If the number is small, the plot will be small, and discontinuities due to the way in which the points are printed by the calculator will become pronounced. A larger value will be less affected by discontinuities and will enable more points to be plotted. A value of 20 should generally give satisfactory results.

iii) O.X: The performance of the program is heavily dependent on the careful choice of this parameter. The initial internal oxygen concentration is multiplied by this decrement factor each time a new point is to be calculated on the plot, in order to calculate the oxygen uptake rate over a range of external oxygen concentrations. If the decrement value is high, the points will be close together and vice versa if the decrement factor is low. However, if the decrement factor is too high, the program will calculate 'duplicate' points on the graph, which will not be plotted but which will increase the run-time of the program.

The choice of a suitable value for O.X will also depend on the value of the diffusion coefficient. If the diffusion coefficient is low, then the decrement factor should also be low in order to avoid the calculation of duplicate points. For a given diffusion coefficient, high values for RA and RC should also be accompanied by a low value for O.X.

iv) CI: This is the initial internal oxygen concentration used to calculate the first point on the graph, and is decremented for each subsequent point by multiplying by O.X. If the diffusion coefficient is low, then the calculated external oxygen concentration will be considerably higher than CI. It should be remembered that the program will not start plotting until the calculated external concentration is less than the base oxygen concentration (CB) defined by the user. Ideally, therefore, CI should be chosen so that the first point calculated is approximately equal to CB. This involves a certain amount of guesswork, but in general if the diffusion coefficient is high, CI should be approximately equal to CB. If the diffusion coefficient is low, then CI should be set to a low value. If CI is set too high, then the first points to be calculated will be at oxygen concentrations above CB and will not be plotted. This may lead to a situation where a considerable time elapses before plotting commences. On the other hand, if CI is too low, plotting may start well below CB and the graph will be incomplete.

If it is only desired to obtain a plot for a root segment in which there is one respiratory system, either of the two following procedures may be adopted:

a) Enter the data for the single system twice, as if there were two systems, but making both RA and RC equal to half the maximum oxygen uptake rate of the single system.

b) Enter the data for one system, and for the second system enter zero for RC and KC, and set CC to a value higher than CA.

III.3 User Instructions

The model has been specifically developed for use with the Texas Instruments TI-59 Programmable Calculator and Printer, and the user is referred to the Manufacturer's Instruction Manual for full details of the operation of the calculator.

STEP	PROCEDURE	ENTER	PRESS	DISPLAY
1	Switch on Calculator & Printer			
2	Partition Storage Area	5	2^{nd} OP 1 7	559.49
3	Enter program manually or from card (see program listing)			
	Enter Initial Data			
4	Initialise entry procedure		A	1
5	Enter data:	RA	R/S	2
		RC	R/S	3
		KA	R/S	4
		KC	R/S	5

STEP	PROCEDURE	ENTER	PRESS	DISPLAY
		CA	R/S	6
		CC	R/S	7
		D	R/S	8
		B	R/S	9
		A	R/S	10
		NR	R/S	11
		CB	R/S	12
		NCB	R/S	13
		O.X	R/S	14
		CI	R/S	0
	Alter Original Data			
6	Initialise alter procedure		2^{nd} A'	RA'
7	Enter only the data to be changed. Original input will remain unchanged unless altered.	RA	R/S	RC'
		RC	R/S	KA'
		KA	R/S	KC'
		KC	R/S	CA'
		CA	R/S	CC'
		CC	R/S	D'
		D	R/S	B'
		B	R/S	A'
		A	R/S	NR'
		NR	R/S	CB'
		CB	R/S	NCB'
		NCB	R/S	O.X'
		O.X	R/S	CI'
		CI	R/S	0
	Print Data Entered			
8	Execute print routine (see III.4)		C	
	Plot Graph			
9	Execute plot routine (see III.4)		B	

III.4 Output

i) Data Listing: Pressing key C will provide a printout of the data entered, in the following format (see III.2 for abbreviations):

```
DATA ENTERED-
     0.012825        RA
     0.012825        RC
        0.004        KA
        0.004        KC
           0.        CA
           0.        CC
    0.0000023         D
         0.05         B
        0.001         A
           5.        NR
        0.281        CB
          20.       NCB
           0.4      O.X
        0.281        CI
```

ii) Plot: Rate of oxygen uptake is plotted on the y-axis as a percentage of the maximum potential rate. The y-axis occupies the width of the printout paper and is therefore fixed. Oxygen concentration is plotted on the x-axis. The length of the x-axis is determined by the user, who must specify the number of 'plot positions' (NCB), each plot position being equivalent to one advancement of the paper. Since rounded values are used by the program for plotting, it is possible that two or more separate points will occupy the same position on the paper. When this occurs, the first point only is plotted, and all other points with the same coordinates are ignored. The final plot is produced starting from an external oxygen concentration defined by the user (CB), down to an external oxygen concentration of zero:

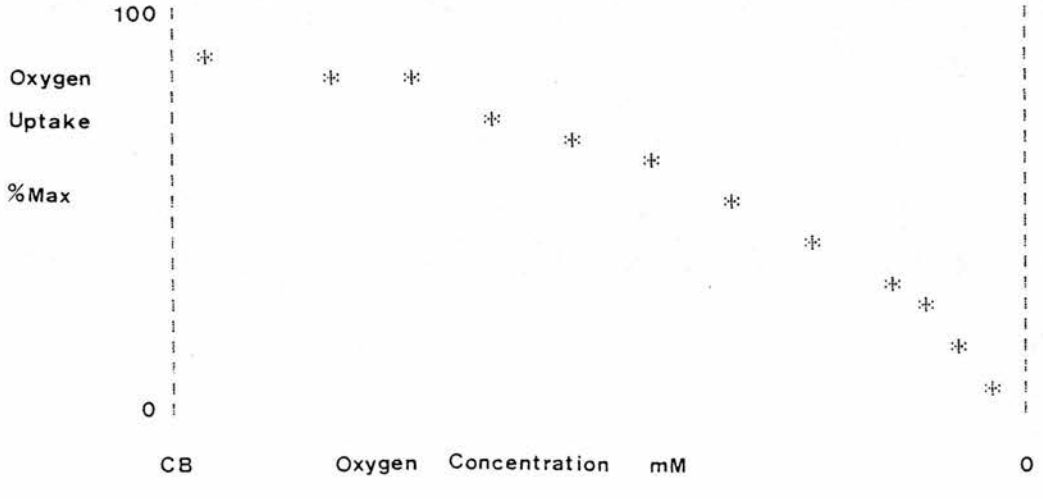

III.5 Diagnostics

The following information is intended to assist the user in the event of any difficulty being encountered when attempting to run the program.

i) Program terminates with a flashing display.

The program will automatically halt execution if any error is encountered while processing. Check carefully that the program and data have been entered correctly and that the calculator is functioning correctly. A zero entry for D, NR, A or CI will also lead to this condition.

ii) Program starts but does not plot any points; program starts plotting only after a long time; program starts plotting immediately, but run-time is excessive.

a) 0.X is greater than or equal to 1.
b) 0.X is too high for the diffusion coefficient being used.
c) CI is too high for the diffusion coefficient being used.
d) CB is very low or zero.
e) NR is excessively high.

iii) Plot shows only a few points, widely scattered.

a) 0.X is too low.
b) CI is too low.

iv) Plot shows no points.

a) CB is less than both CA and CC.

III.6 Program Requirements

i) Memory. The calculator memory must be correctly partitioned to allow space for the 555 program locations. This is achieved by the following key sequence:

5 2^{nd} OP 1 7

ii) Data Registers. Data registers R-00 to R-26 inclusive are used by the program. The following table summarises the contents of each of these data registers. Refer to III.7 for further details.

Register No.	Contents
00	Cylinder count
01	Present plot position
02	Total no of cylinders (= NR initially)
03	Initial oxygen concentration (= CI initially)
04	Present radius
05	D'
06	ϱR
07	ΣC
08	ΣR
09	Δr
10	RA
11	RC
12	KA
13	KC
14	CA
15	CC
16	D
17	B
18	A
19	NR
20	CB
21	NCB
22	O.X
23	CI
24	Smallest COC
25	$B^2 - A^2$
26	Inner radius (= A initially)

Initial data as entered by the user. The contents of these registers are not altered by the plot routine.

iii) Flags. The following flags are used by the program:

Flag 1 - Indicates that system 1 is inactive (see III.7)

Flag 8 - Instructs calculator to halt execution if an error condition is encountered.

iv) Labels. The following labels are used by the program:

A - Data entry routine

A'- Data alter routine

B - Plot routine

C - Data print routine

All branches within the program use 'absolute addressing', or specific program locations rather than labels. For this reason, insertions and deletions should not be made to the program unless all branches are updated accordingly.

III.7 Flowchart.

The purpose of this flowchart is to show in a simplified form the logic used by the program. It does not correspond exactly to the program listing shown in III.8.

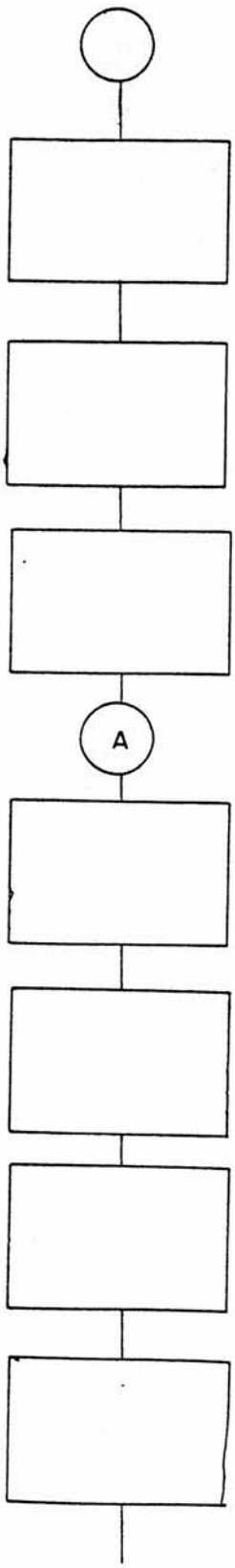

Start

Calculate width of each cylinder:

$$\Delta r = \frac{B - A}{NR}$$

Calculate D', a constant:

$D' = 2 \times 3600 \times \pi$

Print Base Line.

Set cylinder-count to NR

Set present radius, ri, to A

Set cumulative oxygen concentration, ΣC, to CI

Set cumulative oxygen uptake, ΣR, to zero

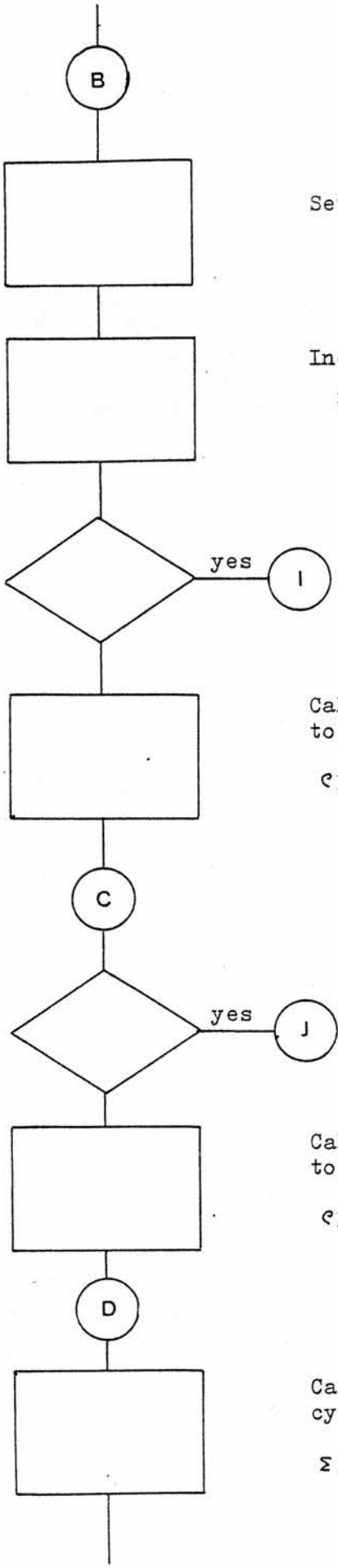

Set 'respiration density', ςR, to zero

Increment present radius, ri, to ri + Δr:

$ri = (ri + \Delta r)$

Is ΣC less than CA?

Calculate respiration density of System 1, and add to ςR:

$$\varsigma R = \varsigma R + \frac{RA}{(1 + \frac{KA}{C})}$$

Is ΣC less than CC ?

Calculate respiration density of System 2, and add to ςR:

$$\varsigma R = \varsigma R + \frac{RC}{1 + \frac{KC}{C}}$$

Calculate acutal rate of oxygen uptake in present cylinder, and add to ΣR:

$$\Sigma R = \Sigma R + \left\{ \frac{ri^2 - (ri - r)^2}{B^2 - A^2} \times \varsigma R \right\}$$

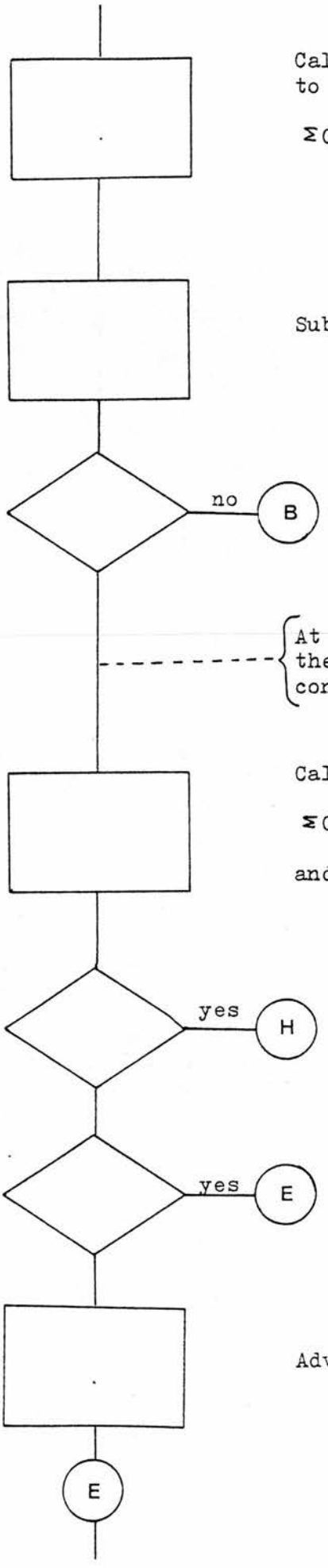

Calculate concentration increment, and add to ΣC to obtain oxygen concentration in next cylinder:

$$\Sigma C = \Sigma C + \left\{ \frac{\Sigma R \times \ln(ri/(ri - \Delta r))}{D'} \right\}$$

Subtract 1 from cylinder-count

Is cylinder-count zero ? (i.e. has the last cylinder just been processed ?)

At this stage, ΣR = rate of oxygen uptake for the whole root, and ΣC is the external oxygen concentration.

Calculate the 'plot position' of ΣC:

$$\Sigma C(plot) = \frac{\Sigma C}{CB} \times NCB$$

and round to an integer.

Is $\Sigma C(plot)$ a 'duplicate point' ? (i.e. has a point already been plotted at this position ?)

Is the paper already positioned at $\Sigma C(plot)$?

Advance paper to $\Sigma C(plot)$

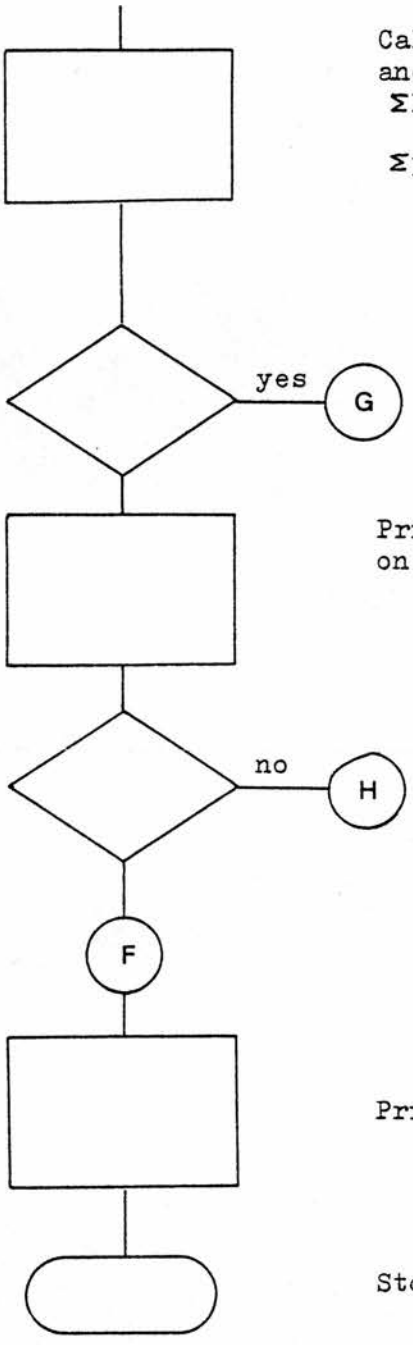

Calculate the respiration rate as a % of maximum, and multiply by 20, taking the rounded value as $\Sigma R(plot)$:

$$\Sigma R(plot) = \frac{\Sigma R}{RA + RC} \times 20$$

Is $\Sigma R(plot)$ zero ?

Print an asterisk on the $\Sigma R(plot)$ point on the y-axis

Is this the last plot position available ? (i.e. is $\Sigma C(plot)$ zero ?)

Print base line

Stop

Plot an asterisk at zero on the y-axis

Advance paper to zero oxygen concentration

Branch to F

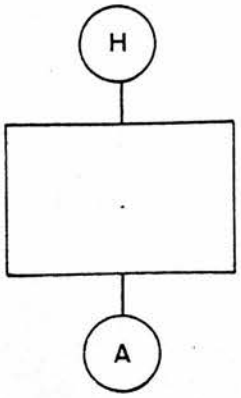

Decrement CI by multiplying by O.X

Branch to A

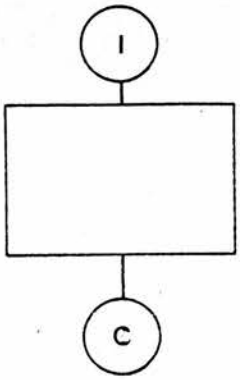

Set flag to indicate that System 1 is inactive

Branch to C

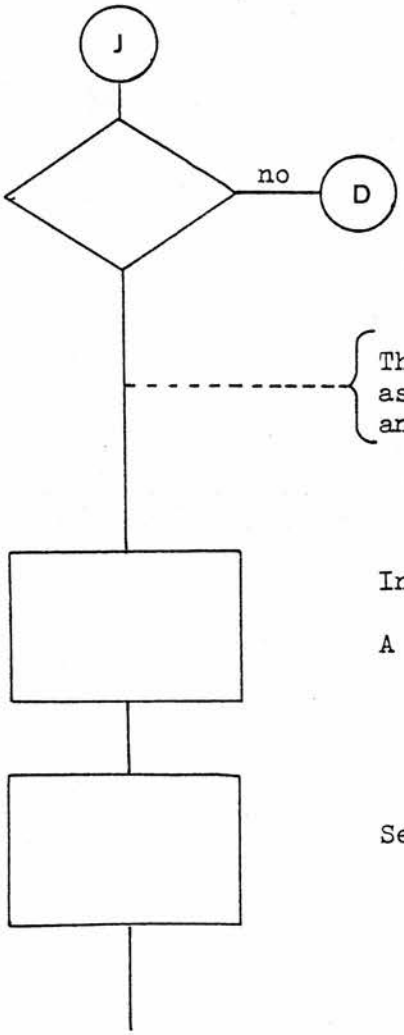

Is flag set ? (i.e. is system 1 inactive?)

The present innermost cylinder is now regarded as inactive, and will not be considered in any further calculations.

Increase inner cylinder radius:

$A = \Delta r + A$

Set CI to the smallest COC

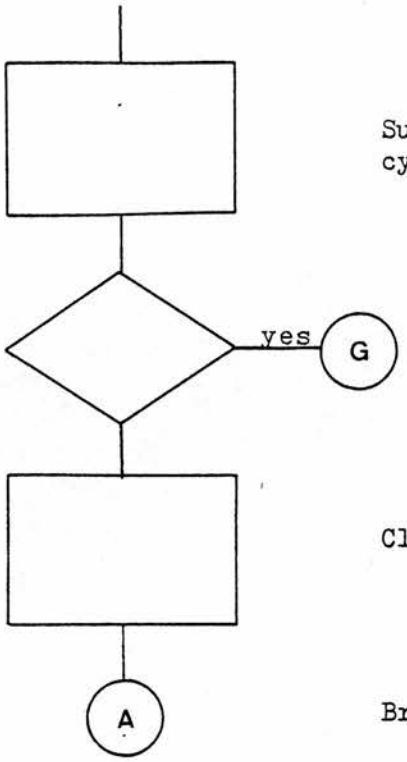

Subtract 1 from NR, the total number of cylinders

Is NR now zero ? (i.e. are all cylinders inactive ?)

Clear flag

Branch to A

III.8 Program Listing

The listing of all program steps, as printed on the calculator printer, is shown on the following pages. The user is referred to the Manufacturer's Instruction Manual for a full description of all the functions used and a translation of the key-codes and abbreviations.

The listing is shown in the following format:

LOCATION	KEY-CODE	INSTRUCTION
XXX	YY	ZZZ

```
000   92 RTN
001   76 LBL
002   12  B
003   22 INV
004   52 EE
005   86 STF
006   08  08
007   22 INV
008   86 STF
009   01  01
010   71 SBR
011   03  03
012   50  50
013   43 RCL
014   19  19
015   59 INT
016   42 STO
017   19  19
018   42 STO
019   02  02
020   43 RCL
021   21  21
022   59 INT
023   42 STO
024   21  21
025   42 STO
026   01  01
027   43 RCL
028   15  15
029   42 STO
030   24  24
031   32 X:T
032   43 RCL
033   14  14
034   77  GE
035   00  00
036   39  39
037   42 STO
038   24  24
039   01  1
040   44 SUM
041   01  01
042   53  (
043   43 RCL
044   17  17
045   75  -
046   43 RCL
047   18  18
048   42 STO
049   26  26
050   54  )
051   55  ÷
052   43 RCL
053   19  19
054   95  =
055   42 STO
056   09  09
057   07  7
058   02  2
059   00  0
060   00  0
061   65  ×
062   43 RCL
063   16  16
064   65  ×
065   89  π
066   95  =
067   42 STO
068   05  05
069   43 RCL
070   17  17
071   33 X²
072   75  -
073   43 RCL
074   18  18
075   33 X²
076   95  =
077   42 STO
078   25  25
079   43 RCL
080   23  23
081   42 STO
082   03  03
083   43 RCL
084   02  02
085   42 STO
086   00  00
087   43 RCL
088   26  26
089   42 STO
090   04  04
091   43 RCL
092   03  03
093   42 STO
094   07  07
095   00  0
096   42 STO
097   08  08
098   00  0
099   42 STO
100   06  06
101   43 RCL
102   09  09
103   44 SUM
104   04  04
105   43 RCL
106   14  14
107   32 X:T
108   43 RCL
109   07  07
110   22 INV
111   77  GE
112   02  02
113   97  97
114   43 RCL
115   10  10
116   55  ÷
117   53  (
118   01  1
119   85  +
120   53  (
121   43 RCL
122   12  12
123   55  ÷
124   43 RCL
125   07  07
126   54  )
127   54  )
128   95  =
129   44 SUM
130   06  06
131   43 RCL
132   15  15
133   32 X:T
134   43 RCL
135   07  07
136   22 INV
137   77  GE
138   03  03
139   02  02
140   43 RCL
141   11  11
142   55  ÷
143   53  (
144   01  1
145   85  +
146   53  (
147   43 RCL
148   13  13
149   55  ÷
150   43 RCL
151   07  07
152   54  )
153   54  )
154   95  =
155   44 SUM
156   06  06
157   53  (
158   43 RCL
159   04  04
160   33 X²
161   75  -
162   53  (
163   43 RCL
164   04  04
165   75  -
166   43 RCL
167   09  09
168   54  )
169   33 X²
170   54  )
171   65  ×
172   43 RCL
173   06  06
174   55  ÷
175   43 RCL
176   25  25
177   95  =
178   44 SUM
179   08  08
```

```
180  43 RCL
181  08  08
182  65  ×
183  53  (
184  43 RCL
185  04  04
186  55  ÷
187  53  (
188  43 RCL
189  04  04
190  75  -
191  43 RCL
192  09  09
193  54  )
194  54  )
195  23 LNX
196  55  ÷
197  43 RCL
198  05  05
199  95  =
200  44 SUM
201  07  07
202  97 DSZ
203  00  00
204  00  00
205  98  98
206  53  (
207  43 RCL
208  07  07
209  65  ×
210  43 RCL
211  21  21
212  55  ÷
213  43 RCL
214  20  20
215  54  )
216  85  +
217  93  .
218  05  5
219  95  =
220  59 INT
221  85  +
222  01  1
223  95  =
224  32 X↕T
225  43 RCL
226  01  01
227  22 INV
228  77  GE
229  02  02
230  90  90
231  67  EQ
232  02  02
233  44  44
234  98 ADV
235  01  1
236  22 INV
237  44 SUM
238  01  01
239  43 RCL
240  01  01
241  61 GTO
242  02  02
243  31  31
244  53  (
245  43 RCL
246  08  08
247  65  ×
248  01  1
249  09  9
250  55  ÷
251  53  (
252  43 RCL
253  10  10
254  85  +
255  43 RCL
256  11  11
257  54  )
258  54  )
259  85  +
260  93  .
261  05  5
262  95  =
263  59 INT
264  29 CP
265  67  EQ
266  02  02
267  78  78
268  69 OP
269  07  07
270  97 DSZ
271  01  01
272  02  02
273  90  90
274  71 SBR
275  03  03
276  50  50
277  81 RST
278  25 CLR
279  69 OP
280  07  07
281  22 INV
282  97 DSZ
283  01  01
284  02  02
285  74  74
286  98 ADV
287  61 GTO
288  02  02
289  81  81
290  43 RCL
291  22  22
292  49 PRD
293  03  03
294  61 GTO
295  00  00
296  83  83
297  86 STF
298  01  01
299  61 GTO
300  01  01
301  31  31
302  22 INV
303  87 IFF
304  01  01
305  01  01
306  57  57
307  43 RCL
308  09  09
309  44 SUM
310  26  26
311  43 RCL
312  24  24
313  42 STO
314  03  03
315  22 INV
316  97 DSZ
317  02  02
318  02  02
319  78  78
320  61 GTO
321  05  05
322  49  49
323  76 LBL
324  11  A
325  01  1
326  04  4
327  42 STO
328  00  00
329  01  1
330  00  0
331  42 STO
332  01  01
333  43 RCL
334  01  01
335  75  -
336  09  9
337  95  =
338  91 R/S
339  72 ST*
340  01  01
341  01  1
342  44 SUM
343  01  01
344  97 DSZ
345  00  00
346  03  03
347  33  33
348  25 CLR
349  92 RTN
350  02  2
351  00  0
352  02  2
353  00  0
354  02  2
355  00  0
356  02  2
357  00  0
358  02  2
359  00  0
```

```
360  69 □P
361  01  01
362  69 □P
363  02  02
364  69 □P
365  03  03
366  69 □P
367  04  04
368  69 □P
369  05  05
370  25 CLR
371  92 RTN
372  76 LBL
373  13  C
374  69 □P
375  00  00
376  01  1
377  06  6
378  01  1
379  03  3
380  03  3
381  07  7
382  01  1
383  03  3
384  00  0
385  00  0
386  69 □P
387  01  01
388  01  1
389  07  7
390  03  3
391  01  1
392  03  3
393  07  7
394  01  1
395  07  7
396  03  3
397  05  5
398  69 □P
399  02  02
400  01  1
401  07  7
402  01  1
403  06  6
404  02  2
405  00  0
406  00  0
407  00  0
408  00  0
409  00  0
410  69 □P
411  03  03
412  69 □P
413  05  05
414  01  1
415  00  0
416  42 STO
417  00  00
418  03  3
419  05  5
420  01  1
421  03  3
422  71 SBR
423  05  05
424  15  15
425  03  3
426  05  5
427  01  1
428  05  5
429  71 SBR
430  05  05
431  15  15
432  02  2
433  06  6
434  01  1
435  03  3
436  71 SBR
437  05  05
438  15  15
439  02  2
440  06  6
441  01  1
442  05  5
443  71 SBR
444  05  05
445  15  15
446  01  1
447  05  5
448  01  1
449  03  3
450  71 SBR
451  05  05
452  15  15
453  01  1
454  05  5
455  01  1
456  05  5
457  71 SBR
458  05  05
459  15  15
460  01  1
461  06  6
462  71 SBR
463  05  05
464  15  15
465  01  1
466  04  4
467  71 SBR
468  05  05
469  15  15
470  01  1
471  03  3
472  71 SBR
473  05  05
474  15  15
475  03  3
476  01  1
477  03  3
478  05  5
479  71 SBR
480  05  05
481  15  15
482  01  1
483  05  5
484  01  1
485  04  4
486  71 SBR
487  05  05
488  15  15
489  03  3
490  01  1
491  01  1
492  05  5
493  01  1
494  04  4
495  71 SBR
496  05  05
497  15  15
498  01  1
499  04  4
500  00  0
501  04  4
502  04  4
503  71 SBR
504  05  05
505  15  15
506  01  1
507  05  5
508  02  2
509  04  4
510  71 SBR
511  05  05
512  15  15
513  25 CLR
514  92 RTN
515  69 □P
516  04  04
517  73 RC*
518  00  00
519  69 □P
520  06  06
521  01  1
522  44 SUM
523  00  00
524  92 RTN
525  76 LBL
526  16 A'
527  01  1
528  04  4
529  42 STO
530  00  00
531  01  1
532  00  0
533  42 STO
534  01  01
535  73 RC*
536  01  01
537  91 R/S
538  72 ST*
539  01  01
```

```
540   01   1
541   44 SUM
542   01   01
543   97 DSZ
544   00   00
545   05   05
546   35   35
547   25 CLR
548   92 RTN
549   22 INV
550   86 STF
551   01   01
552   61 GTO
553   00   00
554   83   83
555   00   0
556   00   0
557   00   0
558   00   0
559   00   0
```
